NTNU – Trondheim
Norwegian University of
Science and Technology

Nonlinear and Time Dependent Analysis of a Concrete Bridge Suffering from Alkali-Silica Reaction

A Case Study of the Elgeseter Bridge in Trondheim.

Maciej Wisniewski
Krzysztof Wojslaw

Civil and Environmental Engineering (2 year)
Submission date: June 2014
Supervisor: Max Hendriks, KT
Co-supervisor: Terje Kanstad, KT
Håvard Johansen, Statens vegvesen
Ragnhild Relling, Statens vegvesen

Norwegian University of Science and Technology
Department of Structural Engineering

ABSTRACT

This thesis reports a case study of the Elgeseter Bridge in Trondheim, which is known to suffer from Alkali-Silica reaction. The main aim is to provide more accurate predictions of the response and capacity of the bridge deck, beams and columns under loading according to håndbok 238 'Bruklassifisering', Norwegian Standards NS 3473 and due to ASR reaction which occurs in this construction. The objective is to form a basis for how ASR mechanisms determined through linear and nonlinear analysis can be used when assessing existing bridges. Concrete expansion due this reaction, the consequences and structural effects are presented. Changes due, to concrete cracking and reinforcement yielding are studied through finite element analyses of this bridge. Recommendations for nonlinear analysis of reinforced concrete slabs with shell and beam elements are established and verified with TNO Diana and SOFiSTiC software. Results from linear and non-linear analysis are verified by comparison with reports. Calculations showed lack of sufficient capacity to shear force and strengthen of the structure is necessary. What is more, this study describes how to use available nowadays methods to prevent the development of ASR reaction in this bridge. Finding relatively accurate solution requires selecting the appropriate methods, the best fitting methods have been considered and have been recommended.

Key words: Reinforced concrete, shear force, expansion of concrete, non-linear end linear finite element analysis, The Alkali-Silica Reaction, bridge, treatment with lithium, crack filling, monosilanes, fiber reinforcement for strengthening concrete structures.

Assumptions and Evidence briefly:

The reason for the formation of cracks in the concrete structure of the bridge is the phenomenon ASR. This is confirmed in later studies by linear and nonlinear analysis of the reinforced slab, columns and beams. This is also proved in a later section of this paper by calculation in accordance with the standard NS 3473 and EC2. Several of reports and our personal investigation also confirm occurrence of this phenomenon in this bridge. Development of ASR reaction is much more advanced on the west side. However, modeling is made with symmetrical response action. The concrete is modelled like a damageable material having elastic and inelastic strains. ASR is modelled using global kinetics including temperature changes. Generally, cracks appearing in the structure, we can divide into two types.

Figure 1. Crack (6 mm width) in internal beam of the bridge.

Cracks which are caused by a phenomenon in itself which begins at microstructural level (components covered by the reaction: columns, plate and exterior beam). And other cracks which are caused by the consequences related to the expansion of concrete from external parts of structure (internal beams of loaded with a combination of three components: shear forces, tensile forces and bending moments).

The fundamental reason why the phenomenon of Alkali Silica reaction occurred in the structure of beams and slab is incorrect performance of the membrane - the protective surface coating of the structure against penetration water and moisture. Moreover the boundary of the pavement plate does not have a secure in the form of cornices and eaves against water penetration.

A first obvious observation from early inspections had shown us that construction doesn't have cross-beams, for that reason stiffness in transverse direction is relatively low. It can be considered that every beam connected with columns works almost independently. That can have also influence for crack which occurs in slab.

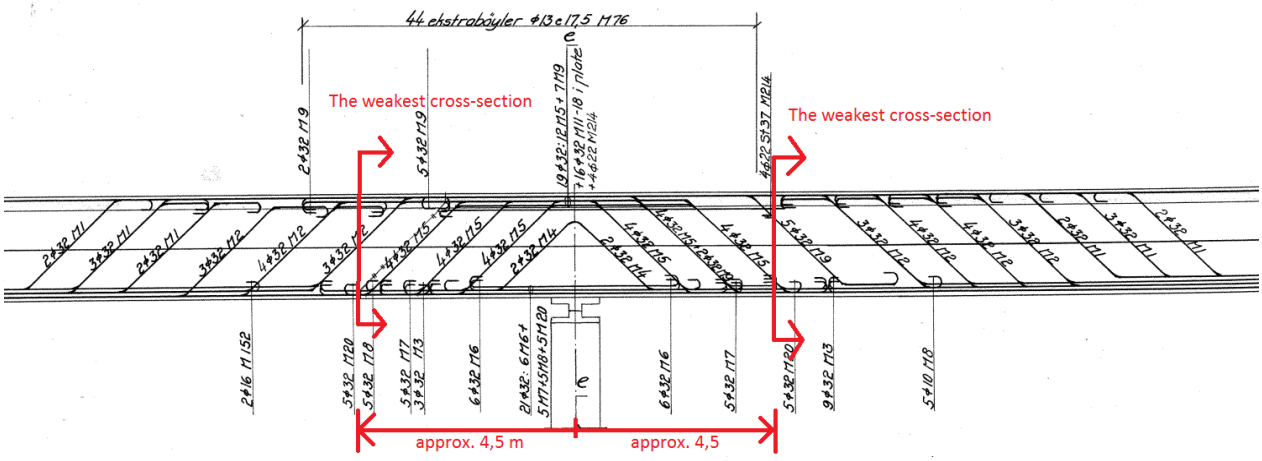

Figure 2. Investigated weakest point of the beam cross-section.

We observed a characteristic repeated phenomenon that in the internal beams are cracked at a distance of 4-5 m from the support. A crack occurs almost within each axis.

By the consequences related to the expansion of concrete from the external parts of bridge – It is confirmed by analysis of our models that internal beams are subjected to large tensile stresses related to ASR reaction. Furthermore, in this aspect through the inspection of the available archival drawings we noticed that the design of the reinforcement has disadvantages. In the recurrent cross-section around of 4-5 m from the support there is a gap in the reinforcement. It is the location of anchoring the upper, lower and bended rods. These facts allow us to assume that stresses in the concrete exceeds the allowable value of tensile as effect of combination of tensile membrane forces, shear forces and also as effect of influence of these weakest points, hence the shapes of cracks in the is not typical as for cracks caused by bandings moments.

In the case of columns are continuously exposed to water action. External especially western pillars are exposed to rain, evidenced by the fact that there are three times more cracks than on the eastern side [4]. Water is present on the columns not only in the form of rain as a liquid and does not work only on the top of structure, but from the sides as well. This aspect is a result from water vapor pressure in the pores of the concrete exposed surrounding atmosphere. In winter, due to the approximately 5- fold higher specific heat of water flowing under the bridge, creating a situation where the steam from the water from the river is in contact with the cold concrete and condenses on the surface. By diffusion water penetrate into the interior parts of the columns. This phenomenon in many cases is neglected. The penetration of steam into concrete structures is according to the so-called higrotermical equilibrium. It all contributed to large increase of moisture content in the concrete.

To prove that the reaction ASR also effects on cracks which occurs in the columns we decided to present the simulation of crack formation. We assumed that the cross section of the column works in 2D plane strain. In the plane strain model type we modeled the quarter of column. To modeling discrete cracking we used line interface elements. It will be shown that deterioration process in columns is advanced, the phenomenon of ASR and steel corrosion is shown.

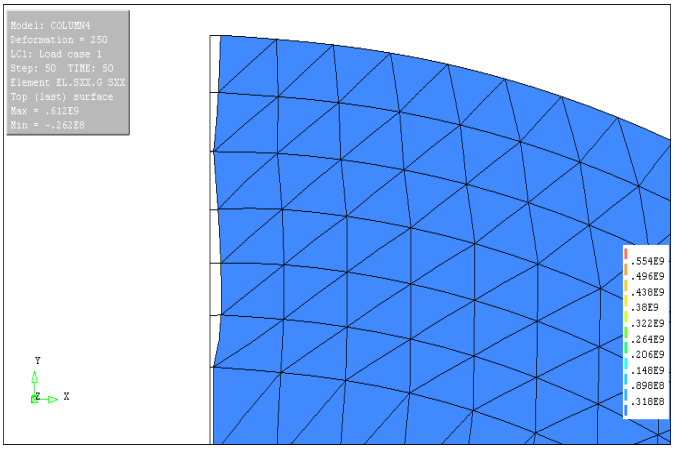

Figure 3. Visualization of crack opening with reinforcement.

This allowed us to assume that the embedded reinforcement of the columns is reduced and more exposed to moisture from rain and steam from the river. This leads to rapidly penetrate the concrete cover and increase the probability of occurrence additional dangerous phenomenon in the structure also increases initiation rate of corrosion in steel.
During observation we also noticed very long longitudinal crack in deck slab. This can be related to ASR expansion of concrete because we observed very characteristic phenomena that this crack occurs exactly on the edge of infection.

Crack also passes through the filters were installed in the slab drainage system. This allows us to assume that the crack is in a weakened section through filters and take place in a cross-section with a large difference in normal forces coming from the expansion of the infected concrete portion.

Figure 4. Corrosion of embedded reinforcement in column *[fot. by Maciej Wisniewski & Krzysztof Wojslaw].*

Proposed solution in a nutshell:

Slab:

Resurface a pavement, curbs and sidewalks. As a result, taken by us under analysis below we strongly recommend use a topical treatment of slab with Lithium under membrane protection after removing the surface of pavement, curbs etc. Afterwards next step will be the application of a new layer of membrane on the bridge slab which will cause that Lithium will be covered and will be actively penetrate and work on reinforcement concrete slab. Application of a new drainage system plate: First and foremost, the most important element is waterproof membrane protection of the slab. Apply new high quality membrane cover on the top surface. It is required filter papers (perforated top) under waterproofing membrane, which is often, especially in a tight, modern waterproofing surfaces neglected. This aspect is a result from water vapor pressure in the pores of the concrete, the moisture in the concrete tends to float upwards and settling on the surface of the waterproof membrane is therefore necessary to apply the perforations. This is to prevent destruction of the top plate cover membrane again. Drainage system dehydration surface drains, manifolds and downpipes, put careful attention to the methods of attaching the filters into the collecting duct, role of fastening steel structures, expansion joints and elements for revision. Consider need for deep drainage system of bridge abutments. Consider also different solutions drainage systems engineering.

Beams:

Fiber Reinforcement Strengthening of the beams is the most appropriate solution. Use of carbon fiber reinforcement with pre-stress system application is necessary. Primarily, internal beams require achievements of sufficient capacity for shear force and sufficient tensile membrane forces which comes from service load and from ASR reaction, respectively. Therefore, the best solution is to use pre-stressed carbon fiber with strips as long as it is possible. The weakest points which have been described in this thesis and places where cracks are already generated require also use glued strips in vertical and diagonal direction. Before Fiber Reinforcement application all the crack should be filled. Rigid polymer- and cement-based grouts may help to stabilize cracks initially, their rigid nature and strong bonding with the substrate concrete often forces cracks to appear adjacent to the grouted area. Crack filling can be taken also to address ASR-induced cracking, primarily through crack filling to minimize ingress of water, chlorides, and other aggressive ions, and ASR-induced expansion by confining the expansion. The last sentences solutions also should be apply to column

Columns:

Using the solution with wrapped fiber reinforcement has been rejected in progress of our analysis. It is proven experimentally that a wrapped fiber strips increases the relative humidity in the concrete structure and this phenomena causes a further development of the reaction. The most appropriate solution chosen from all available are use of electrochemical Lithium Impregnation and after monosilane cover, respectively. Exact principles of electrochemical lithium impregnation have been described on this paper below. Obviously, monosilane was tested on Elgeseter previously and gave very promising results for that reason in our opinion this is proper solution. Formerly, electrochemical lithium impregnation should be done after also crack filling could be taken into account then application of the new structure of monosilane should be prepared. Deteriorated surface of the columns as in the case of column nr #4 in zone 4 should be first replaced with new layer of concrete. All of these treatments are based on the stopping development of ASR by the chemical treatment and by prevents penetration of the water. Further silane allows draining moisture from the concrete. This can provide benefits from the achievement of a relatively low level of moisture below the critical value of 80%. These operations should be prepared especially the central columns in the riverbed from the west where the columns are the most exposed to rain.

Contents

Preface

This thesis investigates the use of linear and non-linear finite element analysis for assessment of reinforced concrete bridge deck slabs, beams and columns subjected to ASR effects loading. As well as finite element analysis was used number of issues about the mechanical properties of reinforced concrete and ASR reaction was taken. It was carried out at Concrete Structures, Division of Institute of Structural Engineering, Norwegian University of Technology and Science. The work on this thesis started January 2014 and ended June 2014 financed by the Norwegian Public Transport Administration.

The work in this study was based on a several reports carried out by the Norwegian Public Road Administration during many of years. The reports were made on the basis of experimental tests by institutions and companies such as: SINTEF, RAMBOLL, and ASS JACOBSEN. Reports experimental program consisted of tests on full scale on existing concrete bridge in Trondheim, subjected to different configurations of measurements of moisture and displacements over the years.

This thesis had been carried out with Professor Max A. N. Hendriks, and Professor Terje Kanstad as a supervisors. We greatly appreciate their guidance, support, encouragement and valuable discussions. We also want to thank Ragnhild H. Relling and Johansen Håvard for their support of our work and permission to use the test data and drawings collected by the Norwegian Public Road Administration. For guidance with FE software we thank Professor Max A. N. Hendriks. For assistance in the construction of reinforcement concrete issues we would like to thank Professor Terje Kanstad. The fruitful discussions provided by all at the Division of Institute of Structural Engineering, Norwegian University of Technology and Science are also greatly appreciated.

1 Introduction

1.1 Background of the project task

Elgeseter Bridge is probably the most thoroughly investigated concrete structure in Norway that has suffered from Alkali-Silica Reaction (ASR). Before 1990, significant reduction of the single expansion joint in the road plate and cracking in other concrete elements were observed. In the early 1990s, when ASR was accepted in Norway as a common deterioration process in concrete structures, a reasonable explanation was provided for damage to the bridge.

Bridges constructions are one of the most susceptible to Alkali-Silka Reaction. Influence of this phenomenon is often critical for the load carrying capacity. Nowadays, design procedures for avoid accuracy of ASR in reinforcement concrete mix are well-known. However, there is still a lack of well-established recommendations for contribution of ASR-reaction in case of old existing structures. Consequently, it is important to examine the appropriateness of current analysis and design methods to describe the actions of Alkali-Silka Reaction. Linear elastic FE gives good results as long as the structure remains un-cracked. Hence, to describe the real behavior of the structure non-linear analysis is needed due to stress redistribution to other regions after cracking.

What is more the diagnosis, assessment and rectification of concrete structures affected by ASR is a complex, difficult and time-consuming process. A major problem facing those involved in identifying and evaluating material and structural damage is the many stages where confusions, contradictions and uncertainties challenge the assessment. Inevitably, assessment of ASR damage is closely and intimately involved with testing. Environment, or most precisely, the changes in climatic and exposure conditions, is probably the most critical factor influencing and modifying accepted concepts of behavior of ASR-affected concrete. Many complex interactive and interdependent parameters involved in controlling the rate of expansion and total expansion. Each structure may have to be assessed and treated individually and independently, while appreciating the known commonalities of the damage process and similar patterns of behavior exhibited by affected structures. However, this master thesis, in our opinion, gives wide and appropriate determination for ASR phenomenon in Elgeseter Bridge. Furthermore this paper gives integrate material and structural design strategy for the assessment and retrofitting of concrete elements of structure damaged by ASR.

1.2 Purpose and scope

The goals of this master thesis:

- To show distribution and re-distribution of shear forces in concrete slabs and beams with respect to bending cracks and yielding of the reinforcement,
- Ensure more exact predictions of the response and capacity of the bridge structure under loading with respect to Alkali-Silka reaction,
- Investigation of the behavior of failures caused by shear forces in reinforcement concrete,
- To demonstrate how a combination of refined structural analyses and engineering interpretation can explain observed deformations and damage of the bridge,
- To investigate whether a common ASR-expansion model for the columns and the deck of the bridge can explain observed cracks,
- Presentation of existing on market repair solutions,
- To propose repair on the Elgeseter Bridge

The overall thrust of this paper is to show that an integrated material and structural design strategy needs to be adopted to develop techniques that are meaning and effective for the identification, evaluation and rehabilitation of concrete elements in reinforcement concrete structures affected and damaged by ASR in order to maintain a capacity of the structure.

Appropriate bridge maintenance activities should be carried out to sustain a required level of performance throughout the whole life cycle. Recently, there has been a considerable increase in repair and rehabilitation methods to restore or enhance deteriorated bridges.
It is a highly complex problem to decide which bridges need maintenance and what kinds of activities are used for the bridge to maximize total benefit. In other words, the bridge maintenance strategy at a network level is an optimization problem to combine the selection of bridges that need repair or rehabilitation with maintenance activities whose total cost should not exceed the given budget. It should maximize the total benefit of bridge maintenance activities.

1.3 Method

The project started with a literature study based on a several reports carried out by the Norwegian Public Road Administration prepared in many of years. Since this master's thesis is closely related to an on-going research project concerning load carrying capacity due to ASR in existing structures, the literature study helped to get an overview of what experiments had been carried out before and what thing may need further investigation. Finite element analyses of a bridge, both where cracking had occurred and had not occurred, were performed in order to identify common parameters for the cases. The results from different analyses are compared.

It is shown that exposure to environmental and a climatic change is the major factor influencing the rate of expansion and total expansion of concrete in real structures. ASR is also closely and intimately involved with testing and test methodologies so that material and structural rectification requires a global approach involving diagnostic methods, tests to establish the potential of future expansion, selective sealing of cracks and protection from environmental attack, structural evaluation using non-destructive test techniques and structural strengthening. In order to investigate columns, non-linear analysis using FE software was required. One typical load and geometry configuration, previously tested on temporary model, was chosen for the study.

2 Alkali- Silka Reaction

2.1 Introduction

The development and improvement of proficient procedures for ASR assessment becomes a demanding need owing to the ageing condition of deteriorate concrete structures. Replacement, rehabilitation or repair requirements demand innovative solutions and at the same time to do not exceed ultimate costs associated with their conduct. All these solutions will help to evaluate the current state of the deteriorated structures but also their future performance to protect newly emerging structures against destructive action ASR.

The alkali-silica reaction is a ruinous chemical process that can occur in ageing concrete. The product of the reaction is an amorphous silicate material which has similar to the gel characteristics. Persistent deterioration of the concrete structure [1] is the result of high expansion properties and may cause cracking in the matrix and in the discrete aggregate of particles. Research and deliberations based on the structural information of this gel at the atomic scale and observation of the macro scale behaviour leads to provide critical information on how to establish the most appropriate repair of the affected structure.

Alkali-silica reaction (ASR) occurs in concrete when alkali from the cement, or from an external source, reacts with free silica presents in certain aggregates to form an alkali–silica gel. The latter has the property of taking in water and expanding. This expansion can cause the aggregate particles and the concrete to crack, and ultimately can damage the concrete. When concrete has become damaged by the alkali-silica reaction, the characteristic feature it displays is a network of cracks, which on the surface of the concrete produces a pattern referred to as ‘map cracking’.

It is obvious that Alkali-silica reaction can lead to the premature distress and loss in serviceability of concrete structures. It have been generally discovered that ASR occurs in concretes with reactive aggregates, when there are sufficient alkalis (K2O, Na2O), and when relative humidity in structure is higher than 85%. In addition, temperature have influence for the time of initiation (induction period) and progress of development of the reaction. Due to ASR takes action, different effects appear inside the concrete, gels and cracks form, gels filling cracks in the aggregates or in the cement paste, gels form reaction rims around aggregate particles, gels fill air-voids in the cement paste and silica gels replacing C–S–H of hydrated cement paste [2, 3].

ASR has been mentioned first time more than 70 years. More than 50 countries around the world has been announced occurrence of this problem [4,5]. The AAR started to be issue

of the first considerations initiated by the scientific community. In the 40s scientists specified first chemical and mineralogical expressions of this reaction (for a historical perspective see Swamy, 1992,[6]).

For instant of the extension of these researches was that symptoms of AAR has been observed in over 100 large dams in the world and have been undertaken into indications of this reaction and evaluation of expensive repairs solutions [7]. Good example is Argentina where more than 100 structures, taken into consideration from variable regions with different climates, deteriorated by ASR have been noted since 1950 (see [8] for a historical perspective). The mineralogical structure of the aggregates is one of the main factors affecting ASR, chalcedony, amorphous silica, tridymite, volcanic glass and cristobalite appear as the ingredient with reactive properties leading to a sudden or normal reaction rate, showing visible signals of reaction in concrete at ages as low as 1 year, determined by the surrounding environment conditions. On the other hand, the very long induction periods usually higher than 10 years is characterized by aggregates as those which are consist of granitic and metamorphic rocks that include mineral species as polycrystalline and strained quartz [9–11]. Different levels of damage evaluation and cracking accuracy appear in concrete microstructure with regard to the kinetic aspects of ASR [12]. Rapid progression of reaction can generate large internal stresses that can act at the interfaces and cement pastes, causing micro and macrocraks. However, the pore solution can be also reached in mixes with strained quartz, where the reactions sources are placed inside the aggregates in active areas (intercrystals). This procedure is very calmly and the invasion is not observed all around the aggregate surface [12]. The results of ASR have been studied by many authors that effect on the mechanical properties of plain and reinforced concrete specimens. According to this considerations most of researchers are agree that ASR significantly effects on the modulus of elasticity and tensile strength of the concrete. Compressive strength reduction is noticeably lower than this is observed in stiffness matrix, being even not untouched in several cases of compressive strength. Therefore the compressive strength is not determinant in assess the quality of concrete deteriorated by ASR.

The appropriate steps of the alkali–silica reaction are not yet sufficient precise neither fully established. However Dent Glasser and Kataoka [13] described that the high (13,5) pH in the pore solution causes dissolution of silica indicating silanol groups which react with the pore solution to form SiO. This deprotonated surface complex adsorbs metal ions from the pore solution, mainly Na+, K+, and Ca2+, to form a gel, which depending on its chemical composition may cause significant expansion. This is considered as a consensus that the general stages take place according to these assumptions.

A very long time it was unknown what gel composition leads to expansion. Prezzi [14, 15] proved and presented a solid foundation to explain the expansion of alkali–silica gels. That can be provided using the double-layer theory.

Several studies [16–20] on synthetic samples have been shown that the structure of the products of ASR have the amorphous character of these silicates. However, that is difficult to get tolerable gel specimens from concrete deteriorated due to ASR that are pure and useful for deep analysis [20].

The alkali hydroxides and the portland of the hydrated cement paste reacted with some structures of silica present in aggregates may form damage in concrete. ASR has been extensively studied (for some more aspects see some examples of consideration [21-23]). The mechanisms that have been described used various models. The mechanisms can be described by two main steps:

- Step 1 - The first siloxane bond break up by hydroxyl ion cause formation of Q_3 tetrahedrons:

$$2SiO_2 + OH^- \rightarrow SiO_{5/2}^- + SiO_{5/2}H$$

A Q4 silicon tetrahedron sharing 4 oxygens with 4 neighbours is represented by SiO2 from a constructional point of view. The Q3 represented by SiO5/2, using a simplified notation, negatively charged tetrahedron in a basic solution. Q4 and Q3 tetrahedrons are constituent elements of the aggregate.

- Step 2 - Hydroxyl ion attack on the Q_3 tetrahedrons to form silicate ions, $H_2SiO_4^{2-}$, $H_3SiO_4^-$, dissolution of silica and small polymers:

$$SiO_{5/2}^- + OH^- + {}^1/_2\ H_2O \rightarrow H_2SiO_4^{2-}$$

Afterwards, sediments of silicate ions by the cations of the pore solution of concrete leads to the formation phases of C–S–H, C–K–S–H and C–N–S–H. The chemical method to measure the degree of reaction in a concrete sub-system has been developed by Bulteel [24] involving the main ASR reagents: ground aggregate, $Ca(OH)_2$ and KOH. This method has allowed us to quantify:

– the number of moles of Q3 tetrahedrons constructed by step 1 and consumed by step 2,
– the number of moles of dissolved silica (Q0 tetrahedrons) constructed by step 2.

Various of theories have been developed and proposed to account for the swelling mechanism induced by the ASR: First of them is the theory of imbibition pressure or osmotic pressure [22,25,26], second is the theory of ion diffusion [27,28], and many various of other like: the theory of crystallization pressure [29,30], the theory of gel dispersion [31] and the theory of electrical double-layer repulsion [32,33]. Unfortunately, none of these theories can explain the experimental results, sufficiently.

The Figure 2.1 has shown the scheme that represents mechanism of the ASR-induced destruction of concrete. The deterioration proceeds according to the following steps:

1) OH− and R+ ions in the pore solution de-polymerize silica rich aggregates to modify to fluid hydrated alkali silicate. The alkali silicate homogeneously wrapper the surface region of the aggregate. Expenditure of OH− ions by the reaction collaborate with the dissolution of Ca2+ ions into the solution.
2) The soft alkali silicate is easily penetrated by the Ca2+ ions into re-polymerize the silicate. The aggregate is now tightly packed with a rigid reaction rim that allows the penetration of not alkali silicate but R+, Ca2+ and OH− ions. The Ca2+ ions penetrate much slower than the R+ ions.
3) The reaction rim is penetrated through the OH− and R+ ions to convert the fresh silicate into bulky alkali silicate. The resultant expansive pressure is stored in the aggregate. The accumulated pressure cracks the aggregate and the surrounding cement paste when the pressure exceeds the tolerance of the aggregate surrounded by the reaction rim and the cement paste.

Model shows that the deterioration of concrete is not caused by the ASR, if the ASR is finished before the creation of the active rim. Aggregate such as fly ash and communal waste incinerator bottom ash are reactive but do not induce the deterioration of concrete, since they are absolutely modified to alkali silicate before the creation of active rims. They have rather tendency to act as pozzolanic materials [34,35] if they absorb alkali ions and therefore reduce the concentration of R+ and OH− ions.

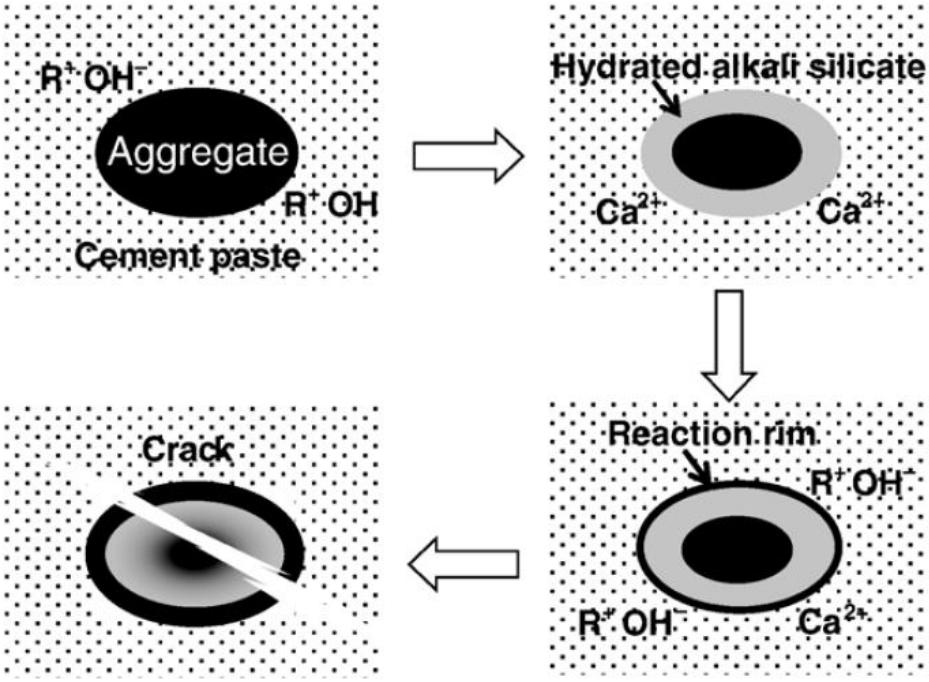

Figure 2.1. Scheme of the mechanism of ASR-induced cracking of concrete.

Two kind of alkali-aggregate reaction (AAR) are currently identified determined by the nature of the chemical properties of reactive mineral; these are:

- Alkali-silica reaction (ASR) which require various kinds of reactive silica (SiO2) minerals, and
- Alkali-carbonate reaction (ACR) which engage certain types of dolomitic rocks (CaMg(CO3)2).

All this category of reaction can act in expansion and cracking of concrete members that can cause a reduction in the existing life of concrete constructions. Map-cracking (Figures 2.2 and 2.3) are the first obvious visible symptoms of accuracy of ASR reaction. On concrete structures affected by either ASR or ACR, the symptoms are generally analogous, and a petrographic tests have to be obtain on samples taken from the structure is usually needed to individualize the two types of reactions. A product from the reaction, the alkali-silica gel, is commonly recognized in concrete influenced by ASR. Occurrence of ACR is limited and restricted to an only few cases in North America. From the other hand, ASR is epidemic throughout North America and worldwide phenomena. The same in case of Elgeseter Bridge, all infected parts are consequences of ASR for that reason, consequently, the vast majority of illustrations shown in this master are typical examples of ASR not ACR. In many circumstances, there may other destructive factors occurs that are contributing to the deterioration investigated. For instant, cyclic freezing and melting of penetrated water in northern regions can extend the cracking initiated by AAR. What is more, embedded reinforcement corrosion can be promoted by exposition for deicing salts and access of chloride ions to cracks caused by AAR in concrete. This may provide pathways to sudden deterioration. Consideration of appropriate measures mitigation should be given to the possibility to use the exact solutions to decrease effect of these and other processes when inspecting a concrete structure for AAR.

Figure 2.2. Map-cracking of a construction beam caused by ASR [*fot. by Maciej Wisniewski & Krzysztof Wojslaw*].

Figure 2.3. Map-cracking of a construction beam caused by ASR [*fot. by Maciej Wisniewski & Krzysztof Wojslaw*].

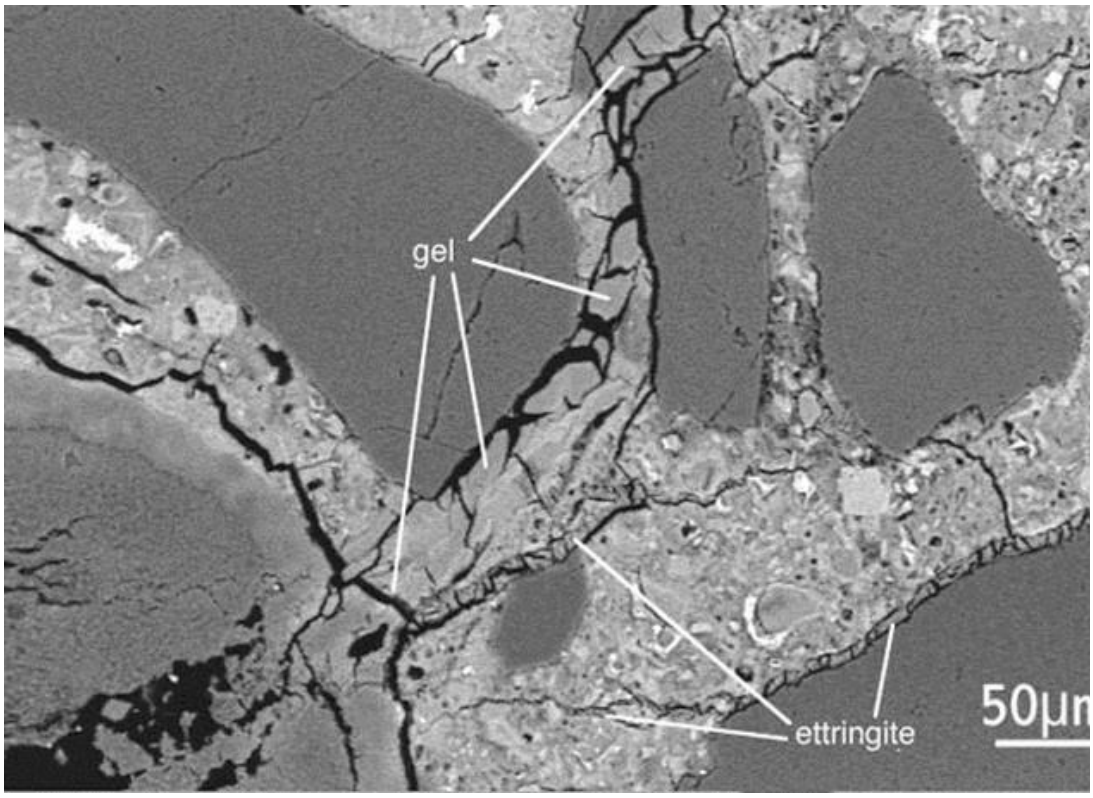

Figure 2.4. Alkali-silica gel in petrographic thin section of concrete taken from an ASR-affected structure.

2.2 Requirements for ASR

Certain forms of chemically active silica minerals occurring in reactive aggregates and the alkali hydroxides in the pore solution of concrete are minor components of chemical activity in aspect of ASR. The product of reaction, an alkali-silica gel, is hygroscopic, and will absorb water and as long as the concrete is in sufficient humidity can swell. Under certain circumstances, the swelling of the gel can lead to expansion of concrete and caused cracking. There are three fundamental conditions for occurrence of ASR; these are:

- Accumulation of alkali hydroxides in the pore solution of the concrete should be sufficient enough. The portland cement is the main source of alkalis in concrete, contained amounts of sodium and potassium. In several cases, supplementary alkalis may be added with other components of the concrete (e.g. aggregates, supplementary cementing materials and certain kinds of admixtures) or as a result of exposure conditions from environment or treatment (e.g. deicing salts or seawater).
- Amount of reactive minerals in the aggregate should be also sufficient enough. The most reactive minerals components are: tridymite, opal, cristobalite, strained quartz, volcanic glass, various forms of microcrystalline and cryptocrystalline.
- Level of humidity. Below a relative humidity of 80 percent ASR is ceased. Unfortunately, since the level of relative humidity in the concrete increases from 80 percent to 100 percent the intensity increases, respectively.

By both dodge of reactive aggregates and regulating the opportunity of occurrence of alkali in the concrete destruction due to ASR can be avoided in new designed construction. There are two ways to regulate the opportunity of occurrence of alkali. The use of low-alkali cement and the use of safety, non-reactive cementing materials are ones of them. In existing ASR-affected structures, the rate of reaction depend on moisture, therefore, the rate of destructive progress, may be tried avoided by lowering the level of relative humidity where it is feasible. Currently, on the world several methods for maintaining of existing structures have been developed. Using appropriate methods a future expansion of ASR in case of existing structures can be wholly blocked.

2.3 ASR in combination with other deterioration processes

After ASR damage has occurred, ASR can be initiated simultaneously with other deterioration processes or may provide the concrete more vulnerable to these processes together. Particularly, when we consider the surface of infected concrete as an open network of cracks, other substances can easily penetrate the structure. This phenomenon of connection of ASR with other deterioration processes unfortunately also occurs in Elgeseter Bridge.

ASR and steel corrosion

Cracking due to ASR provides elements of construction for oxidation and chloride ions from exposed for moisture from river water as well as from rain water and leads to rapidly penetrate the concrete cover and initiate corrosion of embedded reinforcement. One instance of corroded steel in column is shown in Figure 2.5.

Figure 2.5. Corrosion of embedded reinforcement in column *[fot. by Maciej Wisniewski & Krzysztof Wojslaw].*

ASR and freeze-thaw deterioration

The resistance of concrete to cyclic freezing and thawing can be reduced by ASR. Even in case when the concrete is significantly air-entrained. Cracks induced by ASR become starters to saturate the freezing water which will propagate and caused the cracks widen. Flat, horizontal surfaces, such as slab pavements, are particularly vulnerable to this combination of phenomena's.

ASR and delayed ettringite formation

Very often delayed ettringite formation (DEF) has been found in association with ASR. By reduction of the pH in concrete pore solution, ASR can accelerate DEF, therefore expediting the release of sulfates entrapped by the hydrates during elevated-temperature curing. The released sulfates are then free to form ettringite. Formation of ettringite is then

delayed and increases the cracking and expansion which is already contributed by ASR. On the figure 2.6 effects of ASR and DEF is shown.

Figure 2.6. Delayed ettringite formation effect *[fot. by Maciej Wisniewski & Krzysztof Wojslaw].*

2.4 Treating Existing ASR-Affected Structures

Figure 2.7 characterizes the different mitigation opportunities that have been taken into account and are available in the world or we proposed for use in field of Elgeseter structure. These are grouped according to whether they are intended to treat the causes of ASR or the symptoms of the deleterious reaction.

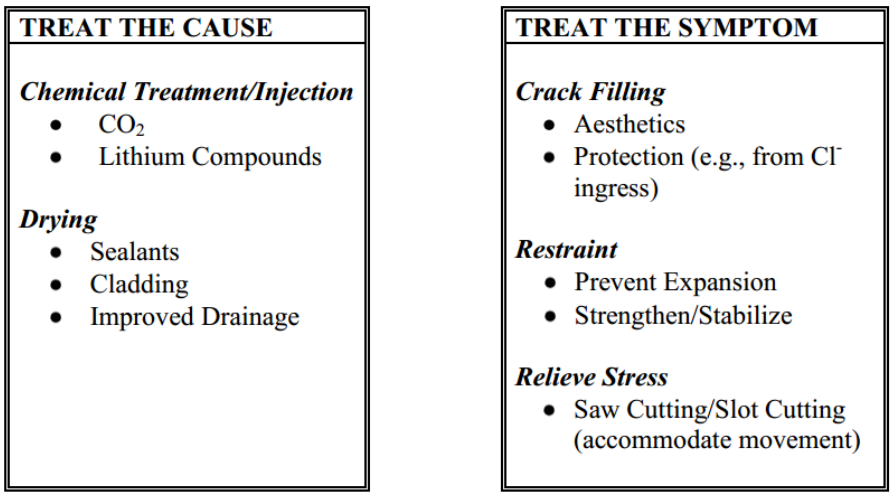

Figure 2.7. Likely options for mitigating ASR-affected structures – treating the cause versus treating the symptom

Two categories of methods for mitigating the effects of ASR exist and can be divided into:

1. Mitigating the symptoms of distress and,
2. Addressing the cause of distress.

Mitigating the symptoms contain: cutting joints which allow further expansion to occur, therefore pressures on neighbor members and stresses within internal parts of the concrete or concrete structures can be relieve. That allows ensuring restraint to further expansion. Cracks filling - caulking cracks with an epoxy compound (or similar) can help reinstate the endurance of the cracked concrete sections and conserve reinforcement which is embedded and exposed for environmental factors influence. From the other hand it not cause, appropriate delay of the rate of expansion concrete and reaction symptoms. In admission, with time if the reaction is let on to progress, new cracks will surely form. To performance cutting joints mechanical equipment have to be used. Joints can also be performed to separate expanding structures from neighbor constructions members as well as to mitigate exceed of internal stresses in pavements. Providing joint space for expansion we not ingrate into the reaction, but only avoid the effects and it is very feasible that the cracking and expansion will continue the progress.

Performance of restraint with using a rock anchors or post-tensioned tendons to that also can be used in structures to prevent unwanted expansion and distortion of the structure. Fiber-reinforced polymers (FRPs) actually are very popular in this field and have been used to wrap structural elements such as beams and strengthening slab and columns in bridges structures and also in the others constructions.

The only two constructive means has been discovered for addressing the cause of damage. To reduce and protect further development of reaction we can use either dry the

concrete solutions to discard the moisture which is necessary to sustain ASR or to eliminate the expansive nature of the reaction by applying lithium compounds.

To reduce the relative humidity in ASR-affected concrete piers structures, silane sealers have been used successfully (see Kojima et al., 1992) and also for instant in case of railway sleepers (Oberholster et al., 1992). Application of Silanes causes that the surface of the concrete is prevented against the penetration of liquid water into the internal parts of construction. In the same time, the moisture is still reduced because water vapor can still exit through the layer, thus the reducing of the relative humidity is in progress in time.

After in section 9 with regard to proposed repair we will briefly discuss each of the options shown in Figure 2.7 and will then focus on those that have the greatest potential for effectively treating ASR-affected Elgeseter Bridge. For each of these options, the merits will be discussed, as well as inherent shortcomings, both in terms of general applicability to field structures and specific application to Elgeseter Bridge.

2.5 General managing structures affected by ASR

Periodic inspection, measurement and monitoring the displacements of different component of the construction using adequate system is basically is currently the most important process in management of ASR-affected structures with concern to the signification of the structure.

Managing structures affected by ASR is a complex process. A condition survey belongs to one part of this process depending on the structure and the requirements of the owner. Owner may also decide that no further testing beyond a detailed site investigation is needed. Measures to mitigate the effects and restrain the rate of the reaction are ones of possible solution, but many of ASR-affected structures remain in service without them. Sudden structural collapse in concrete components affected by ASR is seldom. From the other side, if no measures to mitigate are taken into account with the symptoms or abate the reaction, continuing ASR may result in serviceability problems, increased maintenance costs, accelerated deterioration due to other mechanisms, and reduced service life. As it was mentioned in advance, extent of ASR requires laboratory testing and petrographic examination of cores have influence for significant improvements of tests quality and a certain diagnosis expectation. The results of the laboratory investigation and the symptoms from the site investigation can be combined, that allow an experienced engineer can properly asses the feasible contribution of ASR in the observed deterioration. In the next step may be that immediately recommend measures to mitigate the reaction and its effects can be taken into consideration. However, before deciding on a development of repair/ maintenance a decision may be made to design plan of acting on the structure in order to monitor future

structural behavior. As discussed above, the assessment may be to do nothing more than extend investigation of the structure based on conventional methods, alternatively.

The Figure 2.8 showed scheme where a conventional investigation or particular site inspection may fulfill conditions within the scope of a global consideration of an ASR-affected structure analysis. Field monitoring, laboratory testing, including guidelines in the management of affected structures is provided also in (CSA, 2000; FHWA, 2010). Mitigation methods with suggested repair solution are provided further in this thesis.

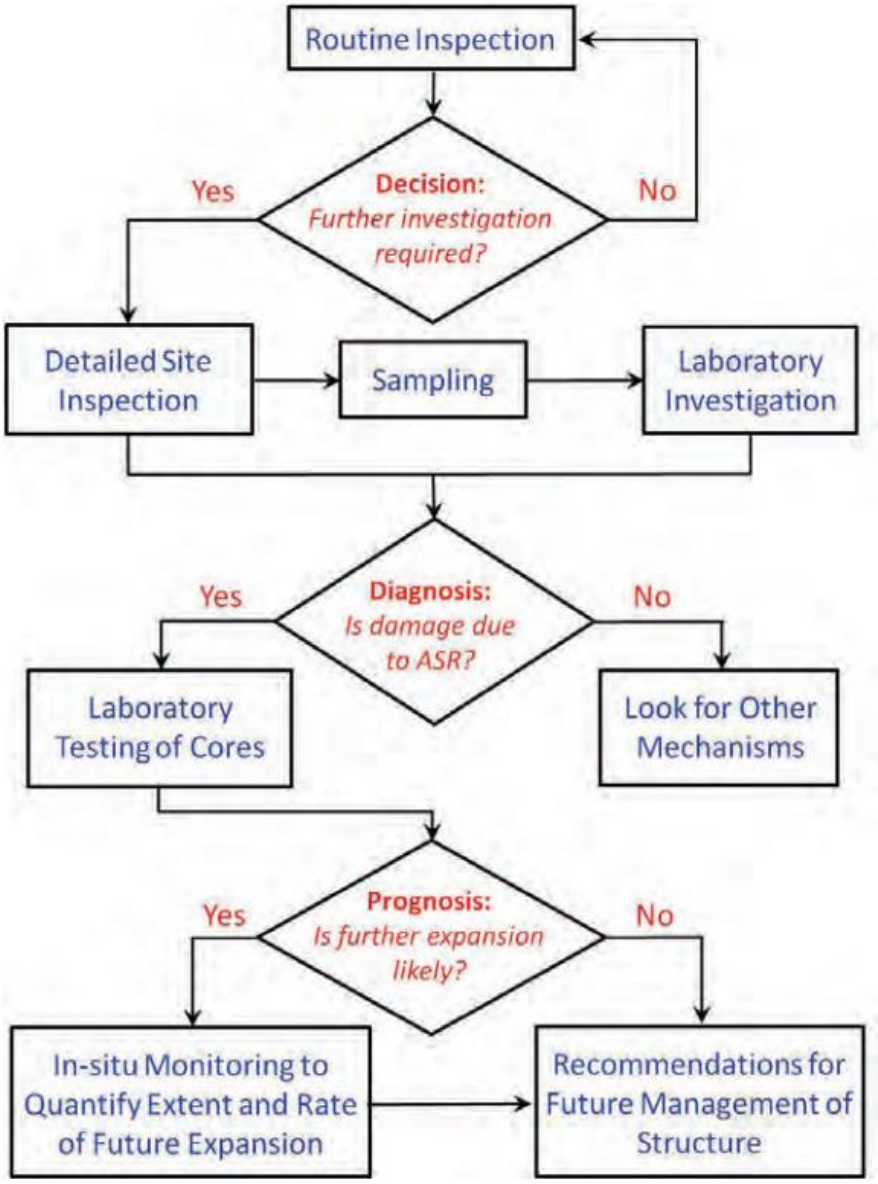

Figure 2.8. Flowchart showing stages in a comprehensive ASR investigation (Modified from CSA, 2000).

3 The Elgeseter Bridge

3.1 General Information

Elgeseter Bridge (Norwegian: Elgeseter Bru) is a bridge in the city and municipality of Trondheim in Sør-Trøndelag, Norway. The Elgeseter Bridge has been main entryway into Trondheim for hundreds of years. The first bridge there is mentioned in 1178. It was on this bridge that the battle between the birkebeiners and the baglers took place in 1199. Two years after the city was destroyed by fire in 1681, the Old Town Bridge (Norwegian: Gamle Bybro) was built. Until then the Elgeseter Bridge was the only connection across the Nidelva. The bridge has been reconstructed many times. In the 16th century it was for a period called "Gårdsbroen" and "Kanikke bro". After the Old Town Bridge was completed, the bridge to Elgeseter fell to decay, and collapsed. In 1863 a railway bridge was constructed at that location for the Trondhjem-Størenbanen railway line to Trondheim. This bridge was called "Kongsgårds bro". The railway bridge was converted into a roadway bridge in 1885, after the train station was relocated to Brattøra[50]. The Trondheim city council decided on 17 March 1949 that the new roadway bridge should be built. Elgeseter bridge was opened in 1951. Nowadays, it is part of the European route E6 highway which passes over the Nidelva river and connects Prinsens street in the Midtbyen area of Trondheim with Elgeseter street in the Elgeseter area of Trondheim in the south. Elgeseter Bridge was built in the period 1949 to 1951[49] and is a unique design for Norwegian construction in this era.

Figure 3.1 Elgeseter Bridge from east side *[fot. by Maciej Wisniewski & Krzysztof Wojslaw].*

3.2 Structure Description

3.2.1 Design

Elgeseter Bridge is an in situ cast reinforced concrete structure. Main carrying elements in this bridge are 4 longitudinal beams in spacing 5.5 m. Integrated reinforced concrete plate with variable thickness base on these beams. Total structural length is 200 m, consist 9 spans. First and last span have 21.25m width, but seven middle spans are 22.50 m each. Southern end the bridge is fixed by a 9 m long abutment structure and supported by a sliding support with expansion joint in the northern end. That was designed only one expansion joint in the entire structure with 200 mm wide. Total width is 23.5 m, carrying a road width of 16.5 m and pedestrian lane on each side of 3.5 m. Longitudinal beams are supported in eight rows with four columns each (with circular Ø 800 mm cross section). Columns are monolithic connected to the beams for all axes except the most northern row, which is mounted with steel plates fastened to the beams. The columns in each row are supported by eight 22-m-long foundation piles which are buried down in the riverbed. Each foundation beam is supported by 78 timber stocks 12–20 m long. The two abutments are supported by several 15-m-long concrete piles located above ground water level. Columns located in the river are protected against ice corrosion by 3-mm-thick steel protection caps at about 0.5 m above high water level.

The concrete used for the construction have shown to be made of alkali-reactive aggregates. This have during the years given expansion of the bridge deck (noticed e.g. as a closing of the expansion joint at the northern end and bending of columns) and extensive longitudinal cracking of the columns. In 2003, the Road Directorate rehabilitated all the northern columns. The major repair work was to move columns back to a vertical position which changed the static scheme.

3.2.2 Orientation

Elgeseter Bridge is coordinated according to normal practice in the Road Directorate. The layout of the Bridge shown in Fig. 3.2 may be described as follows:

Zone 1: southern abutment

Zone 2: first row of columns on the south bank; Columns: Column 1 is located to the west and column 4 to the east;

Zones 3–8: columns in the bed river;

Zone 9: last row of columns on north bank;

Zone 10: northern abutment.

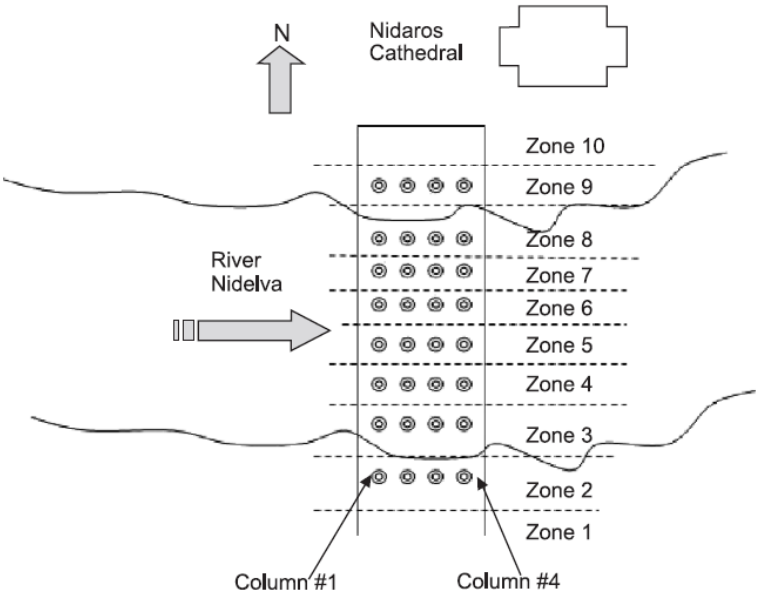

Figure 3.2 Coordination and layout of Elgeseter Bridge with zones and column numbers. V. Jensen / Materials Characterization 53 (2004) 155–170.

3.2.3 Aggregates, cements and concrete mixes

In this section most information come from the expertise report 'Elgeseter Bridge in Trondheim damaged by alkali silica reaction: microscopy, expansion and relative humidity measurements, treatment with mono silanes and repair' made by Norwegian Concrete and Aggregate Laboratory Ltd.

Elgeseter Bridge with its slender elements construction, was real a technological and a constructional challenge for the engineers in the 1950's. It was needed for uniform and high concrete strength required control system and a quality more demanding and appropriate than common practice have ever used in Norway. An intensive testing program was performed to evaluate the best aggregate combination ,aggregate type, cement ratio, type of cement and concrete mixture.

3.2.3.1 Aggregates

In fact and what is very interesting that marine aggregates, then commonly used in Norway, were not selected due to the risk of reinforcement corrosion. For the concrete mixtures in Elgeseter Bridge, the following aggregates were selected:

- Soeberg glaciofluvial fine gravel; grade 0–16 mm;
- Klett glaciofluvial coarse gravel from the river
- Gaula; grade 15–35 mm;
- Trolla crushed rock; 3–15 mm (to replace 4 to 16mm coarse gravel normally used).

For columns, the ratio fine/coarse/crushed aggregate was 50/28/22; for abutments, bridge deck, and foundations, the ratio was 48/29/23 (richer in the coarser grades).

3.2.3.2 Cements

In these times the Portland cement was produced in the two Norwegian cement plants "Dalen" and "Slemmestad". The results form tests with Norwegian standards gave less compressive strength when compared with Swedish and Danish cements. Thereby, a new Portland cement mixture was developed and called Standard-S. Production was place at Dalen factory especially for demand of the Elgeseter Bridge construction. This type of cement contained more gypsum and was more fine grained compared to normal standard cement produced in the 1950s. Still unknown is exact amount of gypsum that was used to this production, but the total sulfur content was probably higher than required by the Norwegian standard. The alkali content is also unknown, but was probably higher than 1 wt.%.

3.2.3.3 Additives

To reduce risk of separation, improve the mixing, and improve resistance to frost, which is important for columns in the river, air entrainment was added to all concretes used in this structure. Test results of concrete mixtures with and without air treatment have shown that concrete with 4.2% air voids is frost resistant even after 200 freeze-thaw cycles. We can say that structure is strongly resistant for frost damage, because any damages has not been observed in any structural elements of Elgeseter Bridge up to the nowadays. From the other side an air entrainment reduced the compressive strength of concrete by 6% for each 1% of added air-void volume. This must be compensated by increasing the cement content or by lowering water/cement ratio. As a final solution, an air-void volume was reduced to about 3% in the final concrete mixes.

In the Table 1 concrete proportions used for Elgeseter Bridge are shown. The material compositions of abutments and beams (concrete quality A) are valid values from the construction work on beams (between columns 5 and 6). The values of columns (concrete quality AA) and foundations (concrete quality A) are accepted values calculated according to Norwegian standards and from the requirement given in the concrete work description.

Concrete proportions of bridge components

Materials/parameters	Abutments and beams	Columns[a]	Foundations[a]
	Quality A	Quality AA	Quality A
Fine gravel (kg/m^3)	888	926	926
Coarse gravel (kg/m^3)	538	518	518
Crushed rock (kg/m^3)	426	407	407
Cement (kg/m^3)	350	450	400
Water/(active) (kg/m^3)	178	180	180
Water/cement ratio	0.51	0.40	0.45
Air (%)	2.9	3	3
Density (kg/m^3)	2380	2482	2432
Construction concrete (m^3)	3150	200	450

Table 1. Concrete proportions used for Elgeseter Bridge.

The Norwegian standard valid in these times required twenty eight days for curing maximum compressive strength values. For the two grades of concrete, these are as follows:
Concrete quality AA: 39.6 MPa;
Concrete quality A: 31.9 MPa.

Norwegian standard NS 427 states that 90% of test results with 100-mm cubes meet these strength requirements. The relationship between water/cement ratio and strength exhibits large scatter and some variation. The variation is the result of adjustments to mixing proportions made to obtain minimum strength requirements specified in the standard. The number of tests, average compressive strength (after the 28-day curing cycle) and calculated variation coefficient are given in Table 2 below.

Average 28-day compressive strength and variation coefficient

Structural elements	Number of tests	Average compressive strength (MPa)	Variation coefficient (%)
Abutments, plate, beams	37	34.2 (35.7)	12.3 (7.5)
Foundations	4	39.1	7.1
Columns	22	40.8 (43.4)	16.2 (10.6)

Parentheses are exclusive results from July 15 to September 12, 1950.

Table 2. Table shows three different groups of concrete components.

3.3 Structural Damage - Collected Data

Elgeseter Bridge is probably the most thoroughly investigated concrete structure in Norway that has suffered from Alkali–Silica Reaction (ASR). Before year 1990, significant reduction of the single expansion joint in the road plate and cracking in other concrete elements were observed. In the early 1990s, when ASR was accepted in Norway as a common

deterioration process in concrete structures, a reasonable explanation was provided for damage to the bridge. This thesis in this section gives brief overview for collected data with a chronological order of bridge damage construction, materials, concrete degradation.

Field inspection in 1989

In 1989, Trondheim municipality (the owner of Elgeseter Bridge) carried out field inspections of several concrete bridges in Trondheim, including Elgeseter Bridge, with the aim to determine actual condition and repair needs [52]. The following statement is quoted from the report:

The expansion joint was repaired in 1985 with epoxy concrete but is today (1989) damaged with resultant ingress of water to the abutment and the shaft bearings supporting the beams. Moreover, the expansion joint is at the end of its life (observing that the width of the joint is approaching zero). A few cracks were observed in beams and road plate. In two columns rust and concrete scaling were observed. Numerous shrinkage cracks were observed on upstream faces of columns. Due to movement of the Southern abutment, cracks up to 10 mm wide were present in walls and roof. Generally, the bridge was in good condition. However, repair work was recommended to be carried out within 5 years. Cost of rehabilitation of columns, girders and beams was calculated to be 6.8 M NOK.

Field inspections in 1990

Because ASR was recently under investigation as a concrete problem in Norway, the road authority responsible for maintenance and functionality of the bridge ordered an assessment of ASR as the possible cause of damage. Therefore, a field investigation was carried out in 1990 [53, 54]. The following observations were reported:
Map cracking typical of ASR occur on southern faces of several columns and the western girder. Long vertical cracks occur in all of the columns, some with crack width up to 1.1 mm. The cracks occur mostly on western faces of columns. Some cracks can be followed from ground level up to the beams (more or less continuous for 10 m). Vertical cracks occurring in beams are probably caused by mechanical movement of the bridge. Inspection of the northern expansion joint revealed that in some places its width was less than 10 mm. Two processes, either separately or collectively, were proposed to explain the movement of the bridge and concomitant reduction of the 200-mm-wide expansion joint:

1. ASR has caused expansion of the beams and the road plate. The expansion of the 200-m-long beams/plate should be ~0.095% after 40 years (i.e., +190 mm).
2. Land movement of abutments has reduced the expansion joint width. The field investigation suggested that ASR could be the reason for observed cracking of the bridge. Core samples were collected for laboratory tests and further documentation.

Laboratory investigations, 1990 and 1991

Three cores with 100-mm diameter and 300–400 mm long were taken from the following structural elements:

- Core 1: from Column No. 2, Zone 9 (see Fig. 3.2 for location);
- Core 2: from Column No. 3 in Zone 9 (see Fig.3.2 for location);
- Core 3: from the western face of a girder at the gangway and about 3 m from southern abutment.

The cores were drilled horizontally into the columns at approximately 1.5 m from the ground. Microstructural analysis was carried out on polished slabs and thin sections impregnated with fluorescent dye. White gel precipitation in air voids and cracks, dark rims around coarse aggregates and cracked aggregates were observed in all the cores. These observations indicate the presence of ASR. The laboratory investigation revealed that deleterious ASR occurred in all the cores. Therefore, it is most likely that ASR caused the observed cracking and expansion. The reaction product inside the sandstone is composed of extremely small cryptocrystalline plate-like crystals. Near the interface with the cement paste, the reaction product transforms into an amorphous gel with shrinkage cracks, as indicated in the figure 2.4 The microstructural study identified the following reacted rock types:

- Sandstone and greywacke (sedimentary rocks);
- Mylonite (cataclastic rock);
- Phyllite (low grade metamorphic rock);
- Fine-grained gneiss (high grade metamorphic rock).

All the reacted aggregates are siliceous rocks (composed of quartz and feldspar) and are today included in the Norwegian negative list of potentially alkali reactive aggregates. In 1990, sandstone, greywacke, phyllite and fine-grained gneiss were known to be potentially alkali reactive internationally [53]. Mylonite and other types of cataclastic rocks (e.g. cataclasite), which have caused deleterious ASR in several Norwegian concrete structures, were first described to be potentially alkali reactive in Norway [53].

Only feldspar survives the process of cataclasis. Classification system was developed by the author [53], namely ,,% cracked aggregates and cracks in paste". The results are obtained by counting aggregates containing cracks and aggregates where cracks run into the cement paste (significant for ASR) as well as number of cracks in the cement paste. This has also been confirmed after more than 50 years' service life. In columns, the water/cement ratios were measured to be 0.35–0.40, which is in agreement with the concrete mix certificate.

In situ measurements

A survey made by Post-doctoral project in 1998 and 1999 which had aims to map the crack pattern in all the columns of Elgeseter Bridge, as well as tests with three monosilane types. A survey was carried out as part of a project in cooperation with the Road Directorate [55].

The main aim was to record cracks in all the Elgeseter Bridge columns located both on the riverbank and in the river. Crack widths were measured 800 mm above the steel protection cap with a crack gauge, and the circumference of columns with a tape measure. Results have given important information on crack widths, number of cracks in columns and distribution of cracks. The data show that crack widths vary from 0.05 to 3 mm, and the number of cracks in columns varies from 5 to 19.

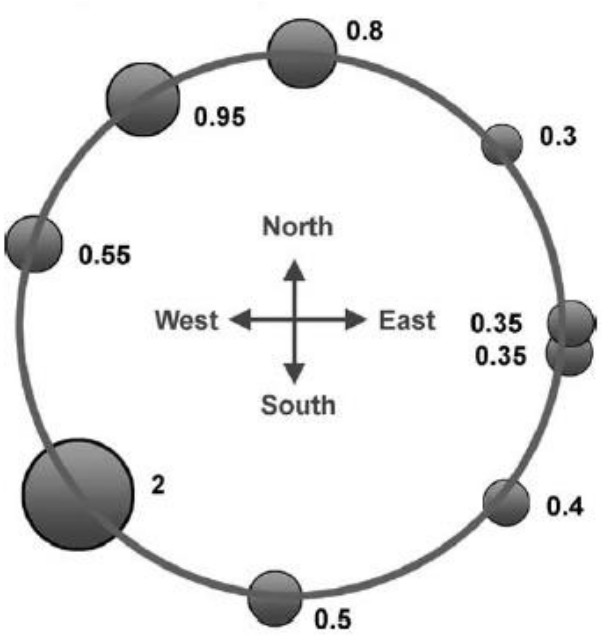

Figure 3.3 Example of crack distribution description in column 1 in Zone 2 about 1 m above ground level. Filled circles are individual cracks with different sizes and numbers are crack widths in mm. So-called Bird's eye view.

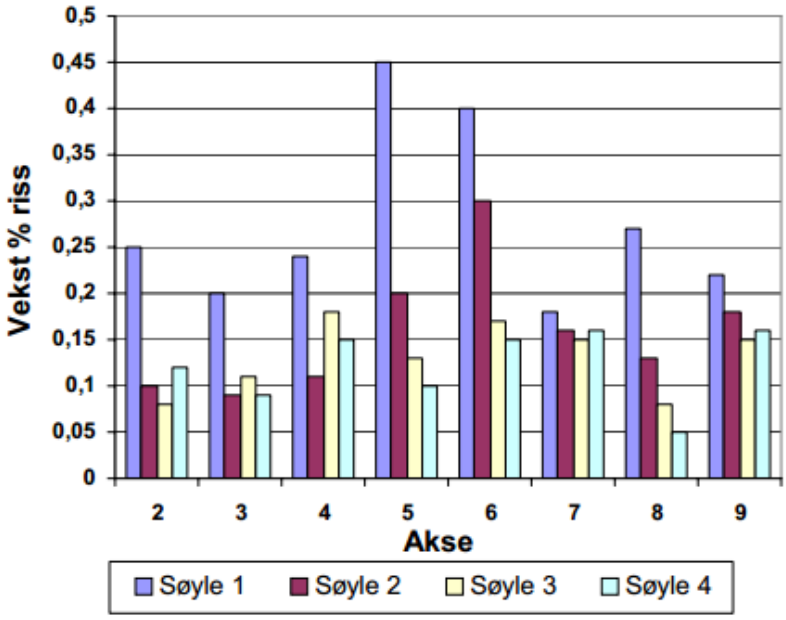

Figure 3.4 Shows expansion data for all the columns in Elgeseter Bridge. Note that the highest expansions occur in columns located in the most westerly row of columns (Column 1) and in the middle of the river (Zones 5 and 6).

Estimations of crack expansions in columns showed highest expansions in columns located most westerly (Column 1) and in the middle of the river.

Undertaken repairs which changed the structure

During to the reduction of the expansion joint to near zero in 2003, rehabilitation of the bridge was urgently needed. It was possibly that expansion of the road plate and beams due to ASR has caused the reduction of the expansion joint, but land movement of the abutments could be another explanation. However, measurements of the inclinations of the northern columns together with the occurrences of ASR in beams and plates suggested ASR to be the main causes of the reduction of the expansion joint. Where expansion of the road plate and beams was caused by ASR only, the road plate and beams should have extended about 200 mm over their 200-m length, i.e., ~0.1% in 50 years.

Moreover, because columns were fastened to the beams, the upper part of the most northern of the columns has moved to the north (possibly 150–180 mm) and was not vertical. Where columns were inclined, the bearing capacity of the bridge was reduced.

If this movement would be allowed to continue, there was a real risk that the columns will fail under tensile stress that will occur on one side. Hence, in 2003, the Road Directorate renovated all the northern columns in Zones 7, 8 and 9 on the bridge. The major repair work was to move columns back to a vertical position. A special steel construction was made to support the beam before demolishing the upper 1m of the column by mini-blasting. A Danish technique was used. The reinforcement was then cut and the column was moved back to a vertical position. Reinforcement was then welded back to the beam and the upper part of the column remolded with concrete.

Figure 3.5 shows the upper part of column 3 in Zone 7 where the concrete has been removed. Note that not all reinforcement was welded back due to rehabilitation[56]. *[fot. by Maciej Wisniewski & Krzysztof Wojslaw].*

3.4 Structural damage - our investigation

In a matter of conducting our inspection of the bridge we noticed a couple of new phenomena. Major signs of alkali silica reaction with combine with other deterioration process were found in columns, which were extensively cracked. The ASR effects were stronger in the columns (zone 2, 3, 4, and 5 in Figure 3.2) rather than in the external beams and external parts of a pavement slab. This can possibly be explained from the different confinement effects, induced passively by the reinforcements and actively by the loads. The same conclusion could be used to explain the swelling redistribution concept in slab. We observed large longitudinal crack in slab in zone 9 between column #3 and column #4. Also we found the explanation for characteristic phenomenon that in the internal beams are cracked in the distance of 4-5 m from the support.

Inspired by these observations, we performed an extensive experimental numerical simulation and calculations to prove that. Furthermore modelling approaches linear and non-linear analysis of columns has been developed. The material model for structural analysis is based on the coupling between the chemical and mechanical loading and aims to be a complementary tool to be used in a structural assessment procedure. The experimental results regarding the mechanical tests on the Elgeseter Bridge are helpful data for the validation of the model.

3.4.1 Columns

The damaging effect of a swelling ASR gel appears to be strongly influenced by compressive stresses in columns, as reported in literature. The coupling effect between chemical and mechanical loading on ASR damage is a key point for testing this hypothesis. The swelling process of concrete affected by ASR appears to be characterized by an intrinsic

This is reported in literature by Larive [57]. The essential is that swelling process is characterized by anisotropic behavior in concrete affected by ASR. According to observation in that report a sample in free expansion condition prefers to swell in the direction parallel to the casting direction; the expansion in this direction ranges from 1.3 to 2.8 times the expansion in the perpendicular directions. The same case exists in columns in our construction.

ASR occurs with other deterioration process in columns. On the Figure 4 the phenomenon of ASR and steel corrosion is shown. This allowed us to assume that the embedded reinforcement of the columns is reduced and more exposed to moisture from rain and steam from the river. This leads to rapidly penetrate the concrete cover and increase the

probability of occurrence additional dangerous phenomenon in the structure also increases initiation rate of corrosion in steel.

Figure 3.6 ASR in combination with corrosion of embedded reinforcement processes in zone 2-5. *[fot. by Maciej Wisniewski & Krzysztof Wojslaw].*

3.4.2 Beams

We observed a characteristic phenomenon that in the internal beams are cracked in the distance of 4-5 m from the support. Cracks occur almost within each axis. By the consequences related to the expansion of concrete from the external parts of bridge - internal beams are subjected to tensile stresses.

Through the inspection of the available archival drawings we noticed that the design of the reinforcement has disadvantages. In the recurrent cross-section around of 4-5 m from the support there is a gap in the reinforcement. It is the location of anchoring the upper and lower rods.

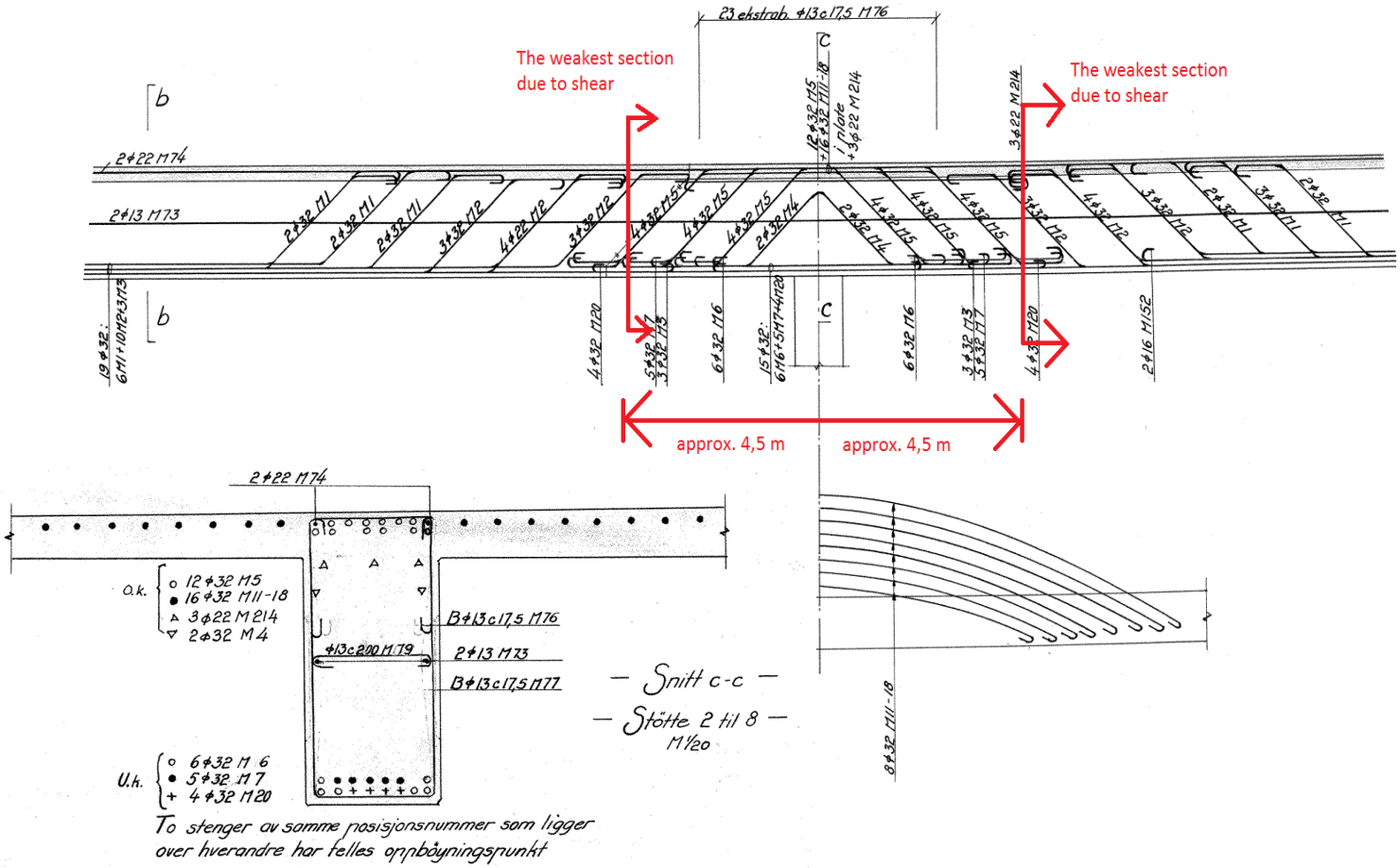

Figure 3.7 Cross sections of the reinforcement beams.

Stresses in the concrete exceeds the allowable value of tensile as effect of combination of tensile membrane forces, shear forces and also as effect of influence of these weakest points, hence the shapes of cracks in the is not typical as for cracks caused by bandings moments

We also suspect that during the performance of construction reinforcement with ribs 32mm of the beams was impossible to bend correctly on building site as it is shown in the drawings.

Exception is cracks in the internal beams between the axis 1 and 2. At this point, the shape of the cracks is typical for bending. Later in this presentation will be show that this place has the highest bending moments that effect on the shape of the cracks.

3.4.3 Slab

During observation we also noticed very long longitudinal scratches deck slab. Figure 3.8 shows the place where the crack occurred. Very characteristic in this place is that the crack occurs almost exactly at the edge of ASR infection. Crack also passes through the filters were installed in the slab drainage system. This allows us to assume that the crack is in a weakened section through filters and take place in a cross-section with a large difference in normal forces coming from the expansion of the infected concrete portion.

Another explanation can be based on the example that tensile concrete specimens with the same aggregate size show, as well known, that the tensile strength is lower along the casting direction. This suggests that the distribution of pores with various shapes and orientations determines both the direction with the weakest tensile strength and the preferred expansion direction. Before microcracking occurs, the swelling is nearly isotropic. Afterwards the gel expansion will induce the propagation of the cracks in the weakest zone (perpendicular to the casting direction), which will mutually influence the further swelling. In conclusion, anisotropic cracking resulting from anisotropic strength properties influences the anisotropic expansion. The same conclusion could be used to explain this case that the swelling redistribution in slab. In specimens subjected to uniaxial compressive loading or lateral constraining the imposed expansion is lower in the restrained direction. Once again the gel expansion induces the crack propagation in the direction which requires less energy dissipation. When the constraints are applied in the lateral direction the gel tends to expand along the longitudinal direction (Fig. 3.8)

Figure 3.8 *Cracks in slab in zone 1 [fot. by Maciej Wisniewski & Krzysztof Wojslaw].*

4 Finite element analysis background

In the engineering society FE analysis provides the opportunity of finding relatively exact results for complicated structures in the most easiest way. That may perform some crucial choices which are obligatory. There are many possibilities to create a FE model; thus it is important to have knowledge what kind of response is expected from the structure that is of interest. Furthermore, that is necessary to make some idealizations of the structure during process of modeling. Before modeling it is mandatory to know the assumptions and precondition of the theory behind the components which will be in structure. Moreover, selections in the process, such as geometry, boundary conditions and mesh density, have influence on achievement a realistic model of structure. In addition, in order to determine a proper model, materials models and element types have to be also wisely and carefully chosen.

4.1 Types of elements

4.1.1 Beam elements

These elements are based on the so-called Mindlin-Reissner theory which does take shear deformation into account. Unlike the classical beam elements of class-I and class-II, the class-III beam elements are based on an isoparametric formulation which assumes that the displacements and rotations of the beam axis normal are independent and are respectively interpolated from the nodal displacements and rotations. Because the displacement interpolation of class-III beams is compatible to the continuum elements they are very suitable for connection to those types of elements. Another advantage of these elements compared to other classes, is that they may be curved due to the fact that they have more than two nodes. The primary strains of the beams are:

- Green-Lagrange strains

$$\varepsilon = \begin{Bmatrix} \varepsilon_{xx} \\ \gamma_{xy} \\ \gamma_{zx} \end{Bmatrix} \quad \text{with} \quad \varepsilon_{xx} = \frac{du_x}{dx} \quad \gamma_{xy} = \frac{du_x}{dy} + \frac{du_y}{dx} \quad \gamma_{zx} = \frac{du_x}{dz} + \frac{du_z}{dx}$$

- Primary stresses

$$\sigma = \begin{Bmatrix} \sigma_{xx} \\ \sigma_{xy} \\ \sigma_{zx} \end{Bmatrix}$$

4.1.1.1 Class-III beams

The CL18B element (Figure 4.1) is a three-node, three-dimensional class-III beam element. Basic variables are the translations u_x , u_y and u_z and the rotations φ_x , φ_y and φ_z in the nodes. The interpolation polynomials for the displacements can be expressed as:

$$\left.\begin{aligned} u_i(\xi) &= a_{i_0} + a_{i_1}\xi + a_{i_2}\xi^2 \\ \phi_i(\xi) &= b_{i_0} + b_{i_1}\xi + b_{i_2}\xi^2 \end{aligned}\right\}$$

i = x, y, z

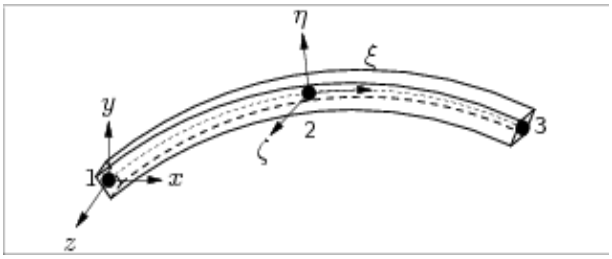

Figure 4.1 CL18B - curved, 3 nodes, 3-D.

Due to these polynomials the strains vary linearly along the center line of the beam. There are 2-points Gauss integration scheme along the bar axis [63].

4.1.2 Curved shell elements

The curved shell elements are based on isoparametric degenerated-solid approach by introducing z*ero-normal-stress.* This shell hypotheses assumes that the normal stress component in the normal direction of a lamina basis is forced to zero: $\sigma_{zzl(\xi,\eta,z)} = 0$. The element tangent plane is spanned by a lamina basis which corresponds to a local Cartesian coordinate system (x_l, y_l) defined at each point of the shell with x_l and y_l tangent to the ξ, η plane and z_l perpendicular to it.

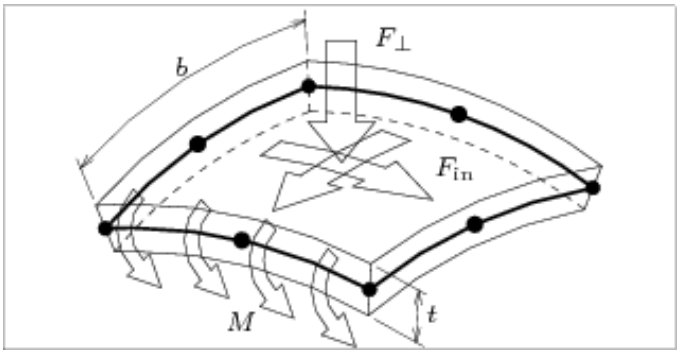

Figure 4.2 Curved shell elements.

The in-plane lamina strains ε_{xx} , ε_{yy} and ε_{zz} vary linearly in the thickness direction. The transverse shear strains γ_{xz} and γ_{yz} are forced to be constant in the thickness direction. Since the actual transverse shearing stresses and strains vary parabolically over the thickness, the shearing strains are an equivalent constant strain on a corresponding area. A shear correction factor is applied using the condition that a constant transverse shear stress yields approximately the same shear strain energy as the actual shearing stress.

Five degrees of freedom have been defined in every element node: three translations and two rotations. Force loads *F* may act in any direction between perpendicular to the surface and in the surface. Moment loads *M* should act around an axis which is in the element face. To avoid shear locking and make results more accurate for the shear forces were used quadrilateral shell elements [63].

4.1.3 Stresses and forces in the curved shell element:

- Cauchy stresses
  Figure 4.3 shows these stresses on a unit cube in their positive direction.

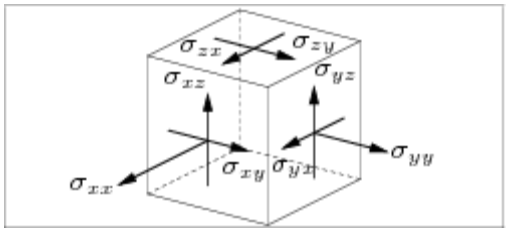

$$\sigma = \begin{cases} \sigma_{xx} \\ \sigma_{yy} \\ \sigma_{zz} = 0 \\ \sigma_{xy} = \sigma_{yx} \\ \sigma_{yz} = \sigma_{zy} \\ \sigma_{zx} = \sigma_{xz} \end{cases}$$

Figure 4.3 Cauchy stresses.

- Generalized Moments and Forces

Figure 4.4 shows these moments and forces on the infinitesimal part dx dy in their positive direction.

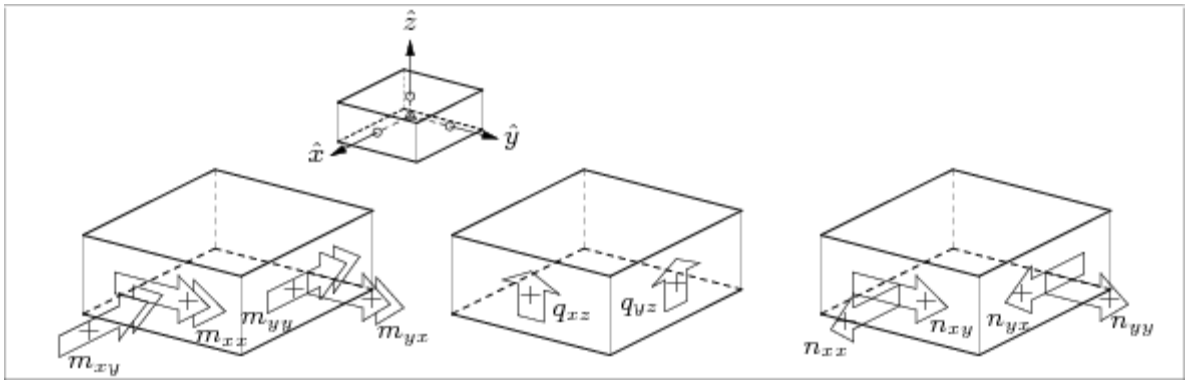

Figure 4.4 Generalized moments and forces.

4.1.3.1 Regular element

The basic variables of regular curved shell elements are the translations *u* and the rotations ϕ. The derived variables are the strains, the Cauchy stresses and the generalized moments and forces.

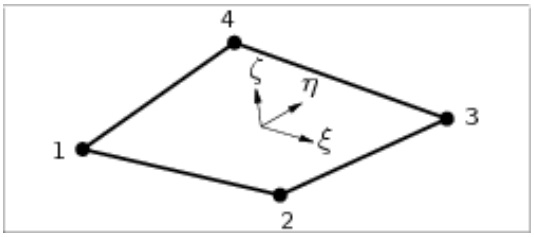

Figure 4.5 Q20SH - quadrilateral, 4 nodes.

The Q20SH element (Fig.4.5) is a four-node quadrilateral isoparametric curved shell element. It is based on linear interpolation and Gauss integration over the *ξ, η* element area. To avoid shear locking, which results in an excessively stiff behavior are modified the transverse shear strain fields. The polynomials for the translations *u* and the rotations ϕ can be expressed as:

$$\left.\begin{aligned} u_i(\xi,\eta) &= a_0 + a_1\xi + a_2\eta + a_3\xi\eta \\ \phi_i(\xi,\eta) &= b_0 + b_1\xi + b_2\eta + b_3\xi\eta \end{aligned}\right\}$$

Typically, for a rectangular element, these polynomials yield approximately the following strain and stress distribution along the element area in a ζ lamina. The strain ε_{xx} , the curvature κ_{xx} , the moment m_{xx}, the membrane force n_{xx} and the shear force q_{xz} are constant in *x* direction and vary linearly in *y* direction. The strain ε_{yy} , the curvature κ_{yy} , the moment m_{yy} , the membrane force n_{yy} and the shear force q_{yz} are constant in *y* direction and vary linearly in *x* direction. The integration scheme over the element area is 2×2 [63].

4.2 Types of material

There are various types of materials which are used for bridge structures, such as concrete, steel, pre-stressing tendons, etc. There are three materials properties which are used for a linear analysis: poisson's ratio, modulus of elasticity and the mass density. Nevertheless, there is large range of material models which can be applied in the diverse analysis types. The intention of the material model is to describe the connection between the deformations of the finite elements and the forces transmitted by them. According to that, material's deformation under external loads should be main criterion of choosing the material model. Concerning steel properties, this material can be modeled with Von Mises plasticity model with a yield criterion.

4.3 Types of reinforcement

Important part in the structural analysis is choosing the appropriate way of modeling reinforcement. Embedded reinforcement can be used for can be modeled reinforced concrete members, which adds stiffness to the model. Mother elements are type of modeling which embeds reinforcement in structural elements. This causes strengthened that concrete elements in the reinforcement direction. Reinforcements do not have degrees of freedom of their own. Material and geometry definition can be described individually, respectively to elements and reinforcements.

4.4 Boundary conditions

Significant role in the structural analysis is selecting the proper boundary. There are several simple assumptions of supports in a static analysis, such as fixed, pinned or roller. However, generally should be taken into account more factors, for example stiffness which has crucial effect on the analysis result. The boundary conditions basically define the restrictions on the degrees of freedom in the nodes. For definition of supported degree of freedom should be defined node number, type and direction. Modeling of supports in FE software demand a conscious thought of each translational and rotational component of displacement in order to simulate reality.

4.5 Meshing

The mesh size determines the precision and quality of the results in the FE software. That exist many different methods of generating mesh and majority of them are based on mesh density. In operation of the mesh generation, elements are defined respect to nodes and the connection between the geometry and mesh is established. Seeing that meshing has important role in the accuracy and stability of the numerical computation, checking quality is always strongly recommended. Control tools are generally available to supply information about elements and their desired shape. The mesh at certain areas of the geometry may need to be refined to improving the quality.

4.6 Types of Analysis

4.6.1 Linear Analysis

The fastest and easiest way to obtain the resultant forces and stresses on a structure subjected to a certain loading is execute linear analysis. The material is treated as elastic and isotropic which needs considerable simplifications and assumptions. Considering the complexity of the reinforced concrete as material the results are not reliable. In places

around supports and concentrated loads appear peak moments and forces. However, in reality, as the concrete cracks at very early stage, these high values will never reach. Thus, allows it to redistribution of the stresses along the structure. Moreover, the reinforcing steel will yield in the cracked tensile zones and let plastic deformations take place with even superior redistribution that is infraction of the elastic assumption. Then, due to the tough non-linear material behavior generate by cracking, selecting a linear method can carry on to wrong results.

4.6.2 Non-linear Analysis

Nonlinear stress analysis enables engineers to quickly and efficiently analyze stresses and deformations under general conditions. Namely, non-linear analysis is a simulation of the response of the structure subjected to increased loading. The main goal is to estimate the extreme load that the structure can carry before it collapses. Simple incremental analysis using non-linear formulations are used to calculate the maximum load. The analysis is sub-divided in increments and equilibrium is found for each increment using iteration methods. Therefore, providing real material and structural response the results are more exact. Since the stress redistribution, and failure mode can be considered, the non-linear analysis will be useful in comprehension the behavior of a structure. Awareness of the limitations is necessary and it is reasonable to validate the modeling method with test results [64].

5 Finite element modeling

The following chapter presents modeled construction in the FEM programs. The modeling process is put forward and verifications of the models by different methods. The main objective of this analysis was to model ASR loading which is applying on the external parts of the bridge. Thus, it is important to predict the horizontal displacements of the deck. Moreover, this involves showing distribution of shear and membrane forces which have a crucial influence on the cracking of concrete. It has been assessed design of the program, location of traffic loads, different in elements and considered various methods withdrawal of results. It forms a good basis for comparison for a study of two different modeling programs. Finally, a comparison is made and discussion of the results from models with different arrangements angle. All the reinforcement was modelled as embedded in curved shell elements as bar reinforcement. In finite element models with these elements, bar reinforcements have the shape of a line.

5.1 Finite element software

5.1.1 TNO DIANA

The name of the DIANA software comes from expression DIsplacement ANAlyzer and obviously is based on displacement method. Program does not bring limitations of the models geometry, thus that models can be set up very realistic. Reinforced concrete models are based on the precise geometry definition of reinforcements and concrete, the clear description of material failure of the steel reinforcements. We put a lot of effort learning program and improving models.

5.1.2 SOFiSTiK

The German company SOFiSTiK is Europe's leading software developer for analysis. The SOFiSTiK FEM Packages are customized solutions to fit all engineering application fields, ranging from 2D Slab design to 3D building and bridge design. All Packages provide the possibility of design according to Eurocodes and many other design codes, plus interactive Post-processing and 64-bit solver.

The entire geometry including boundary conditions are designed identically in both programs. The exception is the taking into consideration of beam elements. Model includes main girders and columns designed as beam elements. Plate is modeled as a mesh of shell elements. In SOFiSTiK, elements are strricte beam while in Diana beams are shell elements

arranged vertically. SOFiSTiK allows us to broader and more detailed analysis regarding the impact of live load vehicles.

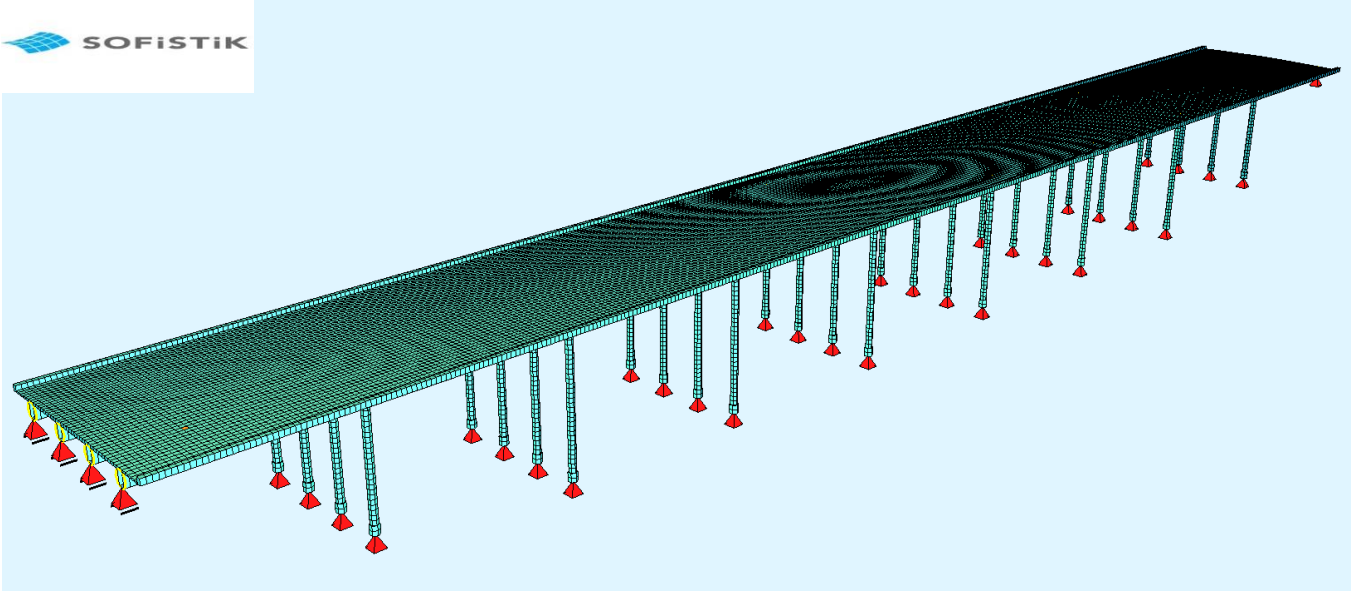

Figure 5.1 Visualization of the structure in Sofistic software. Characteristics: Number of nodes: 20232, Number of elements: 22980.

5.2 Modeling of the columns

In this chapter we focused on the analysis of the columns due to ASR loading. To prove that the reaction ASR also effects on cracks which show in the columns we decided to present the simulation of crack formation. It was assumed that cross section of the column works in two-dimensional plane strain. This is a rough simplification. However, the columns are rigidly attached to the main structure so this approximate approach is considered to be acceptable.

5.2.1 Geometry and FE mesh

Only quarter of column was taken into analysis. Radius of column is equal to 40 cm. Type of elements which were used: 411 nodes and 186 six-node triangular isoperimetric plane strain element (CT12E).

5.2.2 Boundary and load conditions

It was used two various boundary conditions for to different types of analyses. For linear analysis rolling supports were placed on the length 30 cm as show Figure 5.3. Outer part with a width of 10 cm has no loading and supports. In the non-linear analysis to reveal

reality of boundary condition, rolling supports were determined on the entire length of edges. Respectively were blocked movements on the horizontal edge in y-direction and on vertical edge in the x-direction. For crack modeling interface elements were used. Using expansion from temperature of value 0,1% we model ASR loading. In both cases we assumed that ASR reaction affect from the inner part of the column on the radius length equal to 30 cm.

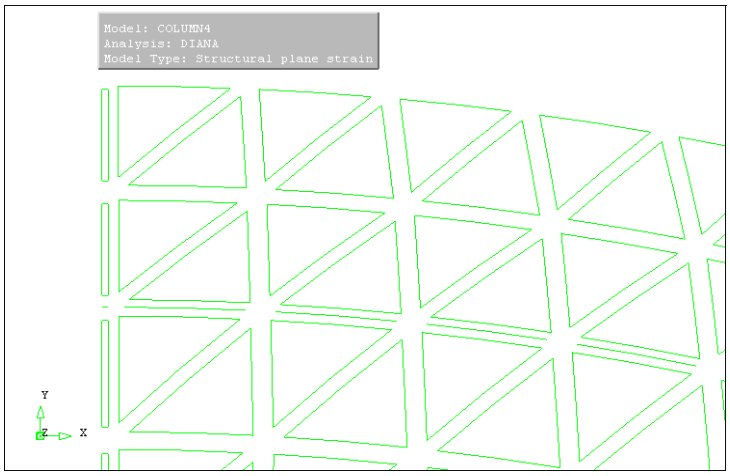

Figure 5.2 Detail of connection interface element with shell and plain strain elements.

5.2.3 Reinforcement

Thus, reinforced was modeled as infinity shell i.e. shaped line having a thickness which is small compared to length. Properties of the steel were established as St. 37 from Table 4. Connection of three different mesh elements which were: interface element, infinite shell and plain strain elements required careful and proper matching types of elements. In the Figure 5.2 it is show how this problem was solved.

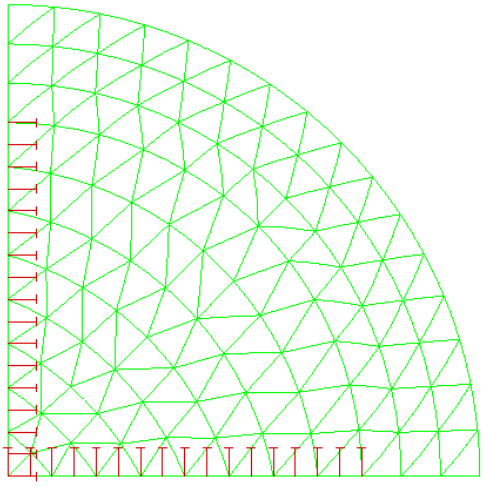

Figure 5.3 Mesh of quarter column.

5.2.4 Interface elements

For the crack interfaces we define a material with linear stiffness moduli:

- D_{11} = 1.0 x 10^8 N/mm^3
- D_{22} = 1.0 x 10^8 N/mm^3

We also specify the nonlinear material parameters for discrete cracking in the interface:

- tensile strength f_t = 2.4 MPa
- fracture energy G_f = 0.08 N/mm
- shear modulus after cracking G_{cr} = 0.001 MPa

5.3 Modeling of the bridge

5.3.1 Geometry

The main carrying elements of the bridge are 4 longitudinal beams wit spacing 5,5m between each other. Cross section of the beam is rectangular 80x143cm. On top there is an integrated concrete plate. The thickness of plat is variable. In the middle of cross-section is equal to 38 cm and constantly decrease to 15 cm. The bridge is made up of 9 spans. Total length of bridge is 200m with spans length 21.25m + 7x22.50m + 21.25m. Total width is 23.5 m, carrying a road width of 16.5 m and pedestrian lane on each side of 3.5 m. Each of the 4 longitudinal beams is supported by 8 columns with the height 15,5 m. Columns have circular cross section Ø 80 cm.

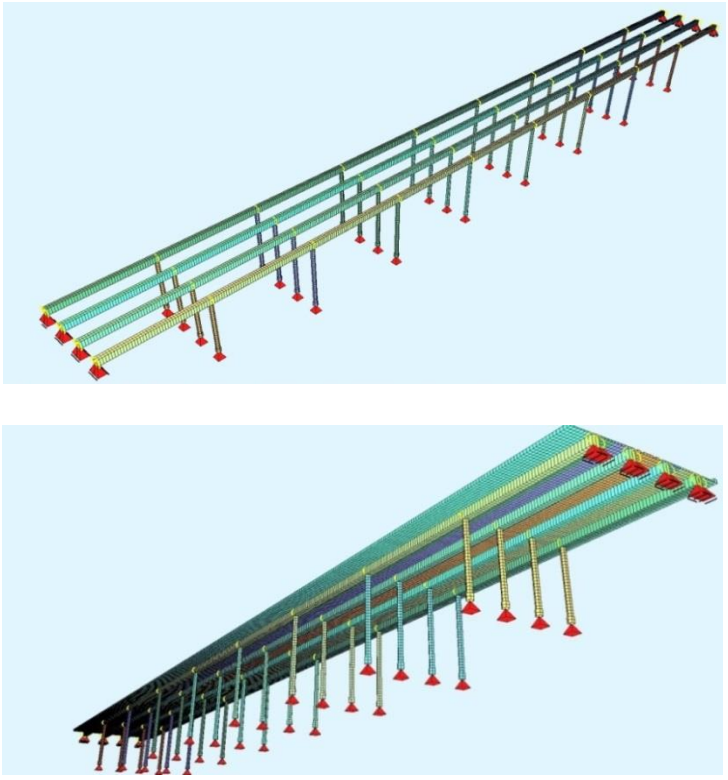

Figure 5.4 Visualization of the structure in Sofistic software.

5.3.2 Materials

5.3.2.1 Concrete

During the years large expansion of the bridge deck has occurred. The concrete used for the construction have shown to be made of alkali-reactive aggregates. Based on cuttings samples tested by SINTEF, the concrete used for the bridge deck consist of 350 kg/m^3 of cement. This is equal to a C25/B20 type concrete, having f_{ck} equal to 16.8 MPa and f_{cd} equal to 12 MPa. For a typical Norwegian type of concrete, the best estimates for E-modulus for load-reaction analyses may be estimated based on the rules from the former standard NS 3473.

This gives:

$$\text{C25 -> } f_{cck} = 20\ \text{MPa} \quad \text{-> } Eck = 9500 \times (20)^{0.3}\text{MPa} = 23\,300\ \text{MPa}$$

Laboratory test show that concrete columns consist of 400 kg/m^3 of cement. This is equal to a C30/B25 type concrete, having f_{ck} equal to 19.6 MPa and f_{cd} equal to 14 MPa. The properties of the concrete modeled in the FE analysis are presented in Table 3.

	f_{cd}	f_{ck}	E_{ck}	v	ρ	Type
	MPa	MPa	GPa	-	kg/m^3	
Deck	12	16.8	23,3	0.2	2500	C25/B20
Columnns	14	19.6	25	0.2	2500	C30/B25

Table 3. Concrete properties.

5.3.2.2 Steel

None of the information about used steel in the bridge has been found. Based on the ,,Betong - uarmert og armert" by Inge Lyse and N. J. Wiig, typical values for materials used at that time was found. The yield limit for St. 37 is 230 MPa, and 340 MPa for St. 52. The reinforcement in the bridge is steel rods without ribs, St. 52 for Ø32 mm and St. 37 for remaining reinforcement. The properties of the steel modeled in the FE analysis are presented in Table 4.

Type	f_{cd}	E_s
	MPa	GPa
St.52	340	200
St.37	230	200

Table 4. Steel properties.

5.3.3 Boundary Conditions

A correct modeling of the supports is important to imitate the actual structural behavior. The boundary conditions in Elgeseter Bridge are asymmetric. Thus, the south edge of the bridge is full fixed in the abutment. However, on the north end are 4 rolling supports, each for a beam. Movable support has blocked movements in the z-direction. Moreover, there exist 32 columns which all of them are fixed in the fundament with piles. All degrees of freedom were blocked in modeling this support.

5.3.4 FE Mesh

Mesh is an ordinary and simple mesh. Almost all elements have the same size throughout all bridge. It is not used a finer division round columns and traffic concentrated loads. All lines are divided into divisions that specify how many elements line should divided into in. The deck mesh elements are rectangular in size 0,5x0,5 m. It is shared so that mesh is satisfactory. It was used 27370 elements of a Q20SH as a shell element with 4 nodes. For columns were used 144 CL18B beam elements.

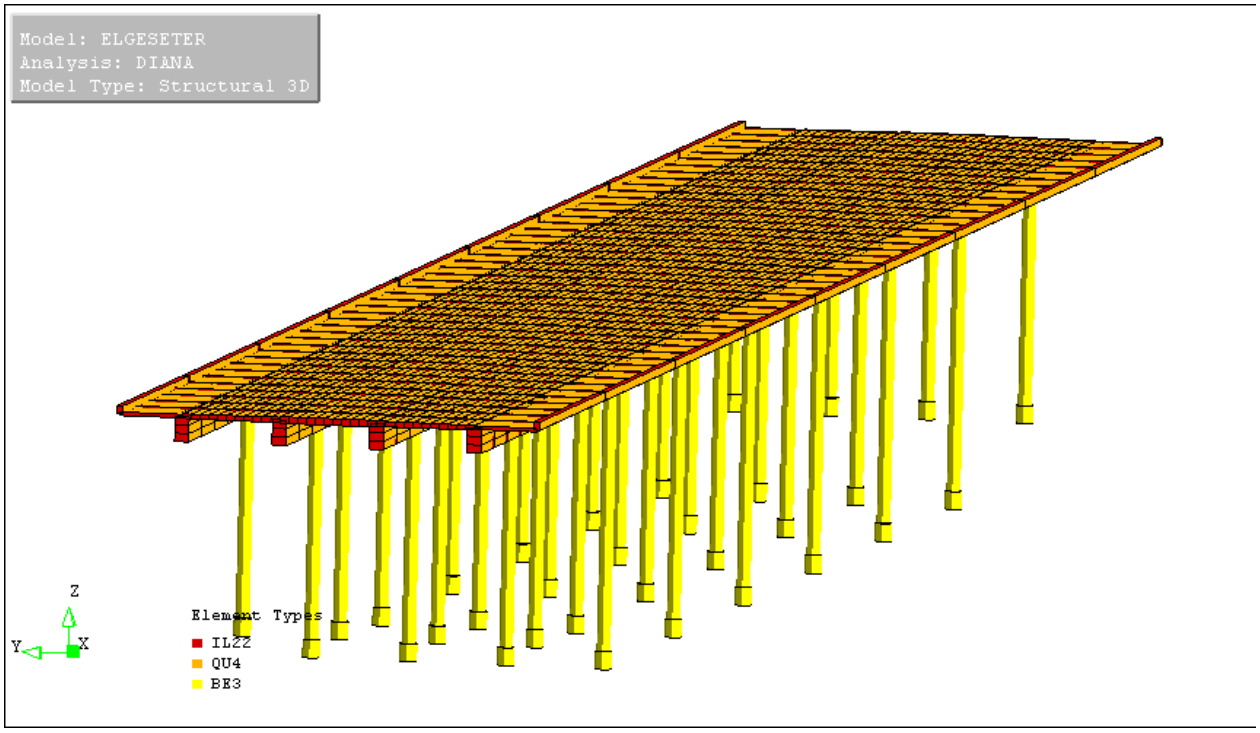

Figure. 5.5 Geometry of the bridge with shown elements types.

5.3.5 Loads

5.3.5.1 Self-weight

The self-weight was modeled as gravity to properly account for the variation of thickness. This load was determined based on the acceleration of 9.81 m/s2 and the density of 2500 kg/m3 for concrete.

5.3.5.2 Weight of equipment and surfaces

Pavement load

Bridge was design with 11 cm thickness of asphalt. After several reparation and maintenance of the pavement the thickness increases. Based on the measurements from April 2012 made by NPRA, thickness of asphalt layer is about 30 cm. This means that thickness has increased three times.
Thickness of layers:

- protective concrete 5cm
- asphalt 30cm
- isolation on the road 1 cm

asphalt:	0,30	· *25,0*	=	7,50	kN/m^2
protective concrete :	0,05	· *24,0*	=	1,20	kN/m^2
isolation:	0,01	· *14,0*	=	0,14	kN/m^2
				8,84	kN/m^2

Sidewalk surface

Thickness of layers:

- concrete pavement 6 cm
- stabilization layer 30 cm
- isolation on the pavement 1 cm

concrete pavement:	0,06	· *24,0*	=	1,44	kN/m^2
stabilization layer :	0,30	· *8,00*	=	2,40	kN/m^2
isolation:	0,01	· *14,0*	=	0,14	kN/m^2
				3,98	kN/m^2

Line load

Cornice 35,0 cm of high and 20,0 cm thickness
Cornice:$0{,}35 \cdot 0{,}2 \cdot 24{,}0 = 1{,}68\ kN/m$
Barrier: $1{,}00\ \frac{kN}{m}$, Curb: $1{,}10\ \frac{kN}{m}$

5.3.5.3 Live load

Choosing of the type of load we done according to ,,Håndbok 238 bruklassifisering - Instructions for classification of bridges and ferry docks in the public road network". Live load is placed on the bridge in the most unfavorable position in the longitudinal and transverse directions within the available transmission distance.

Vertical load

The classification of bridge to the classes:

• Bruksklasse 10 (Bk10)

Lasttype	Lastkonfigurasjon (*) H kN	Bruksklasser			
		Bk10	BkT8	Bk8	Bk6
Vogntoglast	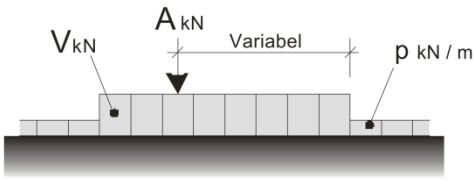 Aksellasten plasseres i ugunstigste stilling	A: 40	32	32	24
		V: 500	400	320	280
		p: 6	6	6	6

Tabel 5 Class of loading (including dynamic), *Håndbok 238 bruklassifisering.*

The concentrated loads, simulating vehicle wheels, were applied on the top of the deck on areas of 0.6 x 0.2 m each. The distance between the loads in the transverse direction was 2000 mm and in the longitudinal direction is placed in most unfavorable place for structure.

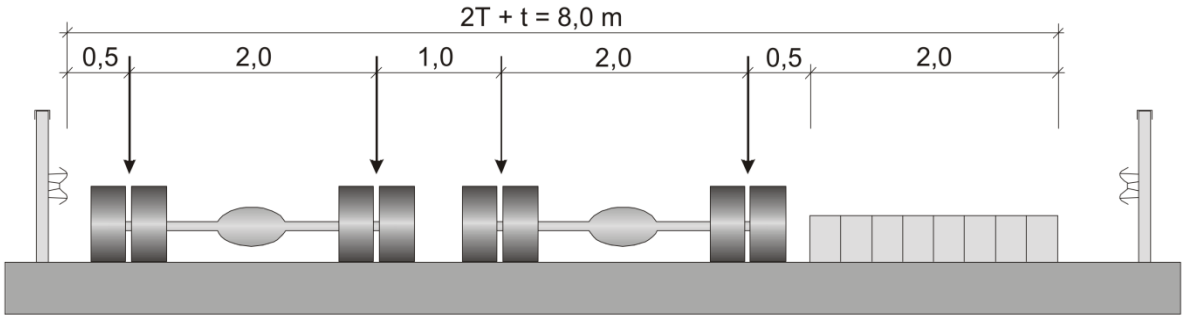

Figure 5.6 Locations of the loads in the cross section of the bridge, *Håndbok 238 bruklassifisering.*

Horizontal loads

Load B

This load comes from braking of vehicle and it is assumed to act on the bridge in longitudinal direction at the height of the road surface and can be simulated as uniformly distributed over the entire travel path width.

Brulengde	Bremselast (kN)			
	Bk 10	Bk T8	Bk 8	Bk6
= 10 m (B_1)	150	120	100	90
= 40 m (B_2)	300	240	190	170

Tabel 6 Value of horizontal load, *Håndbok 238 bruklassifisering.*

$B = 300\ kN$

Load S

This load appears when some of this cases happened:

- side impact ,
- asymmetrical braking of the vehicle,
- impact of skewed

Calculated on the basis of an arbitrarily placed horizontal load $S = 25\%$ of the braking load. The simultaneous occurrence of brake load and the corresponding vertical load. Side load is assumed to act perpendicular to the bridge's longitudinal direction and the height of the roadway[60].

$S = 0{,}25 * B$
$S = 0{,}25 * 300kN = 75\ kN$

5.3.5.4 Pedestrian and cycle load

Pedestrian and cycle path separated from the roadway by a curb should be load by distributed load $q_{ped} = 2\ \frac{\mathrm{kN}}{m^2}$

5.3.5.5 ASR loading

Our knowledge about applying ASR is largely based on very limited data. Mostly we use fact extension of the bridge deck on the moveable supports in the north direction. Figure 5.7 shows us changes of dilatation width during 60 years. Influence of the temperature has been omitted by measure width when construction has the same temperature each year (10°C). We can observe that changes are linear decrease. Value constantly tends toward 0. In the year 2004 when value of gap raised up to critical level 20 mm decided to change all dilatation system. Width of gap increased to 100 mm. Further monitoring of dilatation present reducing the diagram slope and slowing lengthening of the bridge. Based on these data, that the expansion of the concrete within 60 years was around 200mm, we can assume that the free expansion of concrete was 0.1%. We applied temperature load on the external beams and external parts of concrete slab. The same concrete expansion occurs in construction when we put load as a temperature gradient equivalent to 200 °C. We assumed that extension of the bridge external parts, are equal. However, to confirm this assumption should be carried out studies of the free expansion of the concrete used in this construction.

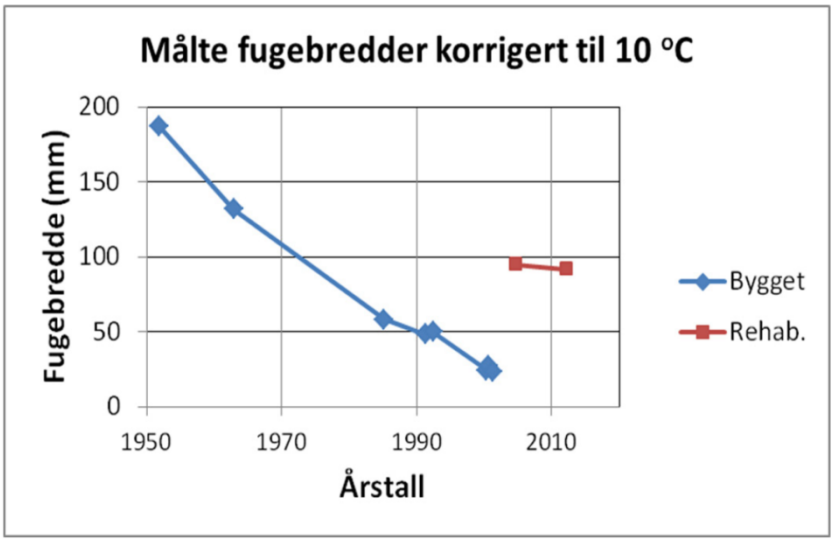

Figure 5.7 Dilatation measurements at the north end of Elgeseter bridge.
„Rehabilitering av brusøyler med alkalireaksjonsskaer. Feltforsøk på Elgeseter bru Sluttrapport."

5.3.5.6 Location of the live load

In Diana software to obtain the most unfavorable location of the movable force, we create the influence field. This influenced field was established to the one of surface element in internal beam. We take into account the element which is located 5 m from the column axe nr 7 for the reason that exactly in this component exists the widest crack. The result is graph which shows us the location of the unit load on the deck which will cause the greatest value of stresses (Sxx) in the beam element.

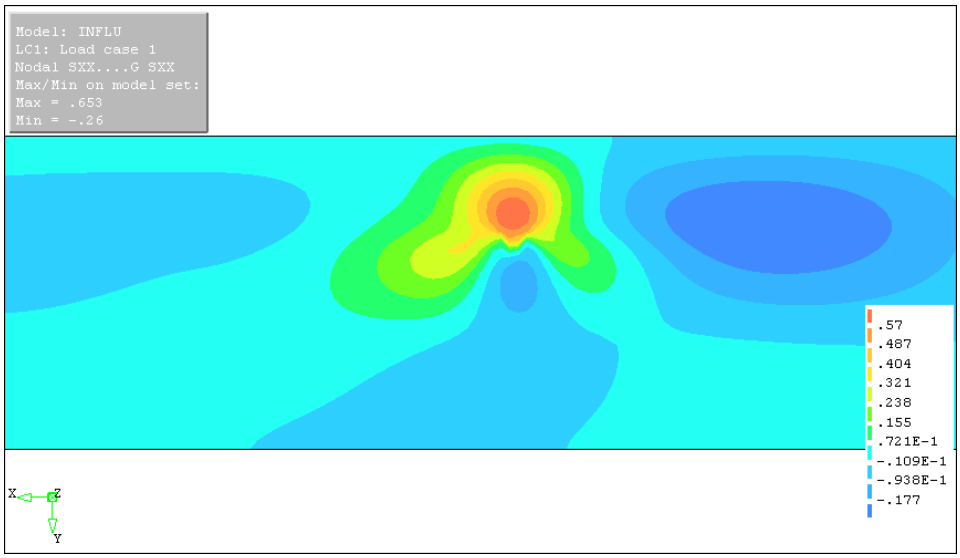

Figure 5.8 Influence field for stresses in X direction for the inner beam.

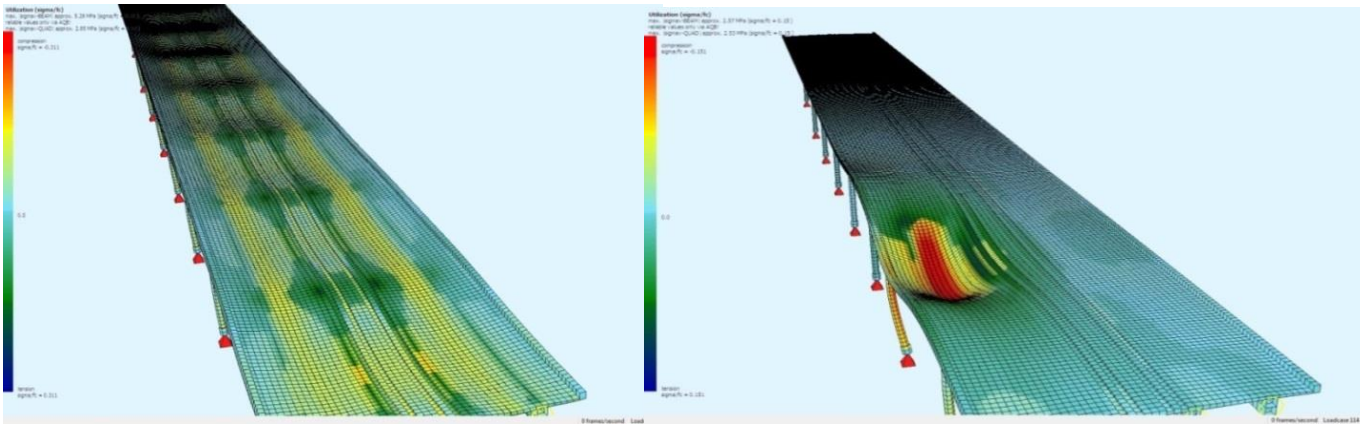

Figure 5.9 and **5.10** Visualization of the impact of live load on the bridge structure. Load case number 5 and 34.

Choose of the type of load we done according to ,,Håndbok 238 bruklassifisering Instructions for classification of bridges and ferry docks in the public road network" .Live load in SOFiSTiK is automatically placed on the bridge end calculated for every possible position in the longitudinal and transverse directions within the available transmission distance. In our case live load comes from vehicle is assumed to moving and act on the bridge in longitudinal direction in each 1 meter in each load case.

SOFiSTiK automatically calculates and generates the worst case load setting. Also calculate envelopes of bending moments shear end normal forces for initiated combination of load cases.

According to the Norwegian Standard for loads for the bridges, the safety factors adopted as the basic system of loads. For the Ultimate Limit State used γf values are summarized in the table below, while the safety factors for Serviceability Limit State adopted as a constant

γf = 1.00.

No.	**Types of loads**	**γ_f**
1	Self weight of construction	1,20
2	Self weight of construction according to no. 1, but as the effect of relieving	0,90
3	Self weight of non-structural elements, such as pavement, curbs etc. and live load	1,50
4	Self weight of non-structural elements according to no. 3, but as the effect of relieving	0,90
5	Forces caused by the influence of rheological	1,20
6	Loads caused by temperature changes and loads of braking and acceleration of vehicles.	1,30

6 Analysis and Results

This chapter show all procedures of analysis which have been done. Afterwards the results from linear and non-linear analysis will be presented. The expansion model for the column and bridge models are the same in the both cases.

6.1 Columns

6.1.1 Linear analysis

Linear analysis can be applied to the crack modeling. That is the simplest method which depends on boundary conditions. Calculations of this model show us the approximate size of crack in the free edges.

The deformation in the x and y direction is equal to 0,435 mm (Figure 6.1). Taking into account that this value is half of the crack, we can say that our crack width is approximately 0,87 mm. Compere with the existing cracks in the column we asses that our assumptions are acceptable.

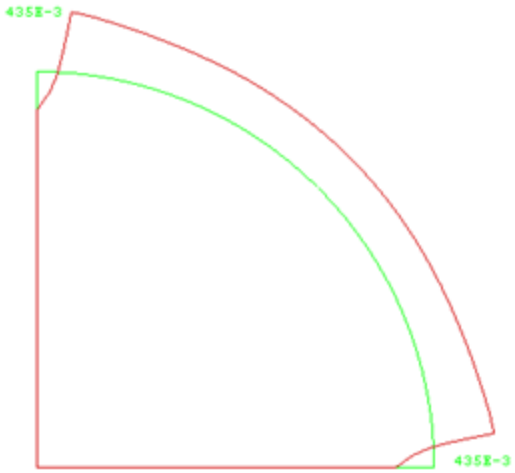

Figure 6.1. Deformation of the column.

6.1.2 Non-linear analysis

An existing crack can modeled discretely using interface elements, which allow an initial crack to open up when the normal traction on the surface of the interface element becomes tensile. Line interface elements are placed between two lines in a two-dimensional configuration. With these elements the interface surface and directions are evaluated automatically from the geometry of the element itself. Therefore, in the present study the existing cracks in the column are modeled using the discrete approach, which enables each individual crack to be modeled as

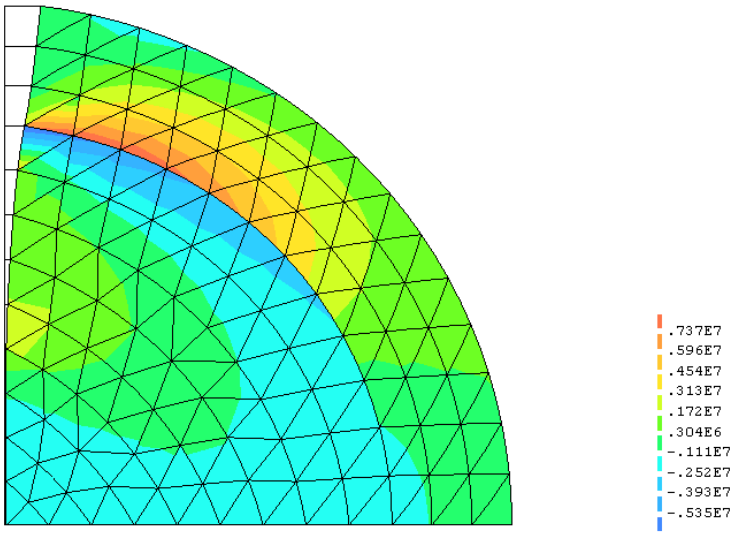

Figure 6.2. Crack opening without reinforcement.

an open crack. Nonlinear structural analysis has to be carried out, which includes crack analysis for the cracking activities that will occur under the presumed incremental time of temperature loading [62].

ASR loading was represented such like in the previous cases as temperature loading. Time steps were established as user specified sizes i.e. step size 0.25 and number of steps equal to 10.

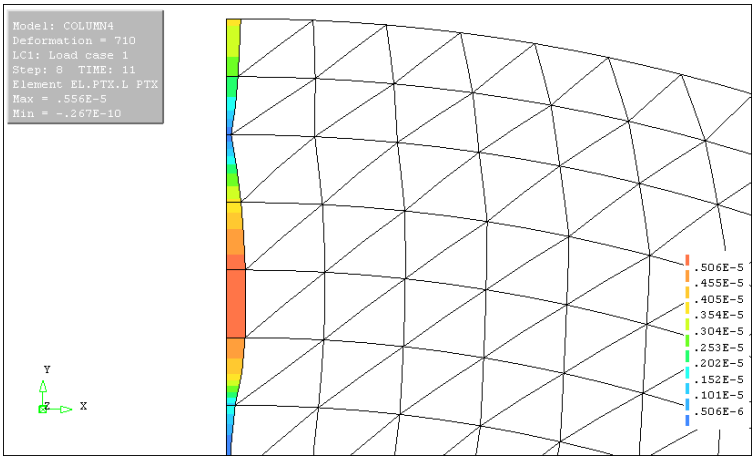

Figure 6.3 Crack opening with reinforcement.

The normal tensile stress in an interface element reached the interface failure stress $f_n > f_t$ so we can assume that element is to undergo damage and cannot carry any loads. The normal traction of the interface was equal to 2,4 MPa. In the figure 6.3 we can observe crack opening which is represented by 26 cracks of the integration points in the interface element.

Based on numerical studies, it is considered that the method may provide an effective way of assessing aging columns based on the crack conditions in concrete and the corrosion of steel reinforcement. Major repairs and renovation of columns must be taken because of the rebar corrosion. Water can easily penetrate concrete through the crack and aggravate reinforcement. In the following chapter solution and method of the repair will be proposed.

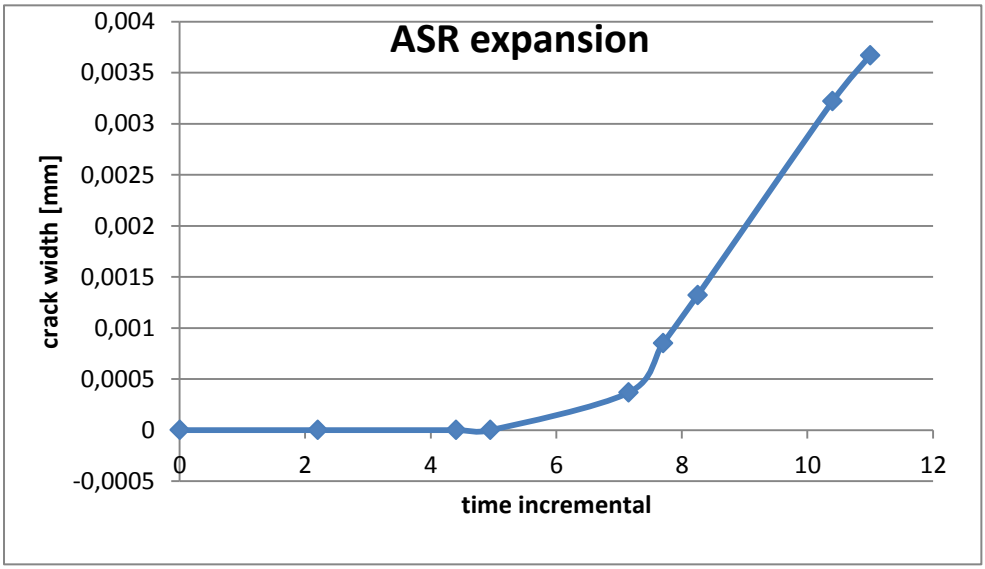

Figure 6.4 Graph shows relationship between ceack width and time.

Slip between reinforcement and the concrete

In our analysis we assume at crack can occur only in the vertical direction. This assumption is not sufficient, because crack can change direction near the bond with the reinforcement. Thus, in further analysis was taken into account bond slip between reinforcement and the concrete. For that has been used interface element placed along the concrete-reinforcement connection. The properties of interface element were established like in the previous case. In the figure 6.5 are presented stresses caused by ASR-reaction. However, any of the integration points along interface element cracked. Unfortunately, we expected cracks of integration points at least in few first elements.

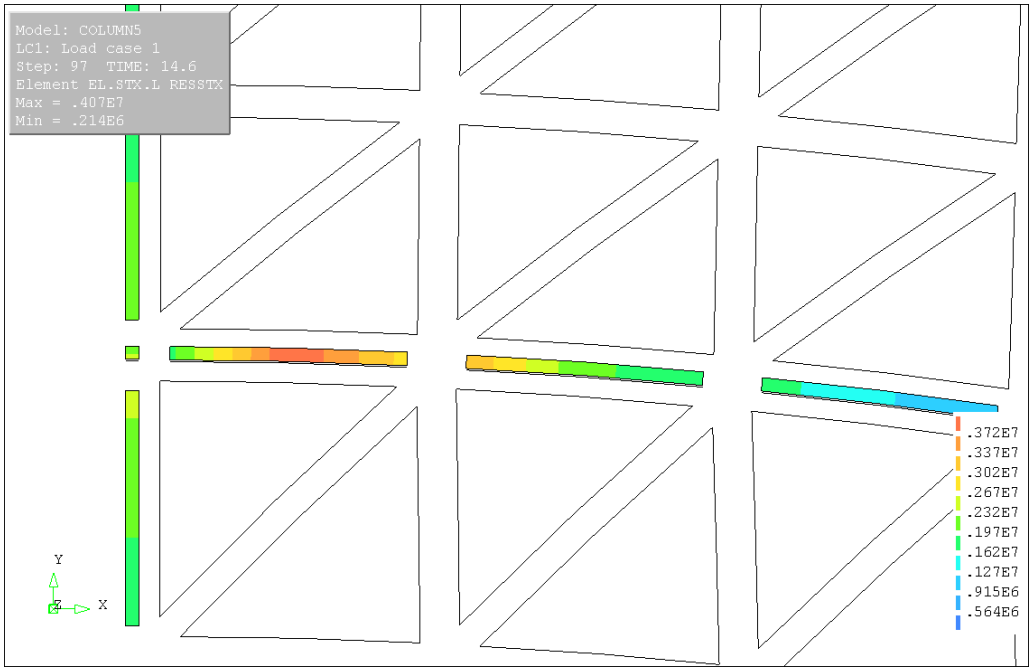

Figure 6.5. Stresses in the interface element.

This problem, in our opinion demands wider and deeper analysis. Horizontal crack which can be initiate close to orbital reinforcement of the column can chip off covering. That cam causes threat to the entire construction due to corrosion of the column reinforcement. We advise to pursuit further consideration in that topic.

6.2 Bridge

In this chapter, the results from analysis in Sofistic and Diana software will be presented. First, bending moment and the shear force distribution in the beams will be shown. Afterwards the results from Alcali-Silca reaction analyses approaches will be presented and compared. Crack pattern and yielding of reinforcement will be presented for a model with accurate shear distribution. At the end the validation and evaluation of the reasonability of the selected model is featured.

Superposition

The results which were calculated with the SOFiSTiK program are stored in the database. The superposition is made separately for each node and for each element or beam section. The task of the program is the determination of envelope for extreme values of the internal forces, displacements and support reactions.

The superposition according to the codes is done with safety factors and combination coefficients for actions are defined by arbitrary load cases. These load cases and combinations of them are superimposed to define an action effect. Whereby Sofistic finds the most unfavorable action effect and after applies the combination factors automatically. To achieve this, the superposition is done in two steps. In the inner step Sofistic finds the extreme value from different load cases of the action effect, and in a second outer process the action effects are combined.

The load cases to be superimposed may be defined unconditionally (e.g. dead load) or conditionally (e.g. live load). In a conditional superposition each load case is only applied if it has an unfavorable contribution.
Each load case is multiplied with scaling factors which are defined above according to Norwegian Standard. For a superposition of linearly analyzed load cases an envelope is formed. The results are visualized and printed below for analysis purposes.

6.2.1 Longitudinal bending moments and shear force redistribution in the beams

6.2.1.1 Self-weight load case

Weight construction was generated by the program Sofistik based on the calculation model amounted to 62888kN.

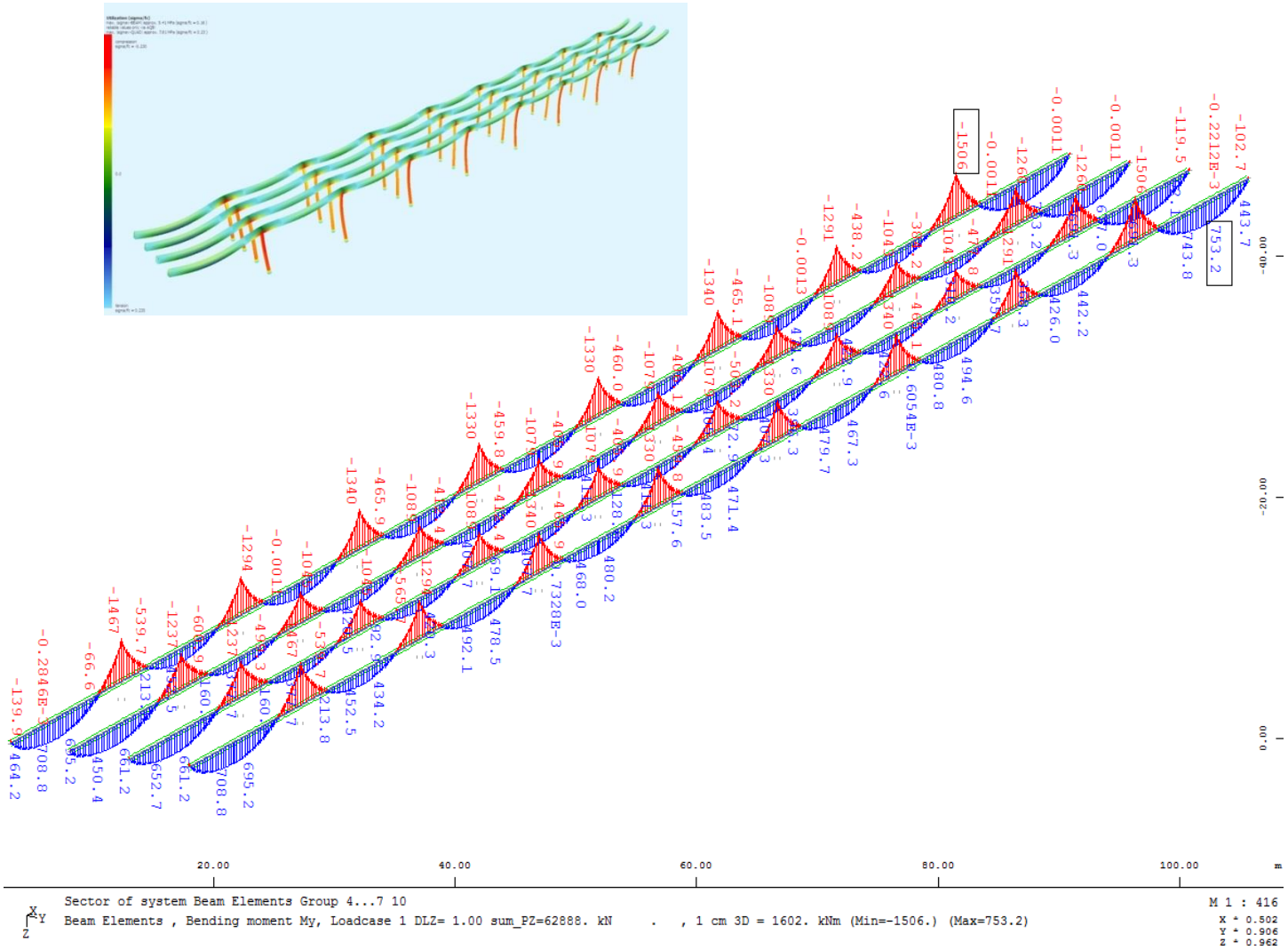

Figure 6.4 and **Table 7** Longitudinal bridge bending moments redistribution for self-weight load case.

Self-weight load case [kNm]	Envelope of bending moments My in axis 6-7:		
	Support:	**¼ span:**	**Mid span:**
Maximum Bending Moment:	-1079	23,6	407,7
Minimum Bending Moment:	-1089	-21,4	407,7
Maximum Global Bending Moment:	753,2		
Minimum Global Bending Moment:	-1506		

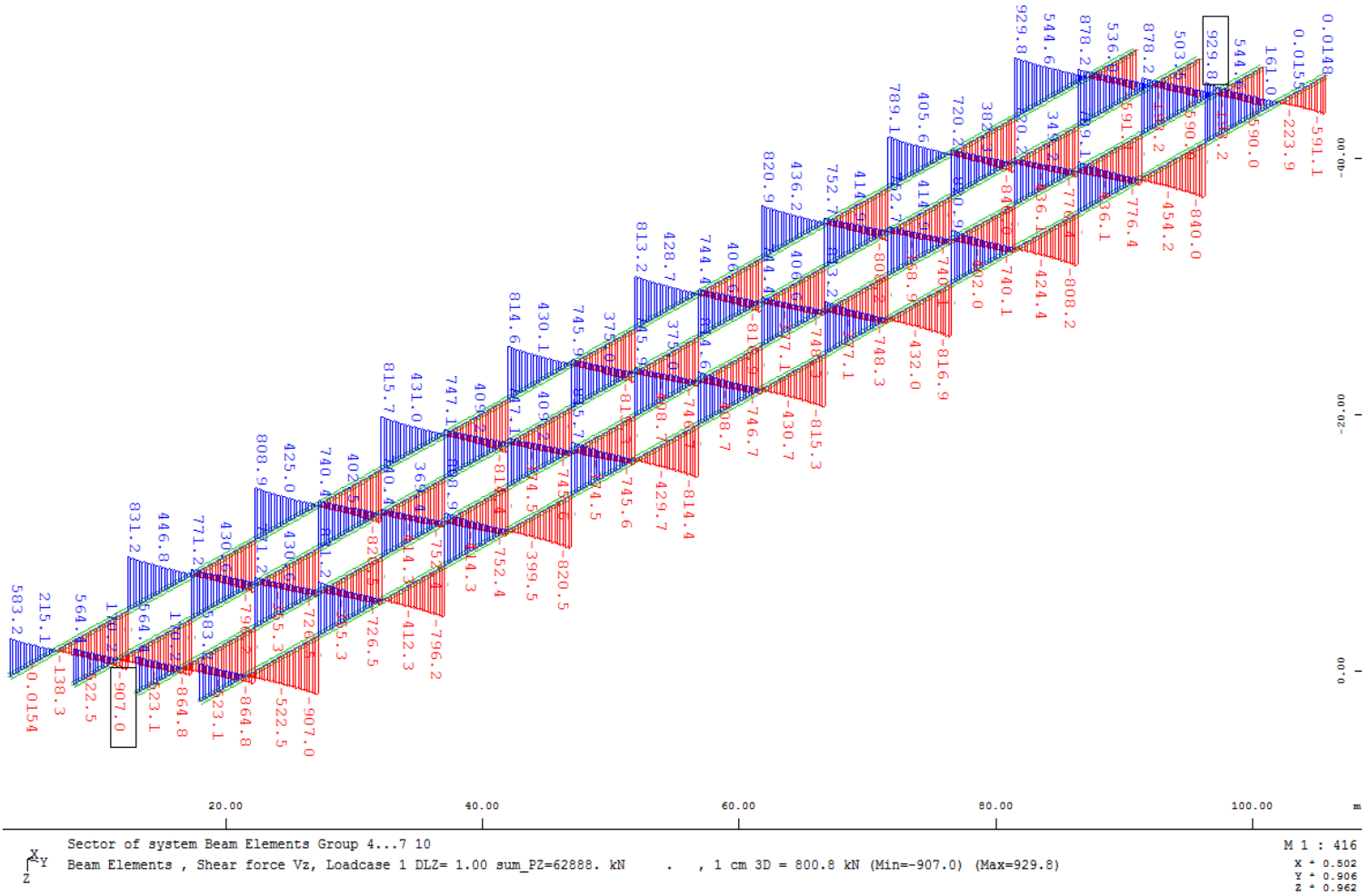

Figure 6.5 and **Table 8** Longitudinal bridge shear force redistribution for self-weight load case.

Self-weight load case [kN]	Envelope of Shear Force Vz in axis 6-7:		
	Support:	**¼ span:**	**Mid span:**
Maximum Shear Force:	747,1	342,9	45,2
Minimum Shear Force:	-745,6	-341,3	-55,8
Maximum Global Shear Force:	929		
Minimum Global Shear Force:	-907		

6.2.1.2 The Ultimate Limit State Combination

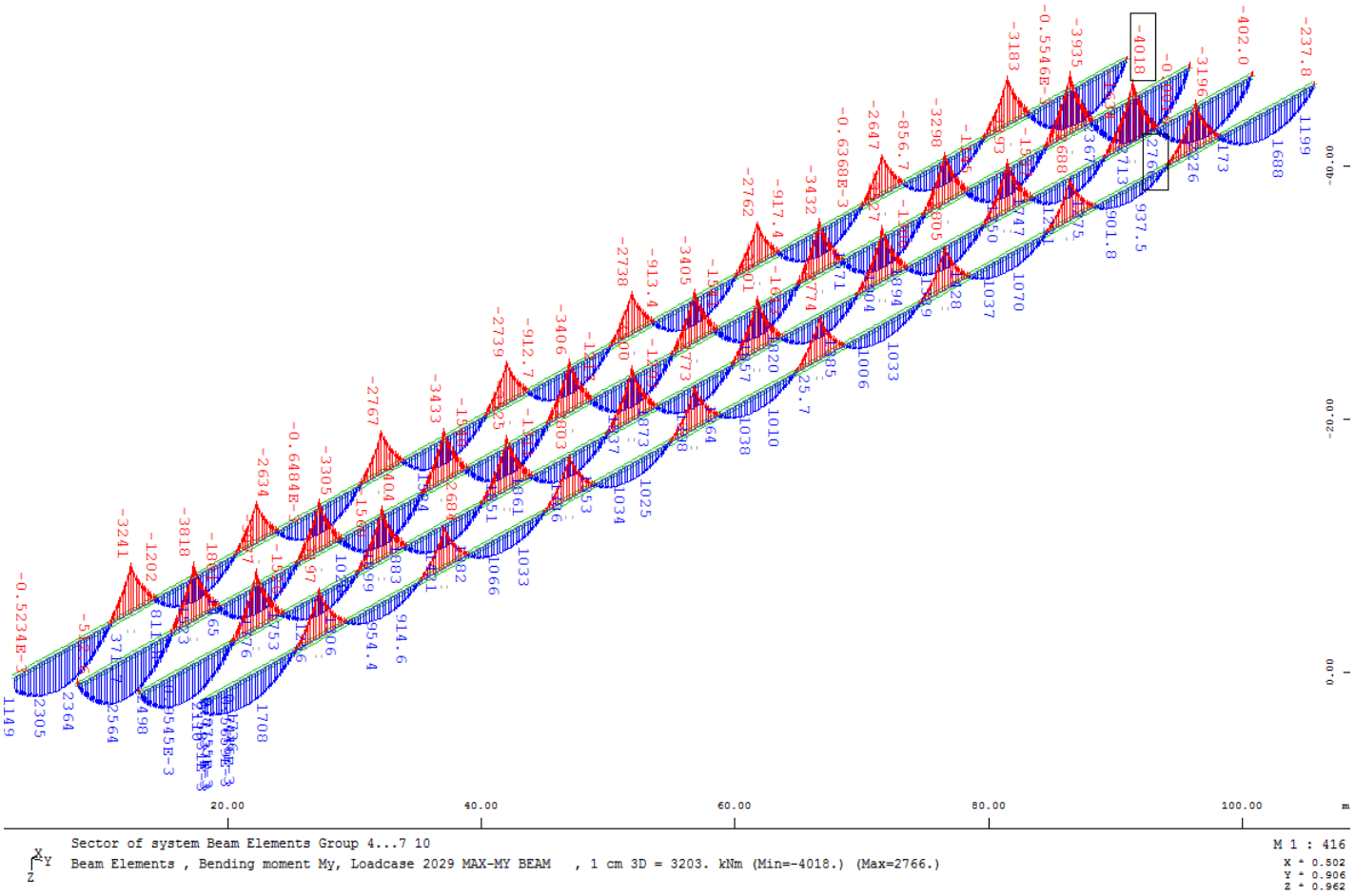

Figure 6.6 and **Table 9** Longitudinal bridge bending moments redistribution for The Ultimate Limit State Combination.

The Ultimate Limit State Combination [kNm]	Envelope of bending moments My in axis 6-7:		
	Support:	**¼ span:**	**Mid span:**
Maximum Bending Moment:	-3406	72,5	1861
Minimum Bending Moment:	-4072	-58,2	1277
Maximum Global Bending Moment:	2766		
Minimum Global Bending Moment:	-4618		

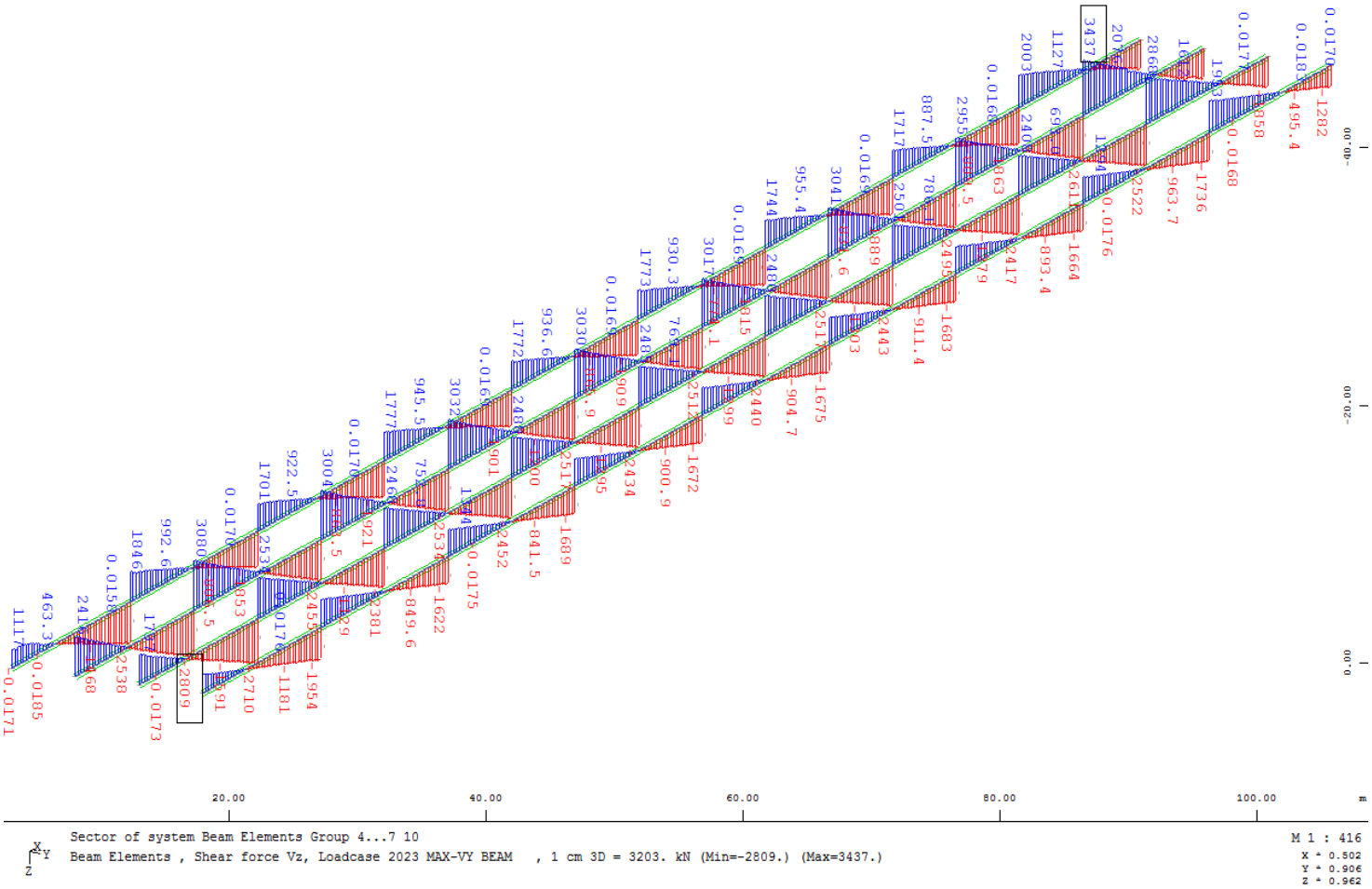

Figure 6.7 and **Table 10** Longitudinal bridge shear force redistribution for The Ultimate Limit State Combination.

The Ultimate Limit State Combination [kN]	Envelope of Shear Force Vz in axis 6-7:		
	Support:	**¼ span:**	**Mid span:**
Maximum Shear Force:	3032	1674	86,3
Minimum Shear Force:	-3023	-1667	-85,2
Maximum Global Shear Force:	3437		
Minimum Global Shear Force:	-2809		

6.2.2 ASR Response – Results in beams and slab

This chapter shows us results of stress and force distribution on the carrying elements and slab due to the Alcali-Silca reaction. Moreover will be present the displacements of the entire structure. The outcome which we preset comes from the linear analysis evaluated in two different software's.

6.2.2.1 Displacements

In the Figure 6.8 we can observe displacement of the entire deck and deflection of the northern rows of columns. Maximal movement of the bridge on the supports is equal to 192 mm. Displacements of the first three rows of columns is equal respectively: 159 mm, 130 mm and 119 mm.

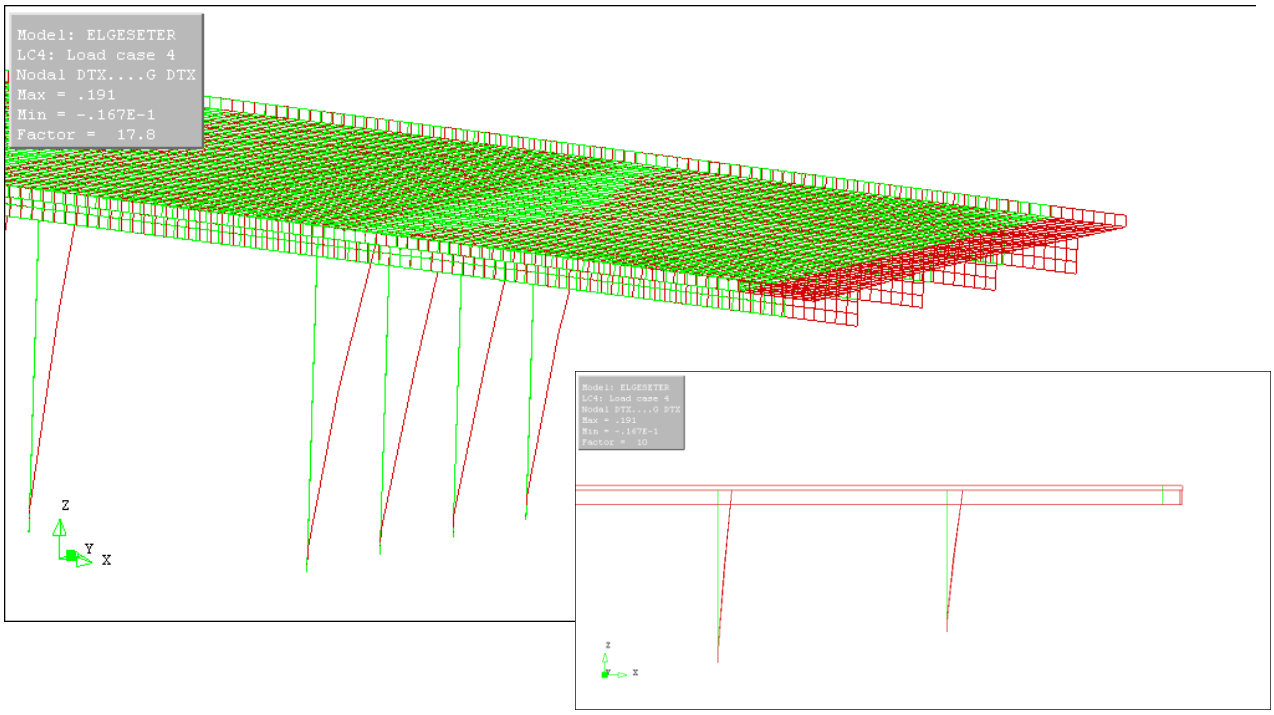

Figure 6.8 Bridge displacements in the X direction.

6.2.2.2 Stress distribution

Identical in terms of the geometry, the external parts of the cross-section of the bridge have been loaded with the ASR reaction. Visualization of the loaded model is shown in figure below. It is characteristic that the greatest stresses occur in the first zone in a place where there was a longitudinal crack observed.

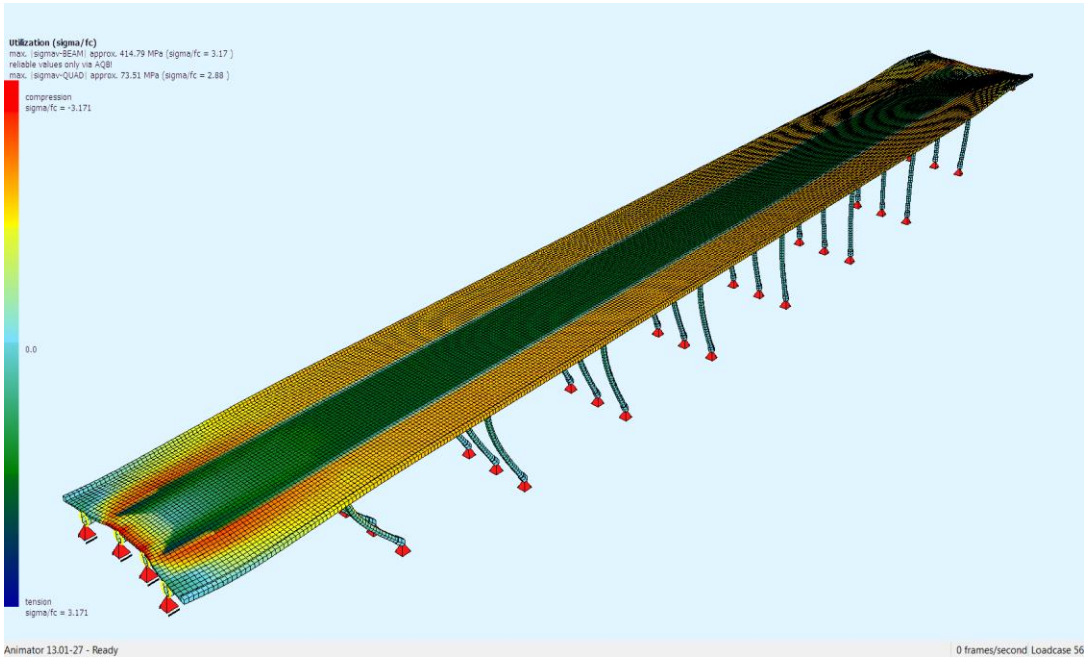

Figure 6.9 Stress distribution on slab due to ASR loading.

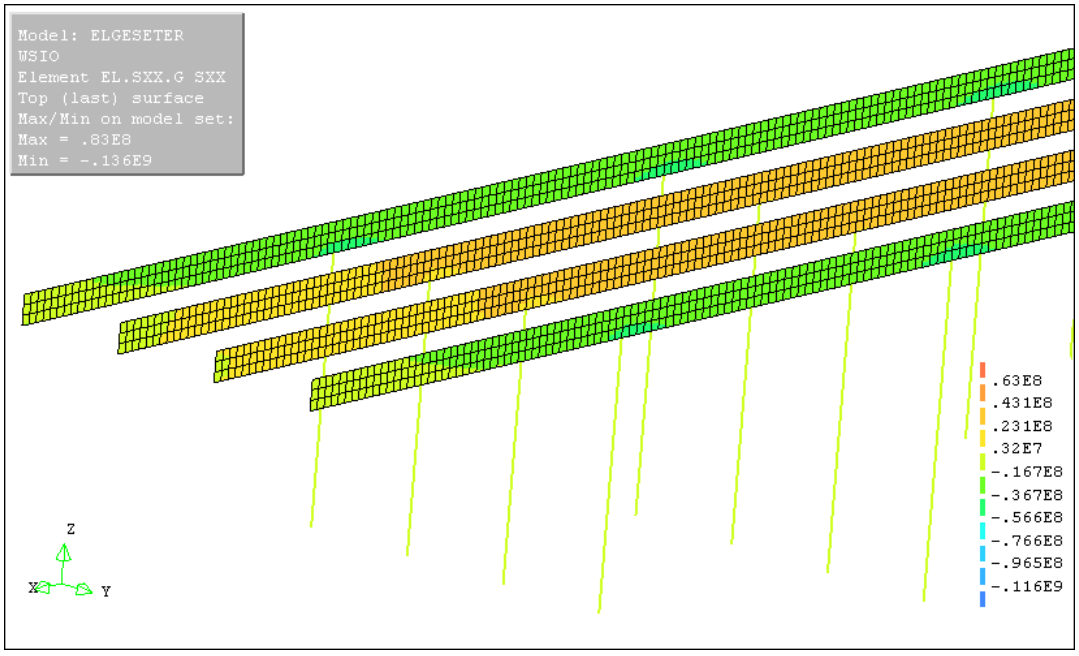

Figure 6.10 Stress distribution on beams due to ASR loading.

6.2.2.3 Tensile force

Very large forces occurring in the internal beams allow us to argue that cracks are caused by the consequences related to the expansion of concrete from the external part of bridge (internal beams are subjected to tensile stress as a result of the ASR reaction from external beams and external part of slab).

As a result of cracks tensile force decreases drastically. The cross-section changes properties. Therefore it is necessary to carry out non-linear analysis of this phenomenon.

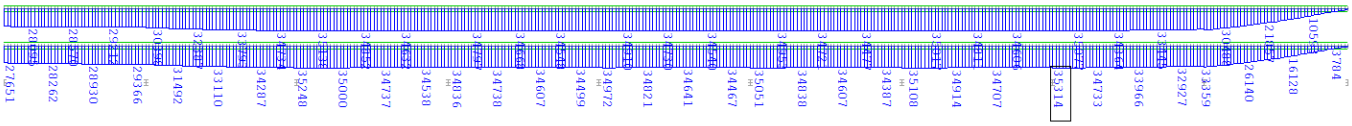

Figure 6.11 Normal Tensile Force distribution due to ASR loading.
Tensile force in internal beams: 35314 kN.

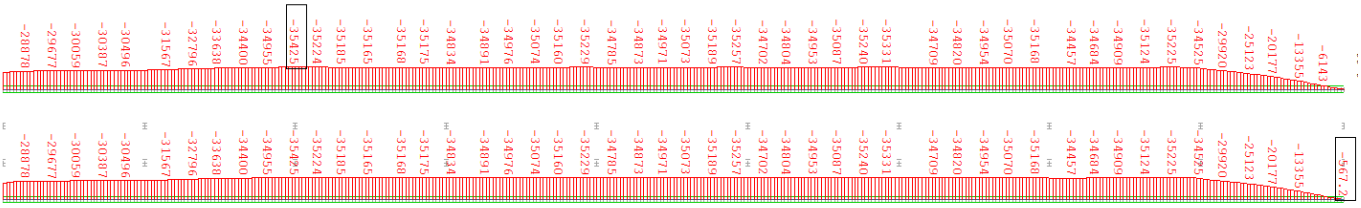

Figure 6.12 Normal Compressive Force distribution due to ASR loading.

Compressive force in external beams: 35425kN.
Tensile force in external beams: 35316kN.

6.2.3 Longitudinal shear force distribution in the slab

The results of the reproduced stresses in model regarding the distribution of the shear force component in longitudinal direction are presented on the Figure 6.13 below.

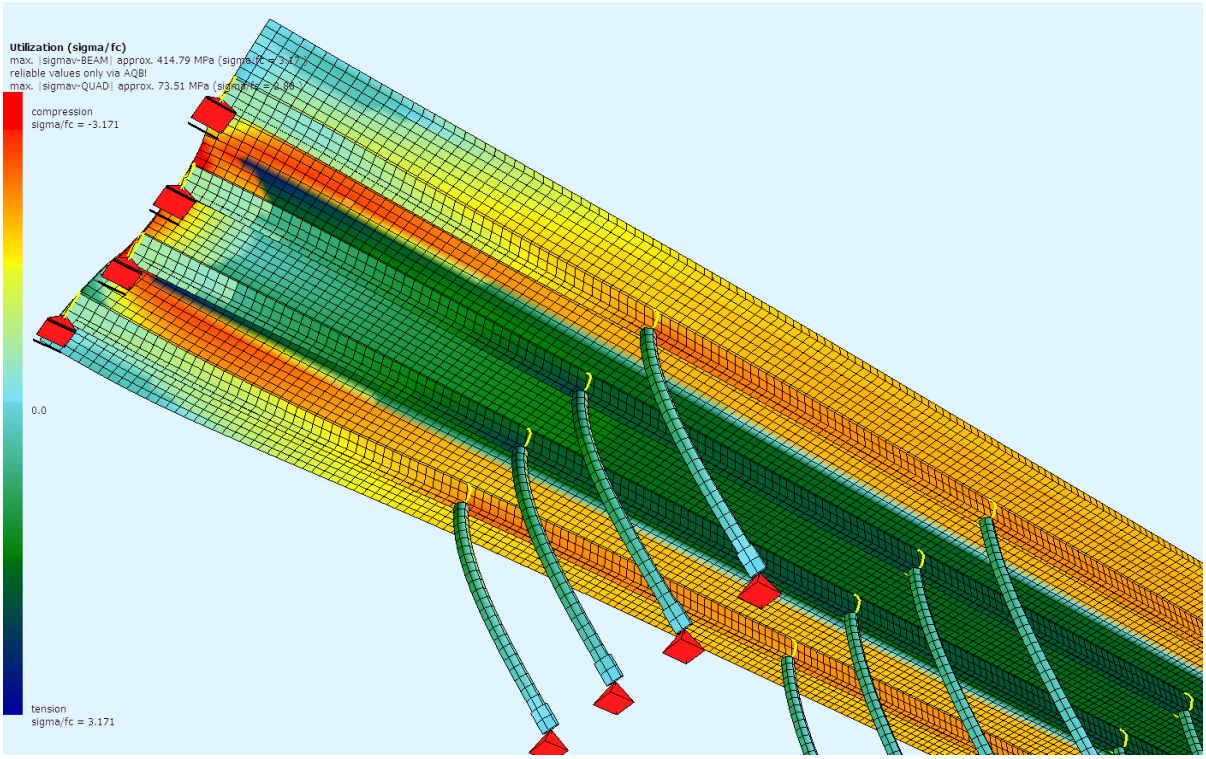

Figure 6.13 Stress distribution due to ASR loading.

7 Engineering Interpretation

7.1 Norsk Standard NS 3473 Simplified Method.

«Prosjektering av betongkonstruksjoner Beregnings- og konstruksjonsregler.»

7.1.1 Simplified method.

12.3.2.1 For structural member without shear reinforcement the capacity of shear at fracture is assumed [67]

$$V_{cd} = V_{co} = 0{,}3 \cdot (f_{td} + \frac{k_A + A_s}{\gamma_c \cdot b_w \cdot d}) \cdot b_w \cdot d \cdot k_v \leq 0{,}6 \cdot f_{td} \cdot b_w \cdot d \cdot k_V$$

$$k_A = 100\, {}^{N}/_{mm^2}$$

$$k_V = 1{,}5 - {}^{d}/_{d_1}$$

$$d_1 = 1{,}0m$$

$A_s - cross$
$- sectional\ area\ of\ the\ inserted\ longitudal\ reinforcement\ on\ tension\ side\ with\ sufficient\ anchorage$

12.3.2.3 Capacity for shear force with axial tensile force can be considered as:

$$V_{cd} = V_{co} \cdot (1 - \frac{N_f}{1{,}5 \cdot f_{td} \cdot A_c}) \geq 0$$

12.3.3.2. Capacity for shear for diagonal reinforcement can be considered as:

$$V_{sd} = \frac{f_{sd} \cdot A_{sv}}{s} \cdot z \cdot (\cot\theta + \cot\alpha) \cdot \sin\theta$$

The remaining longitudinal reinforcement in the weakest cross-section:

- $2Ø32\ M9$
- $3Ø32\ M3$
- $2Ø22\ M74$
- $2Ø13M73$

Cross-sectional area: 50,44 cm^2.

The remaining diagonal reinforcement in the weakest cross-section:

- $3Ø32\ M3$

Cross-sectional area: 24,12 cm^2.
Stirrups:

- $2Ø13$

Cross-sectional area: 2,65cm^2.

7.1.2 Uncracked cross section.

a) contribution from concrete cross-section and longitudinal reinforcement:

$$f_{td} = \frac{f_{tn}}{\gamma_c} = \frac{1{,}4}{1{,}4} = 1{,}0\ {}^{N}/_{mm^2}$$

$$\gamma_c = 1{,}4$$

$$d = 180cm - 2 \cdot 6{,}9cm = 165{,}2cm$$

$$V_{co} = 0{,}3 \cdot (1{,}0\ {}^{N}/_{mm^2} + \frac{100\ {}^{N}/_{mm^2} + 50{,}44\ \mathrm{cm}^2}{1{,}4 \cdot 80cm \cdot 165{,}2cm}) \cdot 80cm \cdot 165{,}2cm \cdot 1{,}0$$
$$\leq 0{,}6 \cdot f_{td} \cdot b_w \cdot d \cdot k_V$$

$$0{,}6 \cdot 1{,}0\ {}^{N}/_{mm^2} \cdot 80cm \cdot 165{,}2cm \cdot 1{,}0 = 792{,}96kN$$

$$b_w = 80cm$$

$$k_A = 100\ {}^{N}/_{mm^2}$$

$$k_V = 1{,}5 - {}^{d}/_{d_1} = 1{,}0$$

$$d_1 = 1{,}0m$$

$$\boldsymbol{V_{co} = 504{,}57kN \leq 792{,}96kN} - condition\ fulfilled.$$

b) contribution from diagonal bend rib reinforcement:

$$V_{sdb} = \frac{f_{sd} \cdot A_{sv}}{s} \cdot z \cdot (\cot\theta + \cot\alpha) \cdot \sin\theta$$
$$\theta = 60°\,, \qquad \alpha = 45°$$
$$z = 0{,}9 \cdot d$$

The yield limit for St. 37 is 230 Mpa and 320 MPa for St. 52
Bend ribs Ø32 are made from St. 52, hence:

$$f_{sd} = 320\,{}^{N}/_{mm^2}$$

$$V_{sdb} = \frac{320\,{}^{N}/_{mm^2} \cdot 2412\ \mathrm{mm}^2}{1000\ mm\ \cdot 1{,}25} \cdot 0{,}9 \cdot 1652mm \cdot (\cot 60° + \cot 45°) \cdot \sin 60° = \mathbf{1086{,}07\ kN}$$

c) contribution from stirrups:

$$V_{sds} = \frac{f_{sd} \cdot A_{sv}}{s} \cdot z \cdot (\cot\theta + \cot\alpha) \cdot \sin\theta$$

$$\theta = 60°, \qquad \alpha = 90°$$

$$z = 0{,}9 \cdot d$$

The yield limit for St. 37 is 230 Mpa and 320 MPa for St. 52
Bend ribs Ø13 are made from St. 37, hence:

$$f_{sd} = 230\,{}^{N}/_{mm^2}$$

$$V_{sds} = \frac{230\,{}^{N}/_{mm^2} \cdot 265\mathrm{mm}^2}{175\ mm\ \cdot 1{,}25} \cdot 0{,}9 \cdot 1652mm \cdot (\cot 60° + \cot 45°) \cdot \sin 60° = \mathbf{207{,}132\ kN}$$

$$\boldsymbol{V_{cd} = V_{co} + V_{sdb} + V_{sds} = 504{,}57kN + 1086{,}07\ kN + 207{,}132\ kN = 1797{,}77kN}$$

12.3.2.3 Capacity for shear force with axial tensile force can be considered as:

Shear capacity can be reduced by the action of the axial tensile force:

$$V_{c1} = V_{co} \cdot (1 - \frac{N_f}{1{,}5 \cdot f_{td} \cdot A_c}) \geq 0$$

$$\boldsymbol{N_f = 35314kN}$$

$$V_{c1} = 504{,}57 \cdot (1 - \frac{35\,314\,000N}{1{,}5 \cdot 1{,}0\,{}^{N}/_{mm^2} \cdot 800mm \cdot 1800mm}) \geq 0$$

$$V_{c1} = -7744{,}68kN$$

$$V_{co} = V_{c1} = 0\ kN$$

The total cross-section of the shear load capacity after reducing:

$$\boldsymbol{V_{cd} = V_{co} + V_{sdb} + V_{sds} = 0\ kN + 1086{,}07\ kN + 207{,}132\ kN = 1293{,}20kN}$$

7.1.3 Cracked cross section.

a) Contribution from longitudinal reinforcement only:

$$f_{td} = 0\,{}^{N}/_{mm^2}$$

$$d = 180cm - 2 \cdot 6{,}9cm = 165{,}2cm$$

$$V_{cd} = V_{co} = 0{,}3 \cdot \left(0\,{}^{N}/_{mm^2} + \frac{100\,{}^{N}/_{mm^2} + 50{,}44\ \mathrm{cm}^2}{1{,}4 \cdot 80cm \cdot 165{,}2cm}\right) \cdot 80cm \cdot 165{,}2cm \cdot 1{,}0$$
$$= 108{,}09kN$$

b) contribution from diagonal bend rib reinforcement:

$$V_{sdb} = \frac{f_{sd} \cdot A_{sv}}{s} \cdot z \cdot (\cot\theta + \cot\alpha) \cdot \sin\theta$$
$$\theta = 60°\,, \qquad \alpha = 45°$$
$$z = 0{,}9 \cdot d$$

The yield limit for St. 37 is 230 Mpa and 320 MPa for St. 52
Bend ribs Ø32 are made from St. 52, hence:

$$f_{sd} = 320\,{}^{N}/_{mm^2}$$

$$V_{sdb} = \frac{320\,{}^{N}/_{mm^2} \cdot 2412\ \mathrm{mm}^2}{1000\ mm\ \cdot 1{,}25} \cdot 0{,}9 \cdot 1652mm \cdot (\cot 60° + \cot 45°)$$
$$\cdot \sin 60° = \mathbf{1086{,}07\ kN}$$

c) contribution from stirrups:

$$V_{sds} = \frac{f_{sd} \cdot A_{sv}}{s} \cdot z \cdot (\cot\theta + \cot\alpha) \cdot \sin\theta$$
$$\theta = 60°\,, \qquad \alpha = 90°$$
$$z = 0{,}9 \cdot d$$

The yield limit for St. 37 is 230 Mpa and 320 MPa for St. 52
Bend ribs Ø13 are made from St. 37, hence:

$$f_{sd} = 230\,{}^{N}/_{mm^2}$$

$$V_{sds} = \frac{230\,{}^{N}/_{mm^2} \cdot 265\mathrm{mm}^2}{175\ mm\ \cdot 1{,}25} \cdot 0{,}9 \cdot 1652mm \cdot (\cot 60° + \cot 45°)$$
$$\cdot \sin 60° = \mathbf{207{,}132\ kN}$$

$$\boldsymbol{V_{cd} = V_{co} + V_{sdb} + V_{sds} = 108{,}09kN + 1086{,}07\ kN + 207{,}132\ kN = 1401{,}29kN}$$

7.2 Norsk Standard NS 3473 Friction Model.

«Prosjektering av betongkonstruksjoner Beregnings- og konstruksjonsregler.»

12.7 Shear Forces in construction joints.

12.7.2 The Capacity of shear along a casting shot with effective area A and reinforcement area A through the interface can be set to:

$$\boldsymbol{V_d = \tau_{cd} \cdot A_c + f_{sd} \cdot A_s \cdot (\cos \alpha + \mu \cdot \sin \alpha) - \mu \cdot \sigma_c \cdot A_c \leq 0,3 \cdot f_{cd} \cdot A_c}$$

$$\alpha - \ reinforcement\ angle\ with\ the\ contact\ with\ surface,$$

$$where\ \alpha\ is\ between\ 90°\ and\ 45°$$

$$\mu - friction\ coefficient$$

$$A_s - area\ of\ reinforcement\ cross - section$$

$$\sigma_c - the\ minimum\ concrete\ tension\ \ acting\ on\ the\ surface$$

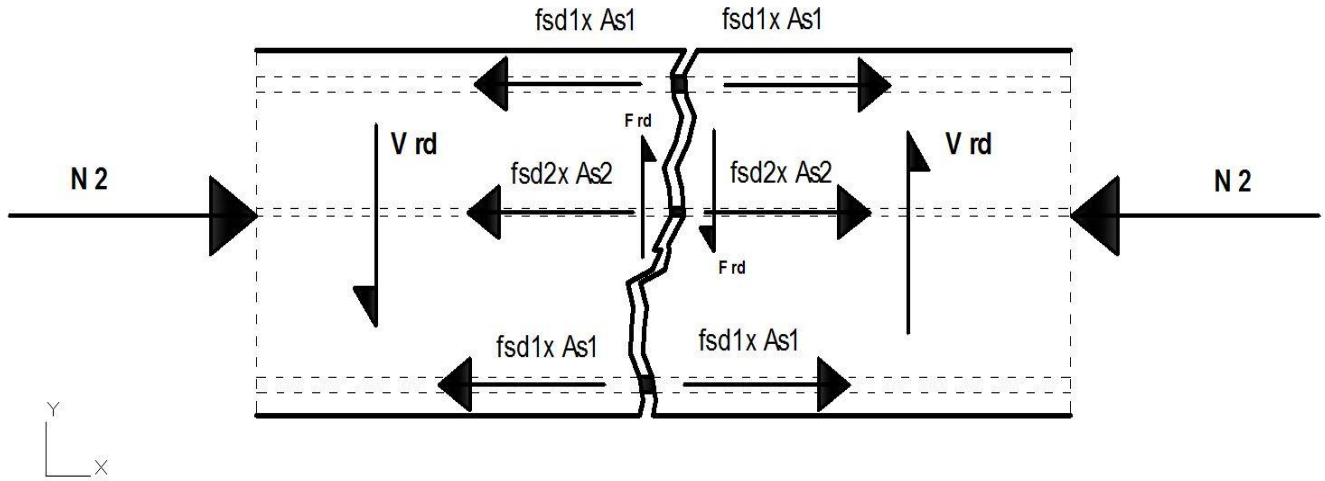

The remaining longitudinal reinforcement in the weakest cross-section:

- $2Ø32\ M9$
- $3Ø32\ M3$
- $2Ø22\ M74$
- $2Ø13M73$

Cross-sectional area: 50,44 cm^2.

The remaining diagonal reinforcement in the weakest cross-section:

- $3Ø32\ M3$

Cross-sectional area: 24,12 cm^2.

<u>According to **Tabell 6:** Verdier for kraftoverføring i støpeskjøter:</u>

<u>Contact surface:</u> $$\sum \boldsymbol{A_s > 0,001 \cdot A_c}$$

$$\boldsymbol{\sigma_c < -0,4\ {}^{N}/_{mm^2}}$$

- smooth
- combination 1:

$$\boldsymbol{\tau_{cd} = 0}$$

$$\boldsymbol{\mu = 0,7}$$

$$\boldsymbol{N_2 = f_{sd1} \cdot A_{s1} + f_{sd2} \cdot A_{s2} + f_{sd2} \cdot A_{s3}}$$

$$\boldsymbol{N_2} = \frac{320\ {}^{N}/_{mm^2} \cdot 804\ \text{mm}^2}{1,25} \cdot 5 + \frac{230\ {}^{N}/_{mm^2} \cdot 380\ \text{mm}^2}{1,25} \cdot 2 + \frac{230\ {}^{N}/_{mm^2} \cdot 133\ \text{mm}^2}{1,25} \cdot 2$$

$$\boldsymbol{N_2 = 1217,9\ kN}$$

$$\boldsymbol{V_{rd} = \mu \cdot N_2 + f_{sd} \cdot A_{sbend} \cdot n \cdot \sin \alpha}$$

$$\boldsymbol{V_{rd}} = 0,7 \cdot 1217,9kN + \frac{320\ {}^{N}/_{mm^2} \cdot 804\ \text{mm}^2}{1,25} \cdot 3 \cdot \sin 60° = 852,53kN + 534,7kN$$

$$\boldsymbol{V_{rd} = 1387,23\text{kN}}$$

7.3 Shear between web and flanges of T-sections. Eurocode 2

Calculation of the longitudinal shear stress [66]**:**

Δx – half of the distance between the section where the moment is 0 and the section where is maximum
h_f – thickness of the slab

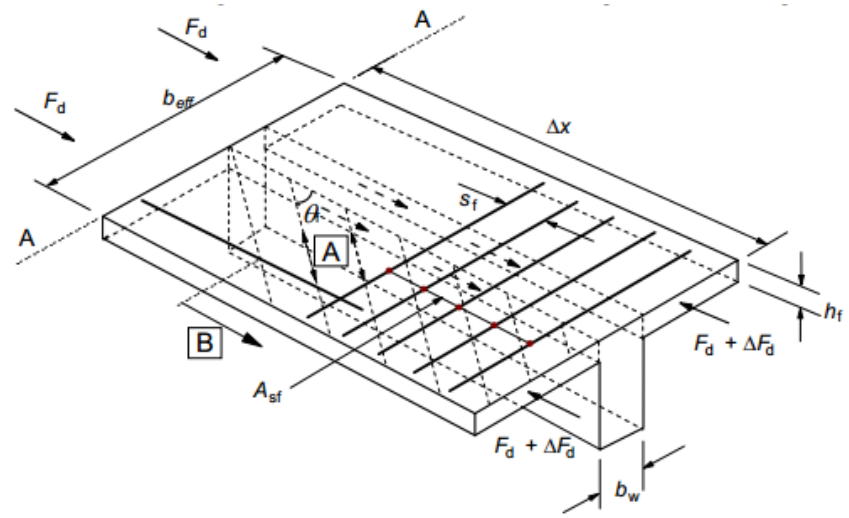

A - compressive struts B - longitudinal bar anchored beyond this projected point (see 6.2.4 (7))

$\Delta x = 0{,}5 \cdot 4{,}26\, m = 2{,}13m$

$h_f = 25\, cm$

$F_2 = 0{,}856 \cdot 10^7 N$ – maximum normal force

$F_1 = 0{,}764 \cdot 10^7 N$ – minimum normal force

$$\boldsymbol{v_{ED}} = \frac{\Delta F_d}{h_f \cdot \Delta x} = \frac{F_2 - F_1}{h_f \cdot \Delta x} = \frac{920000N}{0{,}25m \cdot 2{,}13m} = 1{,}72MPa$$

Crushing of the compression struts

$\theta_f = 45°$

$$v_{ED} \leq v \cdot f_{cd} \cdot sin\theta_f \cdot cos\theta_f v_{ED} \leq 0{,}2 \cdot 16{,}66MPa \cdot 0{,}707 \cdot 0{,}707 = 1{,}66\, MPa$$
$$\leq 1{,}72\, MPa$$

- ***Conditions are not fulfilled***

8 Overview of Mitigation Measures for ASR-Affected Structures

In this section with regard to possible repair we will briefly discuss each of the options shown in Figure 2.7 (section 2.4) and will then focus on those that have the greatest potential for effectively treating in ASR-affected Elgeseter Bridge. All of these options will be presented and discussed. Moreover, both terms of general and specific application to the construction will be talk over.

It is really important that, ASR reaction occurs only when three conditions will be satisfied (as we briefly mentioned before in section 1.2.2)
1) In the concrete are present sufficient alkalies;
2) Sufficient reactive silica within the aggregates must be inherent in the concrete;
3) To maintain the reactions, sufficient moisture must be present within the concrete.

In the case of the willingness of mitigate active ASR by treating the fundamental causes, reducing or eliminating the above factors is necessity.

8.1 Chemical Treatment/Injection

8.1.1 Injecting ASR-affected concrete with CO_2

With regard to sufficient alkalies present within the concrete, it has been suggested that injecting ASR-affected concrete with CO_2 can decrease the alkali content. This manipulation would have the influence of lowering the pH and carbonating the ASR gel (Cavalcanti and Silveira, 1989).

This method has some technical and practical limitations. First of all, injecting gas under high pressure can carry on to meaningful distress in concrete which has already microcracking due to ASR. Secondly, carbonating reinforced concrete can indeed increase the rate of corrosion. This technique would likely has slight influence on ACR as it tends to be powered by a fractional amount of alkalies, and these alkalies can be recycled in the process. Injection of concrete with CO_2 to try to decrease the alkali content occurs to hold slightly or no keep in field structures.

8.1.2 Use of lithium to treat existing ASR-affected structures

Using lithium compounds to treat concrete already suffered from ASR-induced expansion have been tested and that exist several laboratory-based publications about this topic. In researches made by Stark et al. (1993), Stokes et al. (2000), and Barborak et al. (2004) we can find tests done in accelerated laboratories, which show that lithium compounds can decrease future expansion of ASR-affected concrete specimens. The details

of mechanism are still not clear. It is commonly presume that lithium compounds come into the existing gel and modify the nature and behavior of the gel from expansive to essentially non-expansive. The promising results have been received which caused a considerable interest in treating ASR-affected field structures. A particular inspection of past field attempts applying lithium compounds can be found in Folliard et al. (2006). A lot of field trials are still being checked and monitored under current FHWA projects (East 2007) [100].

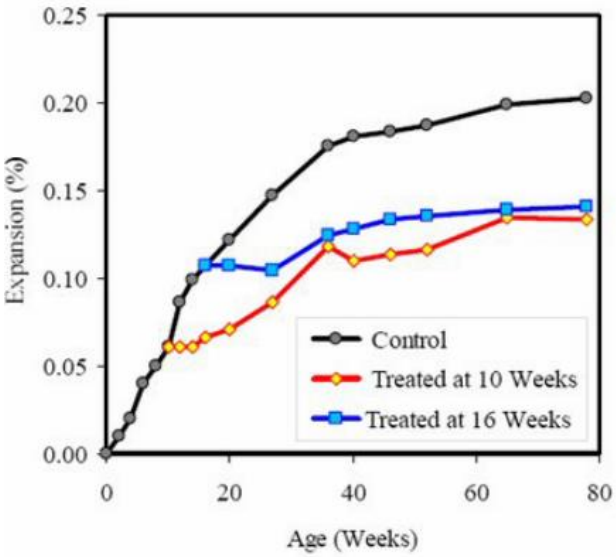

Figure 8.1 Expansion of concrete prisms after treatment with lithium at 10 weeks (expansion = 0.061 percent) and 16 weeks (expansion = 0.107 percent) (Thomas and Stokes, 2004).

8.1.3 Topical Treatment with Lithium

Lithium has been treated by spraying the surface of the many structures in the word, specifically chemical compounds like LiNO3 and LiOH have been used. Application of lithium can be done on diverse types of structures: bridge decks and other bridge components, pavements and median barriers. There are two most popular types of applying lithium: truck-mounted spraying systems (figure 8.2) or hand-held pressurized spray bottles (figure 8.3).

Figure 8.2 Photograph showing topical application of 30 percent-LiNO3 solution to concrete pavement.

Figure 8.3 Photograph showing topical application of 40 percent-Silane Solution (solvent-based) to ASR-affected highway barrier.

The problem which concerns deficiency of penetration in field and laboratory tests in which lithium compounds have been applied topically, force to shift towards more aggressive means of driving lithium into ASR-affected concrete, specifically through electrochemical methods and vacuum impregnation.

Measurement of the depths of penetration of lithium many a times gave quite minimal results, especially for topical applications. Penetration for topical applications frequently was found to be only a few millimeters. In practice, even after three treatments with dosages of lithium (necessary to suppress expansion) measured in heavily cracked pavements penetrated only to the first 2 to 3 mm. Due to an inherent lack of penetration the topical application of lithium compounds shows slightly promise of alleviating ASR in structures. One exception is where ASR is being aggravated in the outer surface by an exterior source of alkalies (i.e. deicing salts).

8.1.4 Vacuum Impregnation with Lithium

Second alternative method to pressure injection is vacuum impregnation which has been used to increase grout penetration into cracked concrete. Numerous of structures have been treated with lithium using this technique. A number these include several substructure elements as beams and columns.

Unfortunately, in research performed under FHWA Project DTFH61-02-C-00097, vacuum impregnation was not found to be effective in the laboratory or in field structures. For example, for ASR-affected bridge columns in which lithium nitrate was applied via vacuum, the depths of lithium penetration were found only to be in the present in the outer 9 to 12 mm, drawing into question whether such an elaborative and expensive vacuuming technique is justified [75].

8.1.5 Electrochemical Lithium Impregnation

The test which lithium nitrate was electrochemically inducted into bridge columns, has shown significant higher depths of penetration. To obtain measured all the way down to the reinforcing steel the dosages were sufficient to reduce ASR.

Hence Electrochemical impregnation techniques have been used to increase lithium penetration on a number of structures (Whitmore and Abbot, 2000). A typical setup (i.e., for a bridge deck) is shown in figure 8.4 and includes the following parameters:

- Technique is based on electrochemical chloride extraction technique.
- Electrode (anode) applied to concrete surface.
- Lithium-bearing electrolyte ponded at surface.
- D.C. voltage (~40 volts) applied between surface anode and embedded steel (cathode)
- Positively charged lithium ions are repelled by the positively charged anode and are drawn towards the negatively charged cathode (steel reinforcement).
- Duration of treatment is typically 4 to 8 weeks [76]

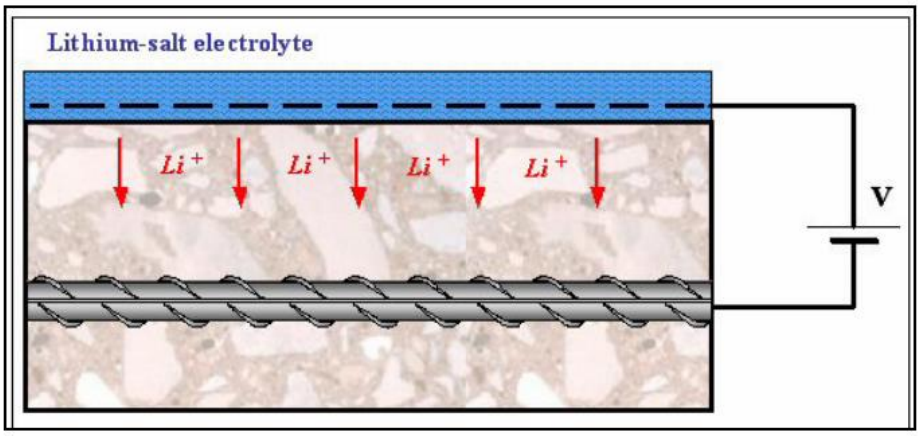

Figure 8.4 Electrochemical lithium impregnation.

In the literature we can find two cases of using this electrochemical technology. These are two bridge decks, one in Arlington, the other in Seaford. In both cases, lithium borate was used as the electrolyte. Cores were taken from the deck in Virginia after 8 weeks of electrochemical treatment. Slices taken from the cores and subjected to chemical analysis revealed the data shown in table 11. The data indicate that significant lithium penetrates to a depth of at least 19 to 32 mm, and these dosages are theoretically high enough to have a beneficial effect on reducing ASR induced expansion.

Depth of slice (mm)	Lithium (ppm)
6–19	315–343
19–32	203–265

Table 11 Penetration of lithium after electrochemical treatment of bridge deck.

Figure 8.5 Electrochemical lithium treatment process. (a) irrigation tubes, wood splices, and metal strips are placed on the column. The metal strips are attached to titanium mesh that

runs inside holes drilled into the sides of the column. (b) A cellulose layer is applied to the side of the column, and (c) plastic sheeting is placed on all sides of the column. The gutters under the sheeting collect excess lithium for reuse [76].

However, the process has disadvantage. Hydroxyl ions are produced at the surface of the reinforcing steel because of the lithium ions which are clearly driven to the reinforcing steel, what generate the steel serves as a cathode in the electrochemical process. Sodium and potassium ions from within the concrete move to the steel surface to provide neutrality and to offset the formation of hydroxyl ions at the reinforcing steel surface. This initiate an growth in the hydroxyl ion concentration and a subsequent increase in alkali (sodium and potassium) concentration near the surface of the reinforcing steel may aggravate ASR-elicited expansion and cracking in this region. Future monitoring expansion, cracking and microstructural evaluations of these should help to establish if the potentially detrimental side effects of electrochemical impregnation outweigh the benefits of the significant lithium penetration [74].

Studies are conducted to judge this treatment technique and to quantify the advantage of this approach. Prosperity of driving lithium all the way to the reinforcing steel is encouraging. However the unfavorable effects of pushing sodium and potassium to the nearness around the steel deserve additionally consideration. The laboratory test clearly has shown effective method in reducing future expansion in ASR-affected concrete. It is necessity at additional lithium-based field test will be carry on, thus helping to quantify the influence of lithium application on residual service life.

8.2 Drying

The most important component of ASR-induced expansion and cracking is moisture. Publications made by Stark (1991) and Pedneault (1996) showed that ASR-induced expansion is significantly decrease preclude or suppressed when a relative humidity (RH) is below of 80 percent. That exist lots of worthwhile methods that can be applied in the field to reduce the internal RH. Proper example of improving drainage preclude for a given structure is diverting drainage from a bridge deck away from an ASR-affected surface. Another mitigation measure is contemplating a cladding. This method precludes the entry of additional moisture. However, the moisture already present within the concrete may be good enough for ASR to become active.

8.2.1 Sealants, Cladding, Siloxanes and Silanes

Applying coating or sealer is more appropriate solution with regard to reducing internal moisture. This method prevents external water from penetrating into the concrete. Moreover, allows water vapor from within the concrete to exit, hence resulting in a general reduction in the internal relative humidity.

A coating or penetrating sealer that will induce decrease in internal relative humidity must ensure the following characteristics:

- Be resistant to water absorption.
- Penetrate to a measurable depth.
- Resist deterioration from ultraviolet (UV) radiation.
- Possess long-term stability in an alkaline environment.
- Be of long-term stability in an alkaline environment; and
- Allow vapor transmission. [75]

Siloxanes and silanes are the most commonly mitigation measures from ASR. Furthermore, they help to decrease two things: ingress of water and external chlorides. First one enhances frost resistance; second one reduces the rate of corrosion of reinforcing steel. In the last few years, silanes have become the essential and serviceable product for these purposes. On the market there is available diversity of silane products. Mainly varying based on the concentration of silane in the specific formulation ranging from 20 percent to close to 100 percent. There are two types of silans due to the type of carrier with which the silane is combined: either water-based and solvent-based. Lithium-based products and silanes are almost always applied at a similar coverage rate and depths of penetration are in the same order of size –a few millimeters. Nevertheless, silanes must only penetrate into the concrete in the outer region to form a functional barrier preventing water from entering but allowing moisture vapor to escape. Unlike lithium compounds, which must penetrate into concrete to reach ASR gel, hence execution the gel less expansive.

To prevent liquid water from entering to the concrete, penetration depths of silan as a typically measured should be 5 or 6 mm. This range of depth is appropriate for these materials to serve their purpose such as allowing internal water vapor to escape, thus decreasing the internal relative humidity of concrete. In order to provide longevity to the treatment as sealers present, deeper penetration of silanes is required. UV radiation or abrasion can remove with time near to the surface of bridge decks. In short, effectiveness of silane will decrease with time, especially due to abrasion and UV effects. It is generally believed at a single application of a silane-based product is not sufficient. Moreover, Carter (1994) reported that the re-application of silane over a surface already treated with silane resulted in deeper penetrations and increase ability to reduce internal moisture. Summarizing, this has been established that re-applying silanes every 5- years or so is prudent.

Benefits of applying siloxanes, and especially silanes have been confirmed by several studies which were focused on reduce future ASR-induced expansion in the field structures. The results of research made by Bérubé et al. (2002a and 2002b) show us dramatic reduction in future expansion. In Figure 8.6 is clearly illustrated at applying silane to highway barriers heavily damaged by ASR, help decrease expansion of the concrete.

Figure 8.6 Barrier wall in Quebec-the section of the wall to the right of the picture has been treated with a silane sealer.

As it was mentioned before, silanes can be quite practical and effective in the field in reducing ASR-induced expansion. However, there are several limitations. In case where moisture is accessible from underneath, silanes will not be as effective as their benefits are only realized from the treated surface.

That can occur on pavements, slabs on grade and wingwalls. Furthermore, wetting and drying cycles are required to decrease internal concrete moisture. For applications where concrete will be fully submerged or not allowed to dry, silanes will probably not function in proper way.

Finally, the last limitation which concern width of the existing cracks. Efficiency of the silanes application drops almost to zero when in concrete are large crack widths. For these, flexible caulking or similar products should be used to seal the larger cracks.

Based on the last progress in researches of products, such as, paints or elastomeric coatings, we can conclude promise in bridging larger cracks and avoiding the need for caulking of individual cracks. The critical situation is when reinforced concrete is exposed to external chlorides or in regions exposed to cycles of freezing and thawing. In this case, need to seal larger cracks become obligatory.

8.3 Crack Filling

Attempts of minimize or manage the symptoms or indication of the harmful reaction at times are more appropriate than direct the fundamental cause of ASR. Naturally, this approach does no arrest reaction but focuses on reducing the influence on the performance or service life of the structure. We will briefly present discussions on measures which can be

used in regard to ASR-induced cracking, mainly through crack filling to minimize entrance of chlorides, water and other aggressive ions. Additionally confining the expansion or allowing for expansion through concrete removal.

Cracks caused by ASR reaction have not only influence on the functioning of a structure, but the cracks serve as access points as well. That causes easily penetration of the concrete by water, chlorides, external alkalies and sulfates. Aggravating ASR and potentially leading to other forms of distress, for instance: frost attack, corrosion of reinforcing steel, salt scaling and sulfate attack. In cases, where structures are subject to aggressive environments or cracking has become dangerous, crack filling is often only one option to choice.

Caulking or flexible grouts are more efficient in filling cracks and conservation water and other substances from entering through the cracks. Although cement-based grouts and rigid polymer may help to stabilize cracks primitively. Strong bonding and rigid nature with the substrate concrete often oblige cracks to appear adjoining to the grouted area. Many of field trials and researches have shown that confinement or physical restraint can meaningfully decrease deleterious expansion due to ASR in the direction of restraint.

8.4 Strengthening of reinforced concrete structures

Nowadays, to restore the integrity of the structure are used two commonly methods; encasement in conventional reinforced concrete and post tensioning in one or two dimensions. These second one is considered to be an effective solution for structural members of bridge structures. To post-tension are used tendons or cables. Nevertheless, because of the periodic distressing which is necessity and that can be disadvantage for large concrete structures. Moreover, that exist another ways of strengthening which is efficient in ensuring containment for selected ASR-affected concrete members. For this purpose reinforcement is used with straps, steel plates and tensioning through bolts. Designing of encapsulating elements should be done very carefully. Otherwise the only advantageous effect of encapsulation may be limited the ingress of moisture. Thus, corresponding reinforcement must be ensured to control stresses due to ASR reaction.

That exists to main common reasons for the strengthening of reinforced concrete structures, change of the primary purpose of use or the degradation of the materials from which it is made (like in our case). We can distinguish also between two types of actions that can improve the quality of construction. The first is to strengthen the structure - these are the operations of increasing the carrying capacity of the structural element, so that it can carry larger loads than assumed on stage of design. The second as for our case is the repair facility - by which we mean actions aimed at restoring destroyed or damaged structural elements to state that it can carry out the designed load class.

8.4.1 FRP and FRCM systems in construction reinforcement

8.4.1.1 FRP systems

One method of reinforcing concrete structures is the use of composite materials. The beginnings of the use of FRP materials were the fifties of the last century. During the next decades, the quality of materials and methods of production automation has significantly improved. The range of reinforcement's assortment includes: mats, strips, ties and rope. They are made of resin matrix reinforced with carbon fibers, aramid or glass. These materials are characterized by high tensile strength, a high strength to weight ratio, high strength to dynamic loads and compared to steel has a high resistance to corrosion. They have linearly elastic characteristics, up to limit loads without permanent plastic deformation [68, 75].

FRP materials, as in the case of glued steel plates are fixed with thermosetting resin. They are used to increase the capacity on the beam for the shear forces and bending moment. Furthermore FRP materials are used in columns to form the spatial state of stress.

The basic components of the FRP system are:

- Strengthened reinforced concrete element with prepared and dust free surface,
- Grounding layer,
- Epoxy filler (to remove inequalities and depressions),
- A first layer of resin,
- Fiber reinforcing element,
- A second resin layer (in the case of CFRP mat),
- Protective layer.

In order to effectively transfer forces to the FRP system, the soil should be appropriately rough. This can be achieved by sandblasting or roughening. The fibers used in composite materials to external reinforcements extend vertically or horizontally, sometimes diagonally. The fabric consist only tightly-oriented fibers without the matrix. In the case of reinforced concrete beams strengthening with pre-stress tapes immediately before being installed to the structure, cause decrease of the stresses in reinforcing steel, the width of cracks and the deflection reduction [68, 75].

8.4.1.2 Methods of attaching FRP systems

The individual elements are fixed to the surface (structural element) with using an epoxy resin matrix subjected to curing. Two methods of curing the matrix are available: cold and heat. Cold curing method is used when applying the sheets to the surface of the reinforced element with dry or wet way. The first, dry method is applied at a weight of 400

g/m2 sheet. In this approach, the mat can be used as the unidirectional and bi-directional fibers.

Strengthening of the element is in two stages: the first takes place in the roll out cold-cure epoxy resin on the surface of the element. The second stage is applied to a dry sheet of this matrix.

The second, wet method is applied to the pre-stressed woven mats of self-weight more than 400 g/m2.In this case, pre-wet resin-impregnated sheet is applied to the surface of the element [68, 75].The method for heat curing the resin matrix is applied both to the sheets of unidirectional or bi-directional fibers. The curing process takes place at low temperature. Hardening of heat is performed by applying heat to the epoxy resin applied to the element. In this type, a pre-impregnated resin fibers which are not generally used to reinforce the structure. They are used in the aerospace industry [68, 75].

8.4.1.3 Methods for strengthening columns

For strengthening columns different systems of banding FRP are adapted, depending on type of material, shape and use of the technology. FRP ties on the surface of reinforced concrete columns can be done using the following methods:

- Winding mats,
- Winding rope (tendon),
- The use of cables,
- Automatic winding,
- attaching prefabricated shells,
- Impregnating resin.

Columns can be wound in a single layer or multi-layer mats or strips laying the spiral or ring. Tapes can be installed manually or in an automated manner. Laying manual is simple and quick to make, but difficult to control. This control applies to quality resin blend to achieve good degreasing and uniform resin saturation, desired compression of the fibers (without excessive creases), control and cure kinetics aspects of sustainability environment before and after curing [68, 75].

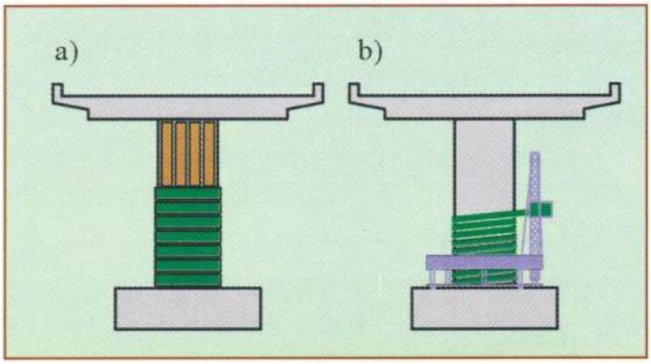

Figure 8.7 Fiber FRP winding around columns: a) composite tape laying, b) automatic rewinding the tape [68].

The most common structural reinforcement is applied as a transverse ties and tape along elements, placed in the areas of potential plastic hinges. The use of bands improves the mechanical characteristics of the columns. At low levels of longitudinal stresses, transverse strains are too small that the band FRP does not contribute significantly to the improvement of the mechanical characteristics of the column. However, when longitudinal stresses exceed the critical stress, increased lateral deformation will influence the cover FRP. Pressure at of the concrete core will become substantial and will depend on the axial deformation of the belt on the level of the pole. This is called passive-type action, which as a result gives a tension band inwardly directed of pressure [68, 75].

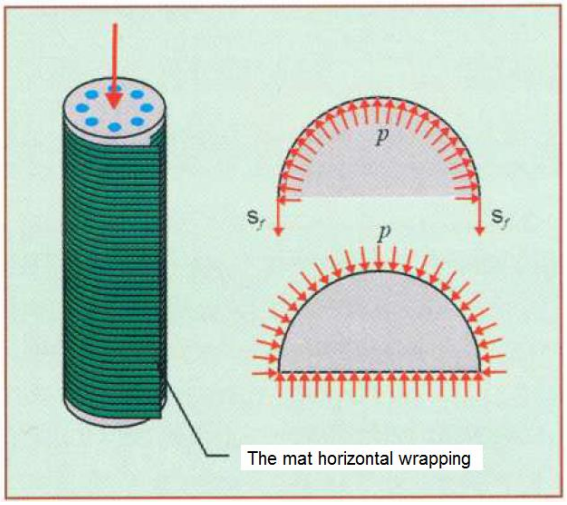

Figure 8.8 The effect of transverse expansion of the concrete and produced horizontal of pressure under an axial load of the concrete core [68].

As a result of the action of pressure in a horizontal concrete core of the column is produced triaxial stress state. Column in this state has a higher ductility and strength. External transverse strengthening has limitations due to the fact that the continuity of reinforcement cannot be provided in column intersections in connections with the foundation and the bents [68, 75].

Strengthening of columns can be also realized through the shallow penetration of rods FRP in cross section. This method encapsulates the bars in grooves provided in the element in the direction of the reinforcement. Connection with the foundation may be obtained by drilling holes in these elements and filling them halfway with epoxy resin. Then the rods are placed in the grooves by pressing it lightly so that the pressed resin flows around the rods. After completion of the deposition of the bars, the FRP wrapper are making to encase both the core and the concrete reinforcing bars [68, 75].

8.4.1.4 Methods for strengthening of the beams

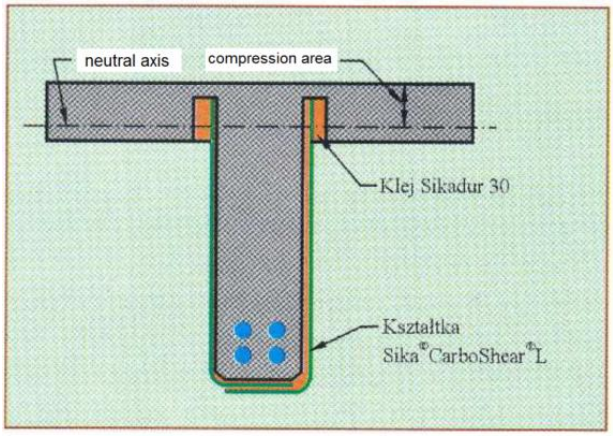

Figure 8.9 Example of shaped L carbon fibers cross sections for strength of the shear zone beams reinforced [68].

To strengthen reinforced concrete beams, such as in the strengthening of columns we shall apply diagonal band to provide appropriate shear capacity and tape along the components to ensure sufficient capacity for bending moments and tensile forces. Tapes are used in both ways: pre-stressed and non- pre-stressed, usually installed in tension zone.

Problems in the applications of FRP systems

As previously mentioned FRP composites are installing to the surface (element construction) using an epoxy resin matrix. However, the mechanical properties of FRP systems depend on the temperature at which the reinforcement works. The limiting value here is the glass transition temperature resins, above which the resin is no longer able to fulfill its role. This temperature falls within the range from 40° to 80 °C.

The whole system then becomes ineffective, regardless of the fibers used (aramid or carbon). Complete loss of adhesion between the resin and the connection thread or between the resin and the surface. Other problem FRP systems are toxic compounds that are released in the presence of a fire [69, 72, and 73].

8.4.1.5 FRCM systems

To solve the problems associated with resistance for higher temperatures FRCM system is available (so-called Fibre Reinforced Cementitious Matrix), based on a matrix of mineral mortar and polypropylene fiber (PBO). The mortar provides a connection of the matrix to the concrete base, and the mechanical strength properties are comparable to the strength of the popular strips of fiber stabilized to the substrate with epoxy adhesive carbon [69, 72, and 73].

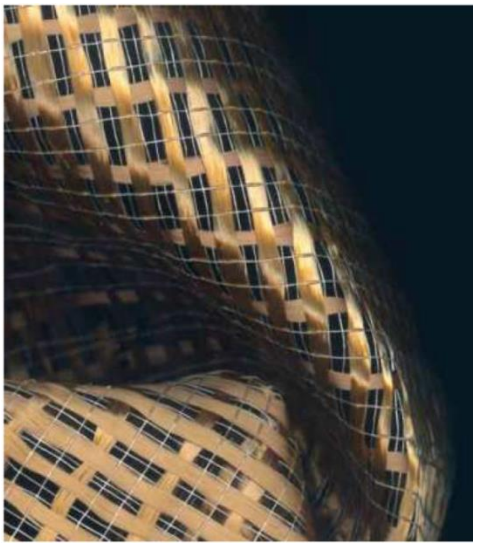

Figure 8.10 PBO fiber system [70].

Figure 8.11 FRCM system with the PBO fiber on a cement matrix applied on the reinforced concrete element [70].

FRCM systems suitable for strengthening reinforced concrete and pre-prestressed concrete elements.

FRCM system with the PBO fiber is used in areas such as:

- Areas of tensile stress,
- Areas of occurrence of shear forces
- Areas of occurrence of twisting moments.

The system is particularly useful for reinforced seismic and paraseismic construction, in order to increase the strength of the elements subjected to bending, shearing or twisting, to increase susceptibility to bending at the ends of the beams and columns, and increase the strength to tensile stresses in the joints between beams and columns [69, 72, 73].

Resistance to heat and moisture

Due to the fact that the system has a mineral binder (inorganic), after curing it is insensitive to temperature including a fire. Additionally, the system is not sensitive to soil moisture as FRP systems. When long-term strengthening of moisture degrades the resin, resulting in the loss of adhesion to the substrate, and thus loss the ability to transfer stresses to the fibers. Under fire conditions FRCM using the system does not emit toxic compounds by using cement mortar [69, 72, 73].

The analysis of samples reinforced by FRCM system with the PBO fiber made in Italy by system manufacturers have shown that the system is not the destruction of the fractured concrete and it is able to carry the load acting on it. Tests were performed on samples with dimensions of 600x150x75 (LxDxH). The mechanism of destruction is shown in the picture below.

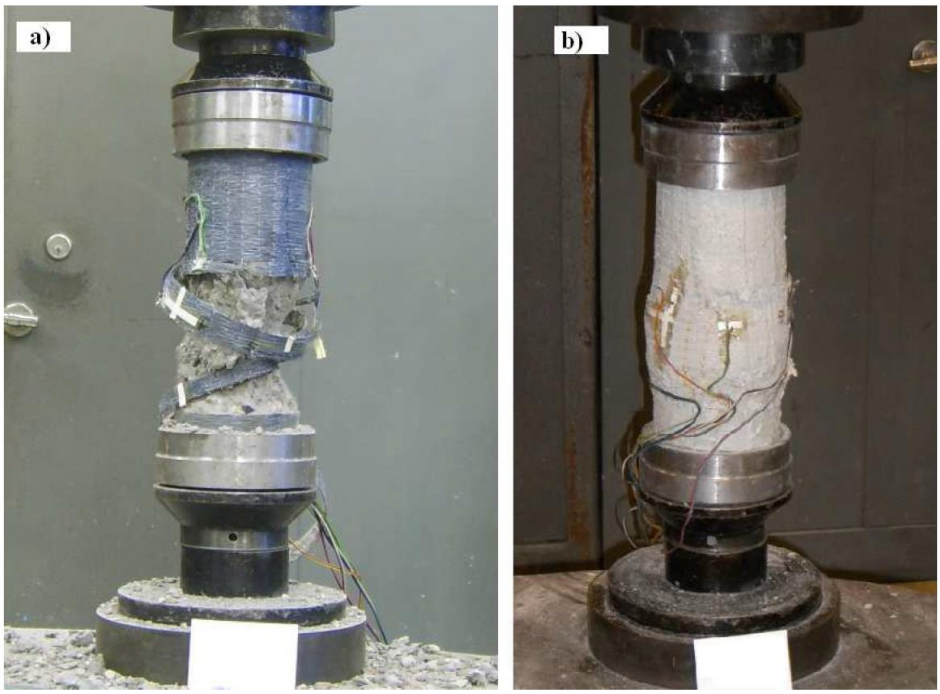

Figure 8.12 a) the destroyed sample reinforced with CFRP system, b) the destroyed sample reinforced with FRCM system with the PBO fiber. (Research had done at the Institute's own Civil Engineering Technical University of Wroclaw).

The sample in the figure 8.12a was destroyed suddenly, with no clear signs of prior to destruction. The sample in the figure 8.12b concrete is destructed, however, has the form of the destruction is completely different. The destruction took place slowly, PBO fiber matrix has deformed (no interruption), and stopping crushed concrete parts inside the reinforcement. Such a mechanism of destruction can give you time to spot potential risks (deformation of the structure) before the final destruction of the reinforced elements and take possible corrective measures or evacuation [69, 72, 73].

8.5 Relieve Stress

Removing sections of concrete near the joints by saw cutting is one of feasible options to lengthen the service life of the structure. That is possible for certain applications for elements suffering from ASR-induced expansion. This operation in Elgeseter Bridge has been done in 2003. Eliminating joint-related failures was achieved by removing part of column close to connection. However, diligence and careful attention must be paid to restoring the intended joint details. Advantage of this approach is stresses relieve. Nevertheless, does gain any benefits in regard to the root cause of the expansion. If the expansion keeps on, it is practicable to apply method frequently but it denies the advantages attain from the preceding concrete removal.

9 Proposed repair solutions

9.1 Columns

9.1.1 Monosilane impregnation

9.1.1.1 Previous Test Repair Aapproaches with Monosilane

After repair in 2003, significant reduction of the only expansion joint and cracking of structural elements were recorded. There are no other evidences that the reaction slows down or becomes dormant without mitigating measures. For that reason in our opinion two of proposal methods to shut down the reaction should be applied. First of possible method is to dry out the concrete to below 80% relative humidity using monosilane and second is chemical treatment of concrete with lithium. Prepared tests with monosilanes have given very promising results and one of the tested products has reduced the relative humidity 50 mm from the surface to less than 80% the results from these tests are described below.

Elgeseter Bridge In 1995 has been developed and pilot tested. The in situ system for measurement was mounted. System show results of relative humidity in concrete and expansion of cracks was on [77]. Measurement sites were installed one beam and columns with 800-mm diameter. Numbers of measure points were equal respectively to eight and four. The main purpose was use of relatively cheap equipment and simple and systematic procedures. In that case, owners of structures could perform all the measurements themselves. The measure of relative humidity was made indirectly by use of wooden sticks (Gonystylus macrophyllum) in stability with the relative humidity in the concrete [78–84].

The diameter of the wooden sticks is 12 mm and length equal to 45 mm. Wooden sticks are mounted into a special fabricated plastic tube with diameter 20 mm drilled into the concrete and injected with epoxy sealers to prevent contact with atmospheric air. In the

concrete, the wooden sticks are in contact with the concrete through four 5 mm holes in the plastic tube. For monitoring in the Elgeseter Bridge, two wooden sticks have been mounted into the plastic tube measuring the relative humidity 50 mm and 250 mm from the surface. For each wooden stick, calibration curves for relative humidity and percent water (electrical conductivity) adsorbed and desorbed are made. That exists evidence at calibration curves vary between wooden sticks, many a time is meaningfully. Then individual calibration curves are constructed for each stick.

Note that the relative humidity 50 mm from the surface reduces thereafter, and that relative humidity is not influenced by temperature fluctuations. Measurements have shown that relative humidity in the concrete varied from 100% to 87% before impregnation with silane. Moreover, profiles have shown that the relative humidity is significantly higher on western faces than on the eastward-facing faces of the columns.

In 1999, 11 new measurement locations were installed on land and in the river as well. The main intend was to measure the effect of monosilane impregnation on ASR, indirectly with measure the relative humidity and expansion of a crack [87]. On three entire columns were applied three different types of silanes. Product dealers applied silane type B and C in September 1999. Type B is a liquid with 40% organosilan ester in isopropanol but silane Type C with creamy consistency. Finally Road Directorate in July 2000 applied Silane Type A, a liquid (100% isobutyltri-ethoxysilan). All the products were applied according to the recommendations and reference [83].

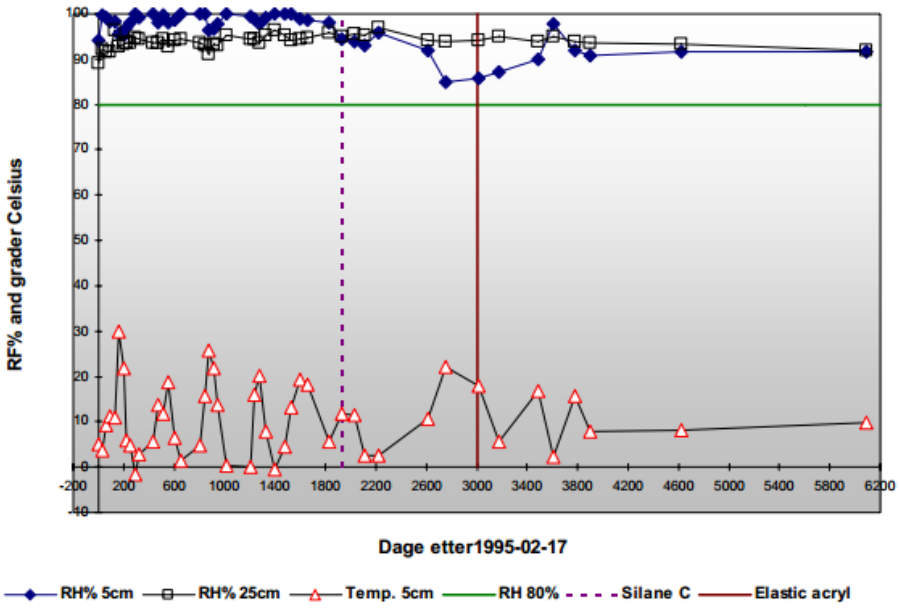

Fig. 9.1. Measurement of relative humidity and temperature at location 8, Column 3, Zone 9. After 1700 days, silane type C was applied to the concrete (vertical detached line).

In the Figs. 9.2–9.4 are presented variability of relative humidity through the center of columns before silane impregnation (untreated), 800–1100 days after applying the impregnate and to the latest measurements after 1057–1357 days [83]. Results are promising. In distance 50 mm from the surface, relative humidity has been decreased, in all the silane impregnated columns. However, in the middle of the column impregnated with silane Type C in distance 550 mm from western face, relative humidity has been insignificantly reduced.

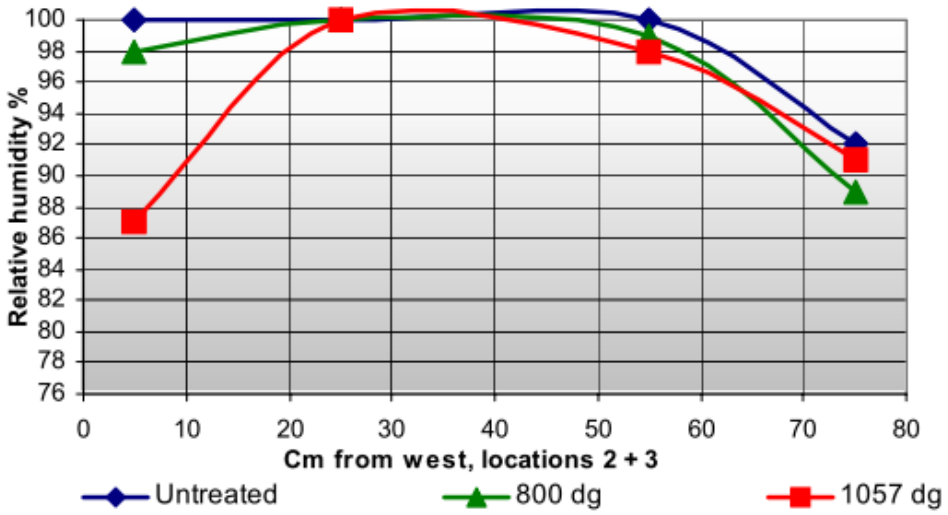

Fig. 9.2. Humidity profiles through column 1, Zone 2 about 1.5 m above ground level. Measurement before impregnation (untreated), 800 and 1057 days, respectively, after silane A was applied.

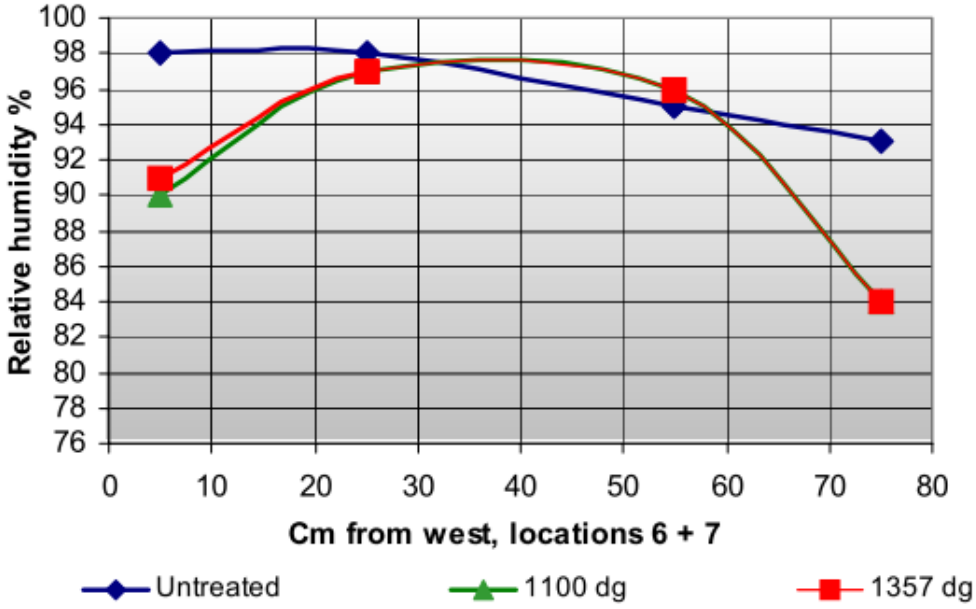

Fig. 9.3. Humidity profiles through column 1, Zone 9 about 1.5 m above ground level measurements before impregnation (untreated), 1100 and 1357 days, respectively. After application of silane type B.

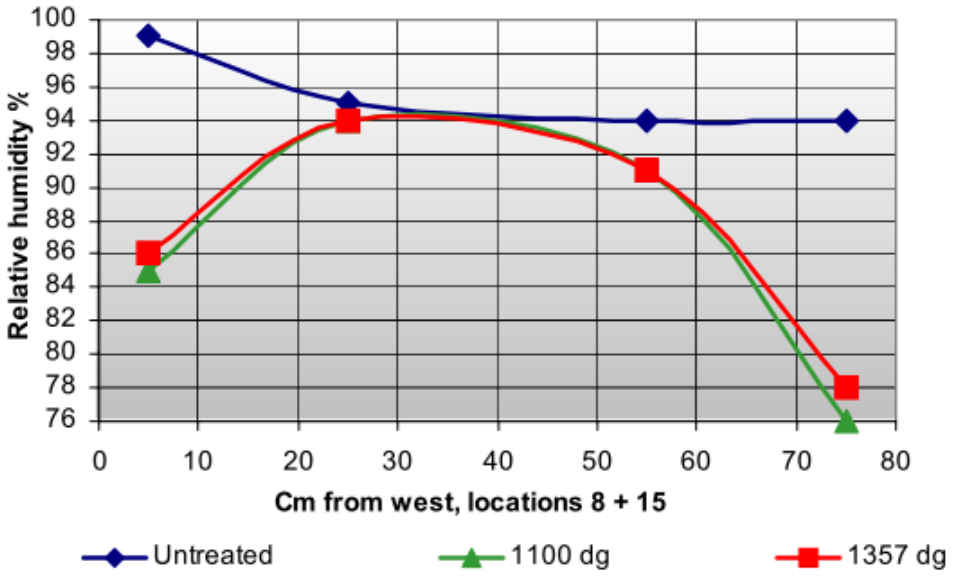

Fig.9.4. Humidity profiles through column 3, Zone 9 about 1.5 m above ground level. Measurements before impregnation (untreated), 1100 and 1357 days, respectively, after silane C was applied.

Humidity is one of the significant parameter from whose the durability of structure depends. Moreover, it is important in reparation of damaged structures with ASR and other deterioration processes. Nowadays, the developments and investigations about surface protection as a measure to decrease the concrete humidity are insufficiently and inappropriate.

In spite of an advanced stage of ASR and massive columns results are promising. As it was stated, results show reducing relative humidity in the concrete 50 mm from the surface after impregnation with monosilane. Furthermore, based on the researches [84-89], creamy consistency monosilane reduces the relative humidity more efficiently compared with the other tested products. It is really hard to interpret the result of measurements crack widths, but if we compere to earlier measurements we can state reducing of crack expansion [82].

9.1.2 Fiber Reinforcement Strengthening of the columns as a not appropriate solution

Performed on the bridge moisture testing prove that the use of carbon fiber for the case of columns increases the moisture of the concrete and hence increases influence of the reaction ASR. Therefore, a solution using carbon fiber on columns raises doubts in our opinion.

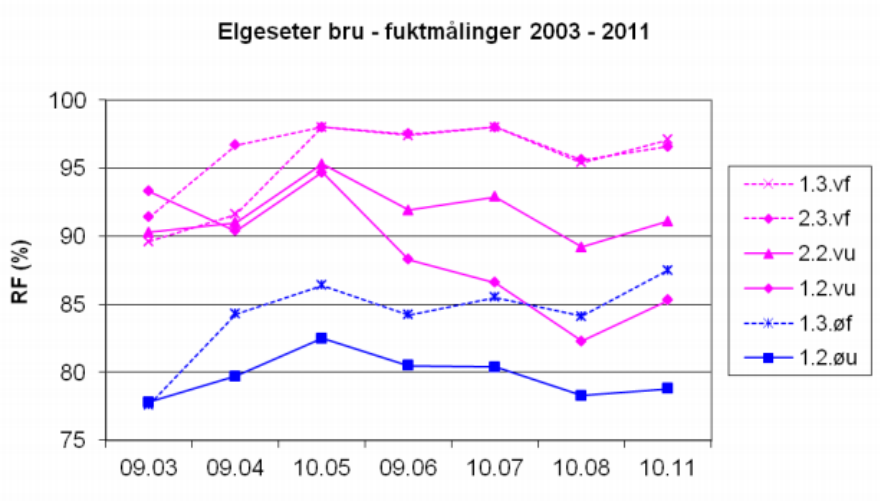

Figure 9.5 Development of relative humidity in concrete pillars in the period 2003 – 2011[88].

On the figure 9.5 above it is shown that columns with fiber reinforcement cover persist higher relative humidity level than columns without any cover. The constant line represent column without cover and the dotted line represent reaction of wrapped columns, respectively.

What is even more important in case of the column currently is not possible to perform pre-stress of fiber reinforcement. For all the reason above using the solution with wrapped has been rejected in progress of our analysis.

9.1.3 Recommendation to use monosilane on columns

The most appropriate solution chosen from all available in the market nowadays are use of electrochemical Lithium Impregnation and after monosilane cover, respectively. Exact principles of electrochemical lithium impregnation have been described on this paper above in section 8.1.5. Obviously, monosilane was tested on Elgeseter previously and gave very promising results for that reason in our opinion this is proper solution. Tests shown that the relative humidity in the middle of columns decreased significantly to a harmless level of about 80%. The average annual relative humidity in the atmosphere is 79–80% in Trondheim. It is considered that this is the lowest possible relative humidity that could be achieved in the bridge columns, with the aid of surface protection. Because of that we recommend also using formerly, electrochemical lithium impregnation should be done first.

Figure 9.6 Zone 4, column #4.

Afterwards we also recommend crack filling which could be taken into account and then application of the new structure of monosilane should be prepared.

In certain cases, however, the structure on the columns is too damaged. Direct application of monosilane layer is pointless and will not provide sufficient insulation from moisture. A good example is here deteriorated structure on the bottom of the column #4 in zone 4. Necessity is therefore replacing the outer surface of the concrete. Only then applying a new layer of monosilane can appropriate protect columns against water penetration.

All of these treatments are based on the stopping development of ASR by the chemical treatment and by prevents penetration of the water. Further silane allows draining moisture from the concrete. These operations should be prepared especially the central columns in the riverbed from the west where the columns are the most exposed to rain.

9.1.4 Electrochemical Lithium Impregnation of columns

More work about this method is in progress to evaluate this treatment technique and to quantify the benefits (and downsides) of this approach. The laboratory tests show, that lithium compounds have clearly influence in reducing future expansion in ASR-affected concrete structures. Large impact on this decreasing has effective driving of lithium all the way to the reinforcing steel. However, the options for treating the cause of ASR in the field are restricted. To totally stop progression of the ASR in columns lithium-based field with collaboration with monosilane protection should be carry on. That also will help remaining the service life of the entire structure. This method is our opinion is perfect to application in our construction of the columns and the effects are very promising and encouraging.

9.2 Slab

9.2.1 Drainage System and Membrane Protection

First step should be a removing a surface of a pavement, curbs and sidewalks. We suspect that when the asphalt will be removed asphalt also cracks on the upper surface of the slab will be visible. Asphalt is a material highly flexible so on the surface of the asphalt cracks are invisible, currently. As a result, taken by us under analysis of this study we strongly recommend use a topical treatment of slab with Lithium. Cracks which may be appeared and be visible after removing the asphalt will allow for deeper penetration of Lithium that can be work more efficiently. Afterwards next step will be crack filling to protect top surface against water penetrate and finally the application of a new layer of membrane on the bridge slab which will cause that Lithium will be also covered and will be actively penetrate and work on reinforcement concrete slab. On the end application of a new drainage system plate is considered: First and foremost, the most important element is waterproof membrane

protection of the slab. Apply new high quality membrane cover on the top surface. It is required filter papers (perforated top) under waterproofing membrane, which is often, especially in a tight, modern waterproofing surfaces neglected. This aspect is a result from water vapor pressure in the pores of the concrete, the moisture in the concrete tends to float upwards and settling on the surface of the waterproof membrane is therefore necessary to apply the perforations. This is to prevent destruction of the top plate cover membrane again. Drainage system dehydration surface drains, manifolds and downpipes, put careful attention to the methods of attaching the filters into the collecting duct, role of fastening steel structures, expansion joints and elements for revision. Consider need for deep drainage system of bridge abutments. Consider also different solutions drainage systems engineering.

9.2.2 Topical Treatment of slab with Lithium under membrane protection

Some of the criteria should be fulfilled consider treating of a structure with lithium-based compounds. That will be possible when the pavement top surface will be removed:

- Lithium treatment is unlikely to “cure” any other deterioration processes such as freeze-thaw damage, corrosion of embedded steel or even alkali-carbonate reaction. Proper diagnosis involves extracting samples for petrographic analysis and other testing in the laboratory.
- There remains potential for further expansion and damage due to ASR [77].

Unfortunately, existing damages cannot be fixed be Lithium treatment. Still are conducted development technologies of treating structures with lithium. At this moment, recommended are protocols for selecting the proper type of treatment. In case of topical treatment applications are relatively simple to perform, and a few general guidelines are provided below.

9.2.3 General guidelines for topical lithium treatment.

• Clean surface (e.g., road sweeper) prior to treatment.
• Do not treat if rain is forecast within 6 hours.
• Keep single application rate ≤ 0.12 L/m2
• Minimum two applications.
• Applications at least 30 minutes apart.
• Ensure uniform surface coverage and no runoff.
• If precipitate forms over > 5 percent of surface, re-wet the surface to dissolve the precipitate. If surface becomes slippery, applications of water should continue until the surface is safe for vehicular traffic.

Amount of individual treatments that can be applied to a structure will be control mostly by economics and other aspects of the repair strategy. In case structure will be treated prior to the application of a concrete or asphalt overlay that can be single treatment be performed. But for example, pavements or bridge decks need treating with appropriate time period and intervals.

The authors are not aware of any studies aimed at evaluating the effect of lithium nitrate on the environment.

9.3 Beams

9.3.1 Fiber Reinforcement Strengthening of the beams

Fiber Reinforcement Strengthening of the beams is the most appropriate solution. Use of carbon fiber reinforcement with pre-stress system application. Primarily, internal beams require achievements of sufficient capacity for shear force and sufficient tensile membrane forces which comes from service load and from ASR reaction, respectively. Therefore, the best solution is to use pre-stressed carbon fiber with strips as long as it is possible. The weakest points which have been described in this thesis and places where cracks are already generated require also use glued strips in vertical and diagonal direction. Before Fiber Reinforcement application all the crack should be filled. Rigid polymer- and cement-based grouts may help to stabilize cracks initially, their rigid nature and strong bonding with the substrate concrete often forces cracks to appear adjacent to the grouted area. Crack filling can be taken also to address ASR-induced cracking, primarily through crack filling to minimize ingress of water, chlorides, and other aggressive ions, and ASR-induced expansion by confining the expansion. The last sentences solutions also should be apply to columns.

10 Discussion and Conclusions

Appropriate bridge maintenance activities should be carried out to maintain a required level of performance throughout the whole life cycle especially, for unique designs structures as Elgeseter Bridge. In 2004 the bridge awarded Concrete Board of Norwegian Concrete Association reasoned that “the bridge is an outstanding, forward-looking and beautiful edifice. By his good technical condition marks the bridge properties of the concrete as a resistant building material.” In 2008 the bridge was protected by the Cultural Heritage. Recently, there has been a considerable increase in repair and rehabilitation projects to restore or enhance deteriorated bridges, it is very important to select proper bridge maintenance activities also subject to constrained budgets. It is a highly complex problem to decide what kinds of maintenance activities are used for the bridge to maximize total benefit in terms of the constrained budget and efficient. In other words, the bridge maintenance strategy at a network level is an optimization problem to combine the selection of bridges that need repair or rehabilitation with maintenance activities whose total cost should not exceed the given budget. It should maximize the total benefit of bridge maintenance activities.

This work was a challenge for the author because of the uncertainties related to research with the unique phenomenon that is ASR, which is usually not present very often in new bridge structures. The concept of the project was development how to analyze the capacity of the Elgeseter Bridge structure in Trondheim. The proposed solutions of repair are prototypes. Calculations and observation showed that the construction do not fulfill the Ultimate Limit State and Serviceability Limit State of the bridge.

10.1 Structural Behavior

This document described an approach for the diagnosis and prognosis of alkali-aggregate reactivity in Elgeseter Bridge structure. A preliminary investigation program of detection of ASR is first presented and allow involves a condition survey aiming at detecting typical visual symptoms of ASR in the bridge, along with a quantitative assessment of the extent of cracking in those structural members most susceptible to ASR. The assessment (diagnosis) of ASR is then completed by calculation of the infected structural members. For instance, the expansion attained to date by the concrete, the current expansion rate and the potential for future expansion, including the temperature and humidity conditions at the site, the water soluble alkali content in the concrete and the restraint conditions in the structural member are proposed. It is generally recognized that the potential for future distress in ASR-affected members is best evaluated through a fairly extensive in-situ monitoring program; however, such a program generally requires years to generate reliable data. Consequently, the approach proposed in this report analyses the results from a series of selected laboratory

investigations, which are used to provide the best estimate possible of the current condition and future behavior of the structure under study, thus allowing one to select reasonable remedial/mitigation actions.

The underlying combination of the Ultimate Limit State includes load associated with vehicle traffic in accordance with Handbook 238. Analysis of the results on the basis of the standard NS 3473 and EC 2 showed that for the combination of the maximum values of forces in the most damaged and cracked bridge components and conditions were as follows:

That was calculated shear capacity in the weakest cross section of the beam. We consider cases with uncracked and cracked concrete. Moreover, to the calculation we take into account influence of the tensile force causes by ASR reaction.

Uncracked:

$V_{cd} = V_{co} + V_{sdb} + V_{sds} = \ 504{,}57kN + \ 1086{,}07\ kN + 207{,}132\ kN = 1797{,}77kN > 1674kN$

Shear capacity can be reduced by the action of the axial tensile force:

$V_{cd} = V_{co} + V_{sdb} + V_{sds} = \ 0\ kN + \ 1086{,}07\ kN + 207{,}132\ kN = 1293{,}20kN < 1674kN$

Based on above calculation state that cross-section has not sufficient capacity to shear force. Enhancement capacity of the structure by using Fiber Reinforcement is necessary.

In combination Serviceability Limit State also according to ,,Håndbok 238 bruklassifisering'' includes all moving load. Examined cases showed that the maximum deflection in span equal to:

$$f_{max} \ = \ 150.5\ mm \ < \ f_{dop} \ = \ L/600 \ = \ 333\ mm$$

that fulfill the conditions of serviceability as for road bridges

Linear and non-linear analyses were used to observe and predict behavior of columns under the expansion of concrete due to ASR reaction. Expansion of the concrete was established to be equal 0,1%. Modeling of crack opening was represented by 26 cracks of the integration points in the interface element. Based on numerical studies, it is considered that the method may provide an effective way of assessing aging columns based on the crack conditions in concrete and the corrosion of steel reinforcement. Moreover, combination of refined structural analyses and engineering interpretation explain observed deformations and damage of the bridge.

10.2 Proposed Repair Solution

In this thesis is that the more accurate prediction of the response and capacity of concrete bridge deck slabs under loading with respect to shear are obtained using the non-linear finite element analysis. Such an analysis describes the real behaviour of the slab since occurrence of cracking in concrete leads to stress redistributions. However, establishing an appropriate method involves many choices in order to obtain a realistic behaviour of the considered structure. It is also crucial that the designer is well aware of the limitations and efficient of the used methods. This thesis allows giving some recommendations that we suggest to use on bridge structure. It may help to establish the repair and rehabilitation projects to become more appropriate and accurate:

Columns:

- **Electrochemical Lithium Impregnation of columns**

Lithium-based admixtures can be used to control expansion due to ASR provided they are used in sufficient quantity is more efficient. It is recommended to carry out this technique before crack filling. This will allow for deep penetration lithium in concrete.

- **Use monosilane on the surface of the columns.**

Lower part of the column #4 in zone 4 and other columns which outer surface is strongly deteriorated need therefore be replaced by the new layer of the concrete after Electrochemical Lithium Impregnation and crack filling. Afterwards applying a new layer of monosilane can appropriate protect columns against water penetration.

Beams:

- **Crack filling**
- **Carbon Fiber Reinforcement Strengthening of the beams**

Slab:

- **Removal of existing pavement, sidewalk, curb, and combination curb and gutter**

Pavement, including base courses, sidewalk, curb, and combination curb and gutter, and other miscellaneous surfaces shall be removed for the full depth thereof. The Contractor shall use suitable equipment, tools, and methods for cutting and trimming as well as removing the materials to the neat lines established by the Engineer and shall not in any manner disturb or damage the sections of base or pavement to be salvaged or adjacent slab and beams constructions members or other surfaces.

- **Crack filling**

For instance the Epoxy crack repair products can be used. The main advantage of epoxies is their amazing compressive strength, which exceeds that of most concrete. That's why epoxies are one of the best choices for cracks requiring structural repair. However, epoxies cure very slowly, generally taking hours to harden. In our case this can be an advantage because it allows time for the epoxy to flow into even the smallest crevices of the cracks.

- **Topical Treatment of slab with Lithium under membrane protection**

Laboratory testing has shown that ASR-affected concrete specimens can be treated topically using lithium-based compounds to slow down the rate of expansion.

Many structures have been treated with lithium using either a simple topical application or electrochemical or vacuum impregnation techniques to increase lithium penetration.

- **Drainage System and Membrane Protection**

The most important thing indisputable need of repair in order to prevent the penetration of water from the atmosphere to the structure of the bridge.

It is recommended that treated structures be monitored and tested to provide information on the efficacy of lithium treatment on the ASR-affected structures in Norway.

Few words from authors:

The design of Elgeseter Bridge with slender structural elements was a technological challenge for the engineers in the 1950s. The requirement for uniform and high concrete strength demanded a rigorous quality control system, which was not common at that time. What is more, ASR was not a known concrete problem in the 1950s, and, therefore, precautions against ASR were not taken. Based on results nowadays, taking into consideration durable time of 60 years of existence of the structure we have to say that bridge was designed as real structural masterpiece made by the Norwegians at these times. We would like to express our admiration for this construction. We are very impressed and also appreciate that we get opportunity to work with this unique construction.

Authors reserve the fact that any of studies aimed at evaluating the effect of lithium nitrate on the environment are not known. The work is not part of the documentation of construction and maintenance of the executive under terms of the construction law and many issues would still have to develop and be submitted for more detailed analysis.

11 References

[1] B. Fournier, M.-A. Bérubé, Alkali–aggregate reaction in concrete: a review of basic concepts and engineering implications, Can. J. Civ. Eng. 27 (2000) 167–191.
[2] T. Katayama, D. Bragg, Alteration of S–C–H and ASR gel in deteriorated concretes, Newfoundland, Canada, Proc. Int. Conf. on Concrete under Severe Conditions, Saporo, Japan, 1995, pp. 1165–1174, 2.
[3] T. Katayama, D. Bragg, Alkali-aggregate reaction combined with freeze/thaw in Newfoundland, Canada Petrography using EMPA, Proc. 10th ICAAR, Melbourne Australia, 1996, pp. 243–250.
[4] T.E. Stanton, Expansion of concrete through reaction between cement and aggregates, Proc. Am. Soc. Civil Eng. 66 (1940) 1781–1811.
[5] B. Fournier, M. Berubé, Alkali-aggregate reaction in concrete: a review of basic concepts and engineering implications, Can. J. Civil Eng. 27 (2) (2000) 167–191.
[6] Swamy, R.N., 1992. The Alkali-silica Reaction in Concrete. Van Nostand Reinhold, New York.
[7] P.K. Mehta, P.J.M. Monteiro, Concrete: Microstructure, Propertiesand Materials, third ed., McGraw Hill, 2006, p.170.
[8] A.S.C. Fava, R.J. Manuele, J.F. Colina, C.R. Cortelezzi, Estudios y experiencias realizadas en LEMIT sobre reacción que se produce entre el cemento y los agregados en el hormigón de cemento portland, Serie Técnica N 85, LEMIT, La Plata, Argentina, 1991, (in spanish) 40 pp.
[9] D. Mc Connell, R. Meilenz,W. Holland, K.T. Greene, Cement — aggregate reaction in concrete, ACI J. Proc. 44 (10) (1947) 93–128.
[10] P.E. Grattan Bellew, Test methodology and criteria for evaluating the potential reactivity of aggregates, Proc. 8th ICAAR, Kyoto Japan, 1989, pp. 279–294.
[11] O.R. Batic, J.D. Sota, Reacciones deletéreas internas, in: E.F. Irassar (Ed.),
[12] J.M. Ponce, O.R. Batic, Different manifestations of the alkali-silica reaction in concrete according to the reaction kinetics of the reactive aggregate, Cem. Concr. Res. 36 (6) (2006) 1148–1156.
[13] L.S. Dent Glasser, N. Kataoka, Cement Concrete Res. 11 (1981) 1.
[14] M. Prezzi, P.J.M. Monteiro, G. Sposito, ACI Mater. J. 94 (1997) 10.
[15] M. Prezzi, P.J.M. Monteiro, G. Sposito, ACI Mater. J. 95 (1998) 3.
[16] X.D. Cong, R.J. Kirkpatrick, S. Diamond, Cement Concrete Res. 23(1993) 811.
[17] X.D. Cong, R.J. Kirkpatrick, Cement Concrete Res. 23 (1993) 1065.
[18] A.R. Brough, C.M. Dobson, I.G. Richardson, G.W. Groves, J.Mater. Sci. 31 (1996) 3365.
[19] X.D. Cong, R.J. Kirkpatrick, Cement Concrete Res. 34 (2004) 1683.
[20] X.Q. Hou, R.J. Kirkpatrick,
[21] L.S. Dent Glasser, N. Kataoka, The chemistry of alkali– aggregate reaction, Proceedings of the 5th International Conference on Alkali– Aggregate Reaction, Cape Town (South Africa), Paper, vol. S252/23, National Building Research Institute of the CSIR, 1981, p. 7.

[22] A.B. Poole, Alkali– silica reactivity mechanisms of gel formation and expansion, Proceedings of the 9th International Conference on Alkali– Aggregate Reaction, London (England), 104 (1), Concrete Society Publications CS, 1992, pp. 782– 789.
[23] H. Wang, J.E. Gillot, Mechanism of alkali –silica reaction and significance of calcium hydroxide, Cement and Concrete Research 21 (1991) 647–654.
[24] D. Bulteel, E. Garcia-Diaz, C. Vernet, H. Zanni, Alkali– aggregate reaction: a method to quantify the reaction degree, Cement and Concrete Research 32 (2002) 1199–1206
[25] L.S. Dent Glasser, Osmotic pressure and the swelling of gels, Cement and Concrete Research 9 (1979) 515– 517.
[26] S. Diamond, ASR: another look of mechanism, Proceedings of the 8th International Conference on Alkali–Aggregate Reaction in Concrete, Kyoto (Japan), 1989, pp. 83–94.
[27] S. Chatterji, Mechanisms of alkali– silica reaction and expansion, in: K. Okada, S. Nishibayashi, M. Kawamura (Eds.), Proceedings of the 8th International Conference on Alkali–Aggregate Reaction in
Concrete, Kyoto (Japan), 1989, pp. 101– 105.
[28] S. Chatterji, N. Thaulow, Some fundamental aspects of alkali– silica reaction, in: M.A. Berube, B. Fournier, B. Durand (Eds.), Proceedings of the 11th International Conference on Alkali–Aggregate Reaction in Concrete, Quebec (Canada), 2000, pp. 21– 29.
[29] R. Dron, F. Brivot, T. Chaussadent, Me´canisme de la re´action alcali– silice, Bull. Liaison Lab Ponts et Chausse´es, vol. 214, 1998, pp. 61– 68.
[30] R. Dron, Thermodynamique de la re´action alcali –silice, Bull. De Liaison des Lab. Ponts et Chausse´es, vol. 166, 1990, pp. 55– 59.
[31] T.N. Jones, A new interpretation of alkali– silica reaction and expansion mechanisms in concrete, Chemistry and Industry 2 (1988) 40– 44.
[32] M. Prezzi, J.M. Monteiro, G. Sposito, The alkali –silica reaction, Part 1: use of the double-layer theory to explain the behaviour of reactionproducts gels, ACI Materials Journal 94 (1) (1997) 10–17.
[33] F.A. Rodriguez, J.M. Monteiro, G. Sposito, The alkali– silica reaction: the surface charge density of silica and its effect on expansive.
[34] R.F. Bleszynski, M.D.A. Thomas, Microstructural studies of alkali–silica reaction in fly ash concrete immersed in alkaline solutions, Adv. Chem. Bas. Mat. 7 (1998) 66–78 (and references therein).
[35] U. Müller, K. Rübner, The microstructure of concrete made with municipal waste incinerator bottom ash as an aggregate component, Cem. Concr. Res. 36 (2006) 1424–1443 (and references therein).
[36] D.E. Stanton, The expansion of concrete through reaction between cement and aggregate, Am. Soc. Civ. Eng. 66 (1940) 1781–1811.
[37] RILEMTC 191-ARP: 'Alkali-reactivity and prevention—assessment, specification and diagnosis of alkali-reactivity', RILEM Recommended Test Method AAR-1: Detection of potential alkali-reactivity of aggregates—petrographic method, Mater. Struct. 36(2003) 480–496.

[38] RILEM TC 106-AAR, 'Alkali aggregate reaction' A. TC 106-2-Detection of potential alkali-reactivity of aggregates—The ultra-accelerated mortar-bar test B. TC 106-3- Detection of potential alkali-reactivity of aggregates-method for aggregate combinations using concrete prisms, Mater. Struct. 33 (2000) 283–293.
[39] RILEM TC 191-ARP: 'Alkali-reactivity and prevention—assessment, specification and diagnosis of alkali-reactivity', AAR-5: Rapid preliminary screening test for carbonate aggregates, Mater. Struct. 38 (2005) 787–792.
[40] RILEM TC 219-ACS 'Alkali–silica reactions in concrete structures': RILEM AAR-4.1—Detection of potential alkali-reactivity of aggregates: accelerated (60 °C) concrete prism test, 2006. (unpublished draft).
[41] RILEM TC 191-ARP: 'Alkali-reactivity and prevention—assessment, specification and diagnosis of alkali-reactivity', RILEM Recommended Test Method AAR-0: detection of alkali-reactivity potential in concrete—outline guide to the use of RILEM methods in assessments of aggregates for potential alkali-reactivity, Mater. Struct. 36 (2003) 472–479.
[42] J. Lindgård, P.J. Nixon, I. Borchers, B. Schouenborg, B.J.Wigum,M. Haugen, U. Åkesson, The EU "PARTNER" Project—European standard tests to prevent alkali reactions in aggregates: final results and recommendations, Cem. Concr. Res. 40 (2010) 611–635.
[43] ASTM C1260—07 Standard Test Method for Potential Alkali Reactivity of Aggregates (Mortar-BarMethod), Annual Book of ASTM Standards American Society for Testing and Materials, 2007, p. 5.
[44] ASTM C1293-08b Standard Test Method for Determination of Length Change of Concrete Due to Alkali–Silica Reaction, Annual Book of ASTM Standards, American Society for Testing and Materials, 2008. p.7.
[45] ASTM C295-08 Standard Guide for Petrographic Examination of Aggregates for concrete, Annual Book of ASTM Standards, American Society for Testing and Materials, 2008, p. 8.
[46] CSA, CSA A23.2-14A-00, Potential Expansivity of Aggregates (Procedure for Length Change due to Alkali–Aggregate Reaction in Concrete Prisms at 38 °C), Methods of Testing for Concrete, Canadian Standards Association, Mississauga, Ontario, Canada, 2004, pp. 246–256.
[47] AFNOR NF P 18-454, Reactivity of a Concrete Formula with Regard to the Alkali–aggregate Reaction, Association Française de Normalisation, Paris, France, 2004.
[48] Norwegian Concrete Association: Alkali–aggregate Reactions in Concrete, Test methods and Requirements to Test Laboratories, NB32, 2005, p. 39.
[49] Trondheim Havn. "Bruer i Trondheim" (in Norwegian).
[50] Store norske leksikon. "Elgeseter bru" (in Norwegian).
[51] Knudsen KE. Report over the concrete work on Elgeseter Bridge, Trondheim. Report Dr Ing A Ass Jakobsen 1951:56 [in Norwegian].
[52] Soerum H. Conditional report on bridges, culverts and gangways maintained by Trondheim Municipality 1990,inspections carried out in 1989, report Technical department Trondheim Municipality, p. 26. In Norwegian.
[53] Jensen V. Alkali Aggregate Reaction in Southern Norway. Doctoral technical thesis 1993, University of Trondheim (NTH), p. 262-9 appendices.

[54] Jensen V. Microstructural analysis on cores from Elgeseter Bridge. SINTEF report STF65 F90033; 1993 (confidential) l.p. 28. In Norwegian.
[55] Jensen V. Post-doctoral project 1998–2000. Norwegian Research Council.
[56] Jensen V. Inspection of repair work on Elgeseter Bridge; 2003 (July).
[57] Larive, C., "Apports combinés de l'expérimentation et de la modélisation la comprehénsion de l'alcali-réaction et de ses effets mécaniques", in *Laboratoire Central des Ponts et Chaussées (LCPC)*. 1998: Paris.
[58] Multon, S. and F. Toutlemonde, "Effect of applied stresses on alkali-silica reaction-induced expansions", *Cement and Concrete Research*, 2006. 36(5): p. 912-920.
[59] Saouma, V. and L. Perotti, "Constitutive model for alkali-aggregate reactions", *Aci Materials Journal*, 2006. 103(3): p. 194-202.
[60] Statens vegvesen Vegdirektoratet (2011) Håndbok 238 Lastforskrifter for klassifisering av bruer og ferjekaier i det offentlige vegnet, ISBN 82-7207-537-7
[61] Statens vegvesen Vegdirektorate (2009) Håndbok 185 Bruprosjektering (normaler).
[62] Jianhong Wang, Zihai Shi, Strength degradation analysis of an aging RC girder bridge using FE crack analysis and simple capacity-evaluation equations, Engineering Fracture Mechanics 108 (2013) Japan
[63] TNO Diana Manual (2012): Diana – Finite element analysis – User's Manual – Analysis Procedures – Release 9.4.4 TNO DIANA BV, Delft, The Netherlands.
[64]Van Dam, T.J., Sutter, L.L., Smith, K.D., Wade, M.J., Peterson, K.R., "Guidelines for Detection, Analysis, and Treatment of Materials-Related Distress in Concrete Pavements—Volume I: Final Report," Federal Highway Administration, Report No. FHWA-RD-01-163, Washington, D.C., August 2002.
[65] Kjell M. Mathisen. Lecture notes; TKT4197-Nonlinear Finite Element, Analysis, Høst 2011.
[66] Eurocode 2 (2001): Design of concrete structures - Part 1: General rules and rules for buildings, European Committee for Standardization (2001), Brussels, 2001.
[67] Norsk Strandard NS 3473 Prosjektering av betongkonstruksjoner Beregnings- og konstruksjonsregler
[68] Kobielak S.: Współczesne betonowe budowle ochronne. Wybrane zagadnienia projektowania Oficyna Wydawnicza Politechniki Wrocławskiej, Wrocław 2005
[69] RUREDIL Via B. Buozzi 1 -20097 San Donato Milanese : Fiber Reinforced Cementitious Matrix (FRCM) – New Developments
[70] Ruredil Technical Notebook, Buildings seismic retrofit with FRCM – Fiber Reinforced
[71] Ruredil Technical Notebook, Cementitious Matrix composite. Concrete and masonry structures. July 2009
[72] Trapko T.: Nośność żelbetowych słupów wzmacnianych taśmami i matami z włókien węglowych. Praca doktorska. Politechnika Wrocławska, 2004.
[73] Wzmacnianie konstrukcji kompozytami FRP, Inżynier Budownictwa, 11/2010.
[74] Smaoui, N., Bissonnette, B., Bérubé, M.A., Fournier, B., and Durand, B., "Stresses Induced by ASR in Prototypes of Reinforced Concrete Columns Incorporating Various Types of Reactive Aggregates," Canadian Journal of Civil Engineering, submitted for publication, 2007.
[75] Fournier, B., et al., "Report on the Diagnosis, Prognosis, and Mitigation of Alcali-Silica Reaction (ASR) in Transportation Structures," Federal Highway Administration, Final Report, 2010.
[76] Michael D.A. Thomas, Benoit Fournier, The Use of Lithium To Prevent or Mitigate Alkali-

Silica Reaction in Concrete Pavements and Structures, Final report, March 2007
[77] Jensen V, Haugen M. Alkali Aggregate reaction in Northern Norway, Report no. 3: in-situ measurement of humidity and expansion. SINTEF-report no. STF22 A96807; 1996. In Norwegian.
[78] Wood JGM. Methods of control of active corrosion in concrete. Proceeding Deterioration of Reinforced Concrete in the Arabian Gulf, October 1985. Bahrain.
[79] APM 106. Humidity measurement, AEC test method. Copenhagen, Denmark. Holte, Copenhagen, Denmark: AEC Consulting Engineer. In Danish.
[80] Apneseth T, Hay M. Test of electrical humidity apparatus, Norsk Treteknisk Institutt, Report from 1992. In Norwegian.
[81] NORDTEST-Metoden. Relative humidity: measured by wooden probes. Nordtest-prosjekt 1993 (April);943–90:23
[82] Jensen V. Elgeseter Bridge: humidity and expansion measurements till 5 September 2002. Assessment of treatment with 3 types of monosilane on columns. NBTL report no. R02001; 2002 (confidential). p. 78. In Norwegian.
[83] Jensen V. In-situ measurement program on Elgeseter Bridge. NBTL project; 2003 (confidential). In Norwegian.
[84] Jensen V. Research project: security of dam structures, Norwegian concrete day 2001-NTNU-SINTEF information day 2001, Sintef report STF 22 A01616; 2001. p. 70–78. In Norwegian.
[85] Jensen V. Relative humidity measured by the wooden stick method in Norwegian concrete structures with and without surface protection. Proceedings Nordic concrete research meeting. Elsinore, Denmark; 2002. p. 150– 3. Oslo, Norway: Norwegian Concrete Society.
[86] Jensen V. Relative humidity measured by wooden stick method in concrete structures: long term measurements and reduction of humidity by surface treatment. SP 212-39, proceedings sixth CANMET/ACI International Conferences, Thessaloniki, Greece; 2003.
[87] Jensen V. Post-doctoral project 1998–2000. Norwegian Research Council.
[88] Rapport from SINTEF, Rehabilitering av brusøyler med alkalireaksjonsskaer. Feltforsøk på Elgeseter Bru. Sluttrapport. Page 23 figure 11.